YAEC-1908, Rev. 1

Vermont Yankee
Cycle 18
Core Performance Analysis Report

November 1995

Major Contributors:

C. Chiu
N. Fujita
B. Hubbard
D. Kapitz
M. LeFrancois
D. Morin
K. Morrissey
J. Neyman
L. Schor
F. Seifaee
R. Smith
K. St.John
R. Woehlke

R40/53

Prepared by: M A Sironen 11/29/95
M. A. Sironen (Date)
VY Nuclear Engineering Coordinator

Approved by: R J Cacciapouti 11/29/95
R. J. Cacciapouti, Manager (Date)
Reactor Physics Group

Approved by: P.A. Bergeron 11/29/95
P. A. Bergeron, Manager (Date)
Transient Analysis Group

Approved by: Eshor for RKS 11/29/95
R. K. Sundaram, Manager (Date)
LOCA Analysis Group

Approved by: R J Cacciapouti for 11/29/95
J. R. Chapman, Director (Date)
Nuclear Engineering Department

Yankee Atomic Electric Company
Nuclear Services Division
580 Main Street
Bolton, Massachusetts 01740

DISCLAIMER OF RESPONSIBILITY

This document was prepared by Yankee Atomic Electric Company ("Yankee"). The use of information contained in this document by anyone other than Yankee, or the Organization for which this document was prepared under contract, is not authorized and, with respect to any unauthorized use, neither Yankee nor its officers, directors, agents, or employees assume any obligation, responsibility, or liability or make any warranty or representation as to the accuracy or completeness of the material contained in this document.

ABSTRACT

This report presents design information, calculational results, and operating limits pertinent to the operation of Cycle 18 of the Vermont Yankee Nuclear Power Station. These include the fuel design and core loading pattern descriptions; calculated reactor power distributions, exposure distributions, shutdown capability, and reactivity data; and the results of safety analyses performed to justify plant operation throughout the cycle.

This report was revised to incorporate the loss of stator cooling transient analysis description and results. The revised MAPLHGR limits are included.

ACKNOWLEDGEMENTS

The author and major contributors would like to acknowledge the contributions to this work by the Vermont Yankee Reactor & Computer Engineering Department for their review of input data and guidance.

TABLE OF CONTENTS

TABLE OF CONTENTS
(Continued)

LIST OF TABLES

LIST OF TABLES
(Continued)

LIST OF FIGURES

LIST OF FIGURES
(Continued)

1.0 INTRODUCTION

This report provides information to support the operation of the Vermont Yankee Nuclear Power Station through the forthcoming Cycle 18. In this report, Cycle 18 will be referred to as the Reload Cycle. The preceding Cycle 17 will be referred to as the Current Cycle. The Cycle 17/18 refueling will involve the discharge of 120 irradiated fuel bundles and the insertion of 120 new fuel bundles. The resultant core will consist of 120 new fuel bundles and 248 irradiated fuel bundles. The General Electric Company (GE) manufactured all the bundles. Some of the irradiated fuel was also present in the reactor in Cycle 16. This cycle will be referred to as the Past Cycle.

This report contains descriptions and analyses results pertaining to the mechanical, thermal-hydraulic, physics, and safety aspects of the Reload Cycle. The MAPLHGR and MCPR operating limits calculated for the Reload Cycle are given in Appendix A. These limits will be included in the Core Operating Limits Report.

This report was revised to incorporate the loss of stator cooling transient analysis description and results. The MAPLHGR operating limits in Appendix A were revised as a result of this transient.

2.0 RECENT REACTOR OPERATING HISTORY

2.1 Operating History of the Current Cycle

The current operating cycle is Cycle 17. To date, the Current Cycle has been operating at, or near, full power with the exception of sequence exchanges, several power reductions, and four short repair outages. The operating history highlights and control rod sequence exchange schedule of the Current Cycle are found in Table 2.1.1.

2.2 Operating History of Past Applicable Cycle

The irradiated fuel in the Reload Cycle includes some fuel bundles initially inserted in Cycle 16. This Past Cycle operated at, or near, full power with the exception of sequence exchanges, several short power reductions, one short repair outage and a coastdown to the end of cycle. The operating history highlights of the Past Cycle are found in Table 2.2.1. The Past Cycle is described in detail in the Cycle 16 Summary Report[1].

TABLE 2.1.1

VY CYCLE 17 OPERATING HIGHLIGHTS

Beginning of Cycle Date	October 24, 1993
End of Cycle Date	March 18, 1995*
Weight of Uranium As-Loaded (Short Tons)	72.02
Beginning of Cycle Core Average Exposure** (MWd/St)	11547
End of Full Power Core Average Exposure** (MWd/St)	21997*
End of Cycle Core Average Exposure** (MWd/St)	21997*
Number of Fresh Assemblies	128
Number of Irradiated Assemblies	240

Control Rod Sequence Exchange Schedule:

	Sequence	
Date	From	To
January 9, 1994	A2-1	B2-1
March 15, 1994	B2-1	A1-1
May 17, 1994	A1-1	B1-1
July 19, 1994	B1-1	A2-2
October 6, 1994	A2-2	B2-2
December 2, 1994	B2-2	A1-2
January 24, 1995*	A1-2	B1-2

---

* Projected dates and exposures.

** Exposures based on the Plant Process Computer accounting.

TABLE 2.2.1

VY CYCLE 16 OPERATING HIGHLIGHTS

Beginning of Cycle Date	April 19, 1992
End of Cycle Date	August 28, 1993
Weight of Uranium As-Loaded (Short Tons)	72.06
Beginning of Cycle Core Average Exposure* (MWd/St)	11417
End of Full Power Core Average Exposure* (MWd/St)	21103
End of Cycle Core Average Exposure* (MWd/St)	21878
Number of Fresh Assemblies	128
Number of Irradiated Assemblies	240

Control Rod Sequence Exchange Schedule:

	Sequence	
Date	From	To
June 14, 1992	A2-1	B2-1
August 9, 1992	B2-1	A1-1
October 15, 1992	A1-1	B1-1
December 7, 1992	B1-1	A2-2
February 9, 1993	A2-2	B2-2
April 6, 1993	B2-2	A1-2
June 6, 1993	A1-2	B1-2

* Exposures based on the Plant Process Computer accounting.

3.0 RELOAD CORE DESIGN DESCRIPTION

3.1 Core Fuel Loading

The Reload Cycle core will consist of both new and irradiated assemblies. All the assemblies have bypass flow holes drilled in the lower tie plate. Table 3.1.1 characterizes the core by fuel type, batch size, and first cycle loaded. A description of the fuel is found in the GE Standard Application for Reactor Fuel[2] and the GE Fuel Bundle Design Reports[3][4].

3.2 Design Reference Core Loading Pattern

The Reload Cycle assembly locations are indicated on the map in Figure 3.2.1. For the sake of legibility only the lower right quadrant is shown. The other quadrants are mirror images with bundles of the same type having nearly identical exposures. The bundles are identified by the reload number in which they were first introduced into the core. Table 3.1.1 provides the key, called bundle ID, which identifies what explicit fuel type is found in each bundle location.

If any changes are made to the loading pattern at the time of refueling, they will be evaluated under 10CFR50.59. The final loading pattern with specific fuel bundle serial numbers will be supplied in the Startup Test Report.

3.3 Assembly Exposure Distribution

The assumed nominal exposure on the fuel bundles in the Reload Cycle design reference loading pattern is given in Figure 3.2.1. To obtain this exposure distribution, the Past Cycle was depleted with the SIMULATE-3 model[5],[6] using actual plant operating history. For the Current Cycle, plant operating history was used through April 22, 1994. Beyond this date, the exposure was accumulated using a best-estimate rodded depletion analysis to End of Cycle (EOC).

Table 3.3.1 gives the assumed nominal exposure on the Current Cycle and the Beginning of Cycle (BOC) core average exposure that results from the shuffle into the Reload Cycle loading pattern. The Reload Cycle End of Full Power Life (EOFPL) core average exposure and cycle capability are provided.

TABLE 3.1.1

ASSUMED VY CYCLE 18 FUEL BUNDLE TYPES AND NUMBERS

	Fuel Type Designation	Reload Bundle ID	Cycle Loaded	Number of Bundles
Irradiated	BP8DWB311-10GZ	R15A	16	40
	BP8DWB311-11GZ	R15B	16	80
	BP8DWB335-10GZ	R16A	17	96
	BP8DWB335-11GZ	R16B	17	32
New	BP8DWB335-10GZ	R17A	18	88
	BP8DWB335-11GZ	R17B	18	32

TABLE 3.3.1

DESIGN BASIS VY CYCLE 17 AND CYCLE 18 EXPOSURES*

Assumed End of Current Cycle Core Average Exposure with an Exposure Window of ± 600 MWd/St[7]	21.92±.6 GWd/St
Assumed Beginning of Reload Cycle Core Average Exposure	12.13 GWd/St
Haling Calculated End of Full Power Life Reload Cycle Core Average Exposure	22.16 GWd/St
Reload Cycle Full Power Exposure Capability (Haling)	10.035 GWd/St

* Exposures based on the SIMULATE-3 accounting.

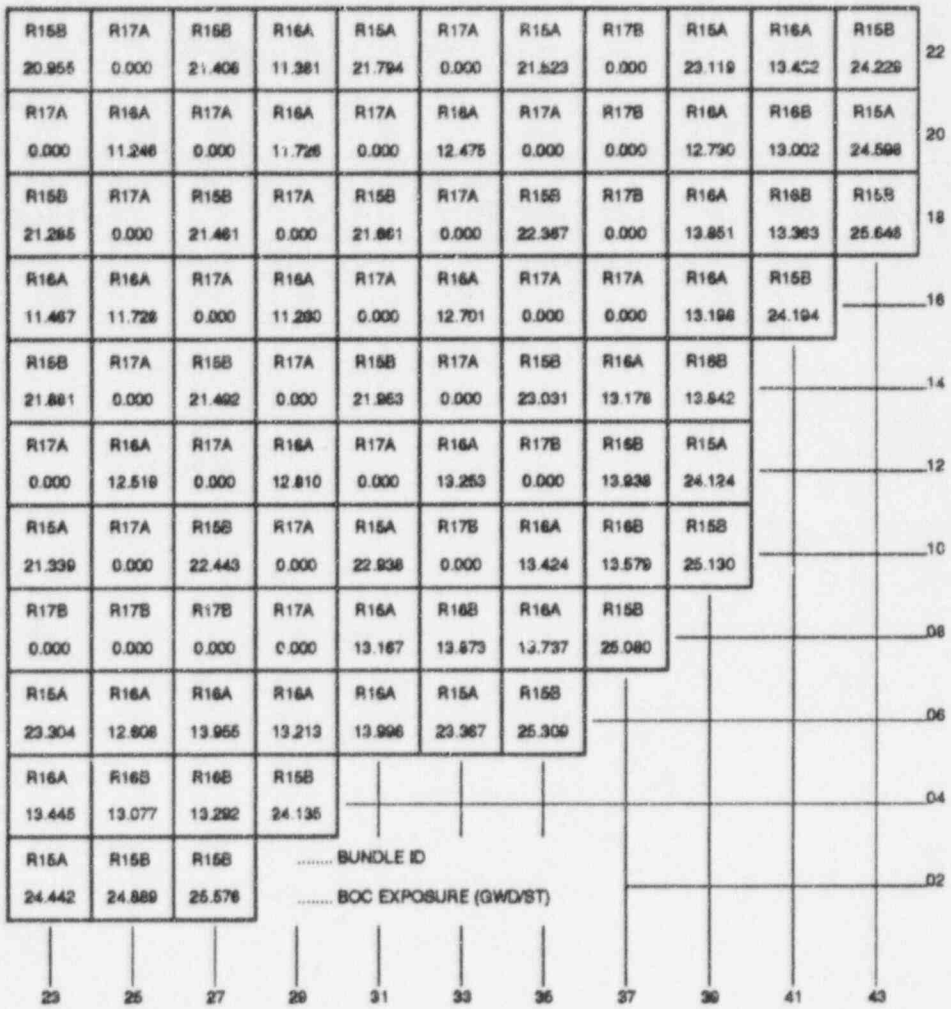

FIGURE 3.2.1

VY CYCLE 18 DESIGN REFERENCE LOADING PATTERN, LOWER RIGHT QUADRANT

4.0 FUEL MECHANICAL AND THERMAL DESIGN

4.1 Mechanical Design

All of the fuel to be inserted into the Reload Cycle was fabricated by GE. The major mechanical design parameters are given in Table 4.1.1 and Reference 2. Detailed descriptions of the fuel rod mechanical design and mechanical design analyses are provided in Reference 2. These design analyses remain valid with respect to the Reload Cycle operation. Mechanical and chemical compatibility of the fuel bundles with the in-service reactor environment is also addressed in Reference 2.

4.2 Thermal Design

The fuel thermal effects calculations were performed using the FROSSTEY-2 computer code[8],[9],[10]. The FROSSTEY-2 code calculates pellet-to-cladding gap conductance and fuel temperatures from a combination of theoretical and empirical models including but not limited to fuel and cladding thermal expansion, fission gas release, pellet swelling, pellet densification, pellet cracking, and fuel and cladding thermal conductivity.

The thermal effects analysis included the calculation of fuel temperatures and pellet-to-cladding gap conductance under core average and hot channel conditions. The core average calculations integrate the responses of individual fuel batch average operating histories over the core average exposure range of the Reload Cycle. These gap conductance values are weighted axially into 12 axial nodes by power distributions and radially by volume. The core-wide gap conductance values for the RETRAN system simulations, described in Sections 7.1 and 7.2, are from this data set at the corresponding exposure statepoints. Table 4.2.1 provides the core average response of gap conductance.

The hot channel gap conductance values, which are input to the hot channel transient calculations (Section 7.1), were evaluated for the limiting fuel bundle type as a function of the assembly exposure for two axial power shapes, a 1.4 chopped cosine and the Reload Cycle's Haling. The hot channel calculations assumed the following as required by the NRC Safety Evaluation for

FROSSTEY-2[11]: 1) appropriate allowances to account for manufacturing uncertainties and 2) the worst axial power shape prior to the transient. The peak power node was placed at the maximum average planar linear heat generation rate (MAPLHGR) limits. Gap conductance values for the hot channel analysis were determined using the limiting bundle exposure. The limiting bundle is defined as the bundle with the lowest MCPR or the highest power, if different, within the exposure range of interest. The limiting exposure for the bundle is defined by the exposure which produces the highest bundle average gap conductance within the interval of interest. The SIMULATE-3 rodded depletion (Section 5.1.2) provided predictions of the limiting bundle exposure for each exposure interval. Table 4.2.2 provides the hot channel gap conductance values for the two axial power shapes. Results are presented for the bounding exposure for the chopped cosine shape and at the four exposure statepoints for the Haling shape.

4.3 Operating Experience

All irradiated fuel bundles scheduled to be reinserted in the Reload Cycle have operated as expected in past cycles of Vermont Yankee. Off-gas measurements in the Current Cycle indicate no fuel rod failure.

TABLE 4.1.1

NOMINAL FUEL MECHANICAL DESIGN PARAMETERS

Fuel Bundle*	Irradiated Fuel Type	New & Irradiated Fuel Types
Bundle Types	GE8X8NB	GE8X8NB
Vendor Designation	BP8DWB311-10GZ & BP8DWB311-11GZ	BP8DWB335-10GZ & BP8DWB335-11GZ
Initial Enrichment,w/o U_{235}	3.11	3.35
Rod Array	8X8	8X8
Fuel Rods per Bundle	60	60
Outer Fuel Channel		
Material	Zr-2	Zr-2
Wall Thickness, inches	0.080	0.080

* Complete bundle, rod, and pellet descriptions are found in References 2 through 4.

TABLE 4.2.1

VY CYCLE 18 CORE AVERAGE GAP CONDUCTANCE VALUES

Axial Node	Gap Conductance (BTU/hr-ft^2-°F)			
	BOC	EOFPL-2000 MWd/St	EOFPL-1000 MWd/St	EOFPL
1	1190	1830	1960	2115
2	2345	3600	3715	3840
3	2445	3810	3875	4140
4	2455	3820	3895	4185
5	2495	3860	3955	4325
6	2610	3945	4150	4560
7	2600	3940	4140	4555
8	2625	3960	4180	4565
9	2525	3880	4005	4455
10	2420	3760	3850	4080
11	1880	2860	2990	3125
12	675	1015	1120	1225

TABLE 4.2.2

VY CYCLE 18 HOT CHANNEL GAP CONDUCTANCE VALUES*

FOR HALING AXIAL POWER DISTRIBUTION

Axial Node	Gap Conductance (BTU/hr-ft^2-°F)			
	BOC**	EOFPL-2000 MWd/St**	EOFPL-1000 MWd/St**	EOFPL**
	10.95 GWd/St***	10.016 GWd/St***	10.95 GWd/St***	11.472 GWd/St***
1	3360	3040	3360	3590
2	7850	7520	7850	8330
3	9630	9530	9630	9500
4	9630	9780	9630	9500
5	9630	9880	9630	9500
6	9650	9890	9650	9500
7	9650	9890	9650	9500
8	9650	9890	9650	9500
9	9650	9890	9650	9500
10	9450	8150	9450	9500
11	6580	6130	6580	6930
12	1530	1460	1530	1570

* The hot channel gap conductance values are derived for the BP8DWB335 fuel type because it is conservative compared to the other fuel types.

** Core Average Exposure.

*** Peak Bundle Exposure.

TABLE 4.2.3

VY CYCLE 18 HOT CHANNEL GAP CONDUCTANCE VALUES*

FOR 1.4 CHOPPED COSINE AXIAL POWER DISTRIBUTION

Axial Node	Gap Conductance (BTU/hr-ft^2-°F)			
	BOC**	EOFPL-2000 MWd/St**	EOFPL-1000 MWd/St**	EOFPL**
	12.15 GWd/St***	10.008 GWd/St***	11.472 GWd/St***	12.15 GWd/St***
1	750	790	760	750
2	1510	1410	1480	1510
3	5040	3690	4680	5040
4	7920	8000	7500	7920
5	9730	10450	9970	7930
6	9780	10450	10020	9780
7	9810	10450	10020	9810
8	9810	10450	10020	9810
9	9810	8570	9150	9810
10	7230	6210	7070	7230
11	2640	2260	2520	2640
12	950	960	950	950

* The hot channel gap conductance values are derived for the BP8DWB335 fuel type because it is conservative compared to the other fuel types.

** Core Average Exposure.

*** Peak Bundle Exposure.

5.0 NUCLEAR DESIGN

5.1 Core Power Distributions

The Reload Cycle was depleted using SIMULATE-3 to give both a rodded depletion and an All Rods Out (ARO) Haling depletion.

5.1.1 Haling Power Distribution

The Haling depletion serves as the basis for defining core reactivity characteristics for most transient evaluations. This is primarily because its flat power shape has conservatively weak scram characteristics. Sensitivity studies have shown that the limiting pressurization transient results are more conservative when calculated using the Haling power distribution as the initial power shape.

The Haling power distribution is calculated in the ARO condition. The Haling iteration converges on a self-consistent power and exposure distribution for the burnup step to EOFPL. In principle, this should provide the overall minimum peaking power shape for the cycle. During the actual cycle, flatter power distributions might occasionally be achieved by shaping with control rods. However, such shaping would leave underburned regions in the core which would peak at another point in time. Figures 5.1.1 and 5.1.2 give the Haling radial and axial average power distributions for the Reload Cycle.

5.1.2 Rodded Depletion Power Distribution

The rodded depletion was used to evaluate the misloaded bundle error and the rod withdrawal error because it provides the initial rod patterns and more accurately defines the local characteristics prior to the transient evaluations. It was also used in the rod drop worth and shutdown margin calculations because it depletes the top of the core more realistically than the Haling depletion. The rodded depletion also provides the hot channel bundle exposures for the gap conductance calculation.

To generate the rodded depletion, control rod patterns were developed which give critical eigenvalues at several points in the cycle and peaking similar to the Haling calculation. The resulting

patterns were frequently more peaked than the Haling, but were below expected operating limits. However, as stated above, the underburned regions of the core can exhibit peaking in excess of the Haling peaking when pulling ARO at EOFPL. Figures 5.1.3 and 5.1.4 give the ARO radial and axial average power distributions for the Reload Cycle rodded depletion at EOFPL.

5.2 Core Exposure Distributions

The Reload Cycle exposures are summarized in Table 3.3.1. The projected BOC radial exposure distribution for the Reload Cycle is given in Figure 3.2.1. The Haling calculation produced the EOFPL radial exposure distribution given in Figure 5.2.1. Since the Haling power shape is constant, it can be held fixed by SIMULATE-3 to give the exposure distributions at various mid-cycle points. BOC, EOFPL-2000 MWd/St, EOFPL-1000 MWd/St, and EOFPL exposure distributions were used to develop reactivity input for the core wide transient analyses.

The rodded depletion differs from the Haling during the cycle because the rods shape the power differently. However, rod sequences are swapped frequently and the overall exposure distribution at end of cycle is similar to the Haling. Figure 5.2.2 gives the EOFPL radial exposure distribution for the Reload Cycle rodded depletion.

5.3 Cold Shutdown Margin

Technical Specifications[12] state that, for sufficient shutdown margin (SDM), the core must be subcritical by at least 0.25% $\Delta K + R$ (defined below) with the strongest worth control rod withdrawn. Using SIMULATE-3, a search was made for the strongest worth control rod at various exposures in the cycle. This is necessary because rod worths change with exposure on adjacent assemblies. Then the cold K_{eff} with the strongest rod out was calculated at BOC and at the end of each control rod sequence. Subtracting each cold K_{eff} with the strongest rod out from the cold critical K_{eff} defines the SDM as a function of exposure. Figure 5.3.1 shows the results.

The cold critical K_{eff} was defined as the average calculated critical K_{eff} minus a 95% confidence level uncertainty. Then all cold results were normalized to make the critical K_{eff} equal to 1.000.

Because the local reactivity may increase with exposure, the SDM may decrease. To account for this and other uncertainties, the value R is calculated. R is defined as R_1 plus R_2. R_1 is the difference between the cold K_{eff} with the strongest rod out at BOC and the maximum cold K_{eff} with the strongest rod out in the cycle. R_2 is a measurement uncertainty in the demonstration of SDM associated with the manufacture of past control blades. It is presently set at 0.07% ΔK[13],[14]. The shutdown margin results, summarized in Table 5.3.1, show that the shutdown margin for the Reload Cycle is greater than the Technical Specification limit of 0.32% ΔK.

5.4 Maximum K_∞ for the Spent Fuel Pool

Section 5.5E of the Technical Specifications requires that the K_∞ for any bundle stored in either the new fuel vault or the spent fuel pool not exceed 1.31 to ensure compliance with the K_{eff} safety limit of 0.95. The bundles used in the Reload Cycle do not exceed the specifications in Section 5.5E, as shown in Table 5.4.1. These values are obtained from CASMO-3G[15].

TABLE 5.3.1

VY CYCLE 18 K_{EFF} VALUES AND SHUTDOWN MARGIN CALCULATION

Cold Critical K_{eff}	1.0000
BOC K_{eff} - Controlled With Strongest Worth Rod Withdrawn	0.9872
Cycle Minimum Shutdown Margin Occurs at BOC With Strongest Worth Rod Withdrawn	1.28% ΔK
R_1, Maximum Increase in Cold K_{eff} With Exposure	0.00% ΔK

TABLE 5.4.1

VY CYCLE 18 MAXIMUM COLD K_∞ OF ANY ENRICHED SEGMENT

Bundle Type	Maximum K_∞
BP8DWB311-10GZ	1.20
BP8DWB311-11GZ	1.20
BP8DWB335-10GZ	1.22
BP8DWB335-11GZ	1.22

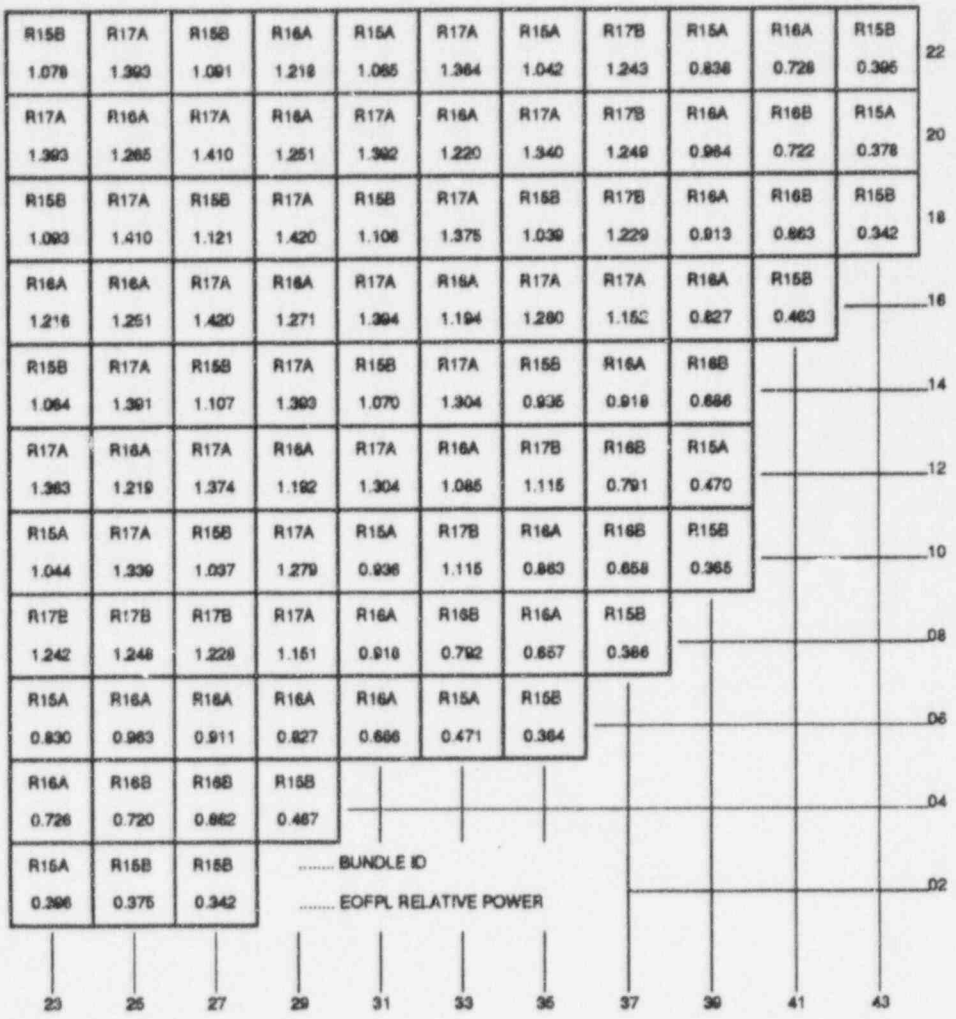

FIGURE 5.1.1

VY CYCLE 18 HALING DEPLETION,
EOFPL BUNDLE AVERAGE RELATIVE POWERS

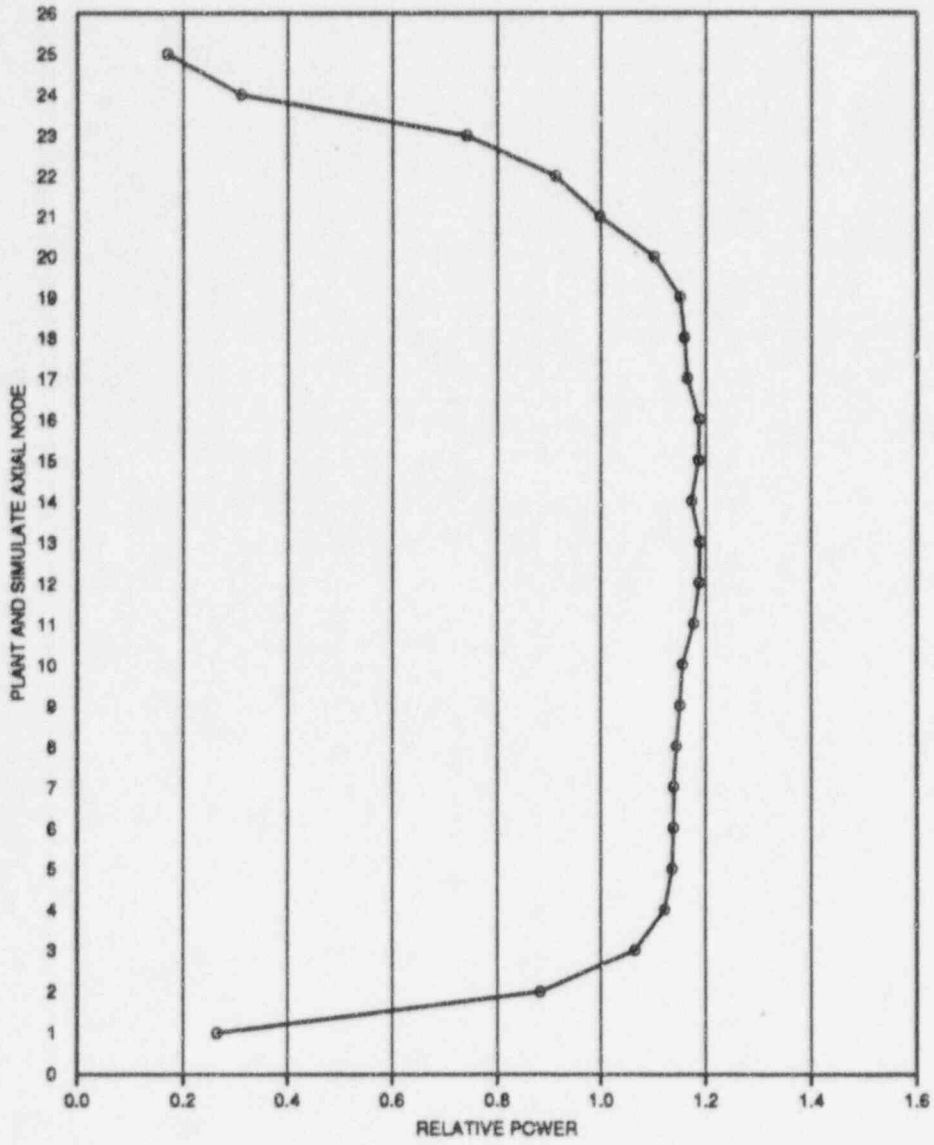

FIGURE 5.1.2

VY CYCLE 18 HALING DEPLETION, EOFPL CORE AVERAGE AXIAL POWER DISTRIBUTION

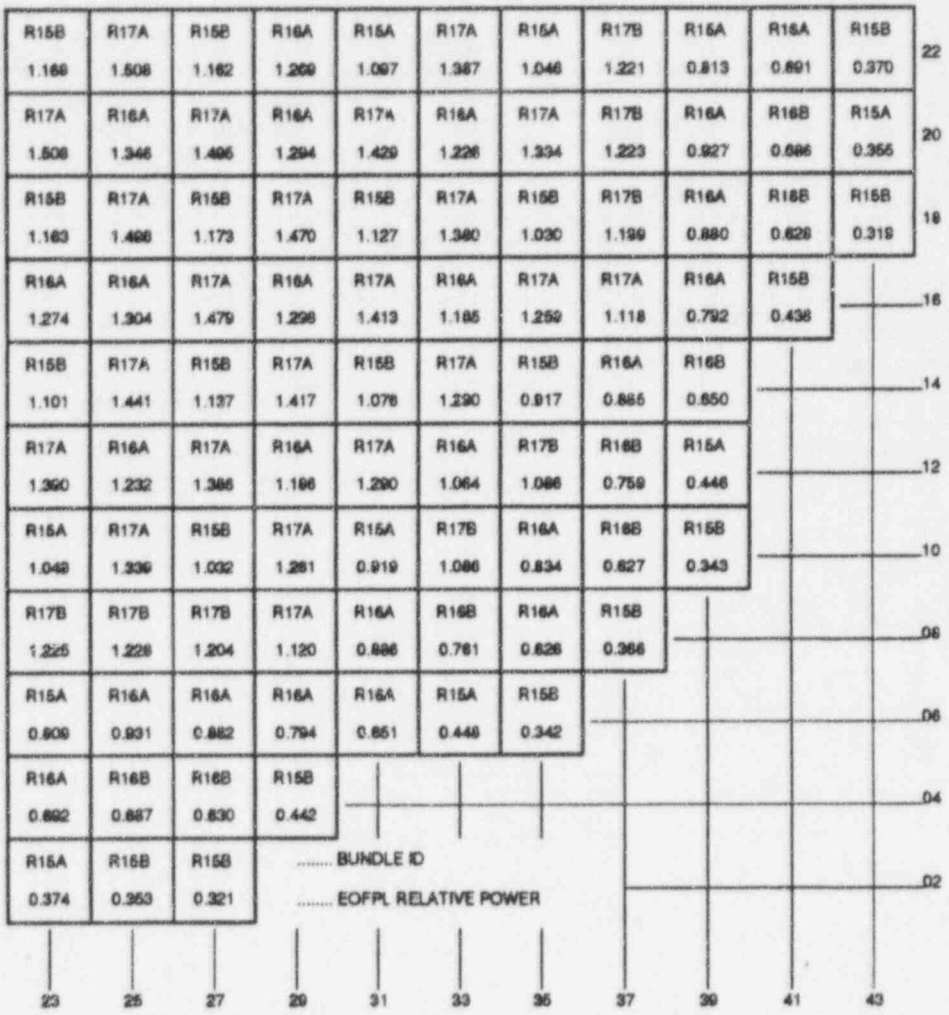

FIGURE 5.1.3

VY CYCLE 18 RODDED DEPLETION - ARO AT EOFPL,
BUNDLE AVERAGE RELATIVE POWERS

FIGURE 5.1.4
VY CYCLE 18 RODDED DEPLETION - ARO AT EOFPL
CORE AVERAGE AXIAL POWER DISTRIBUTION

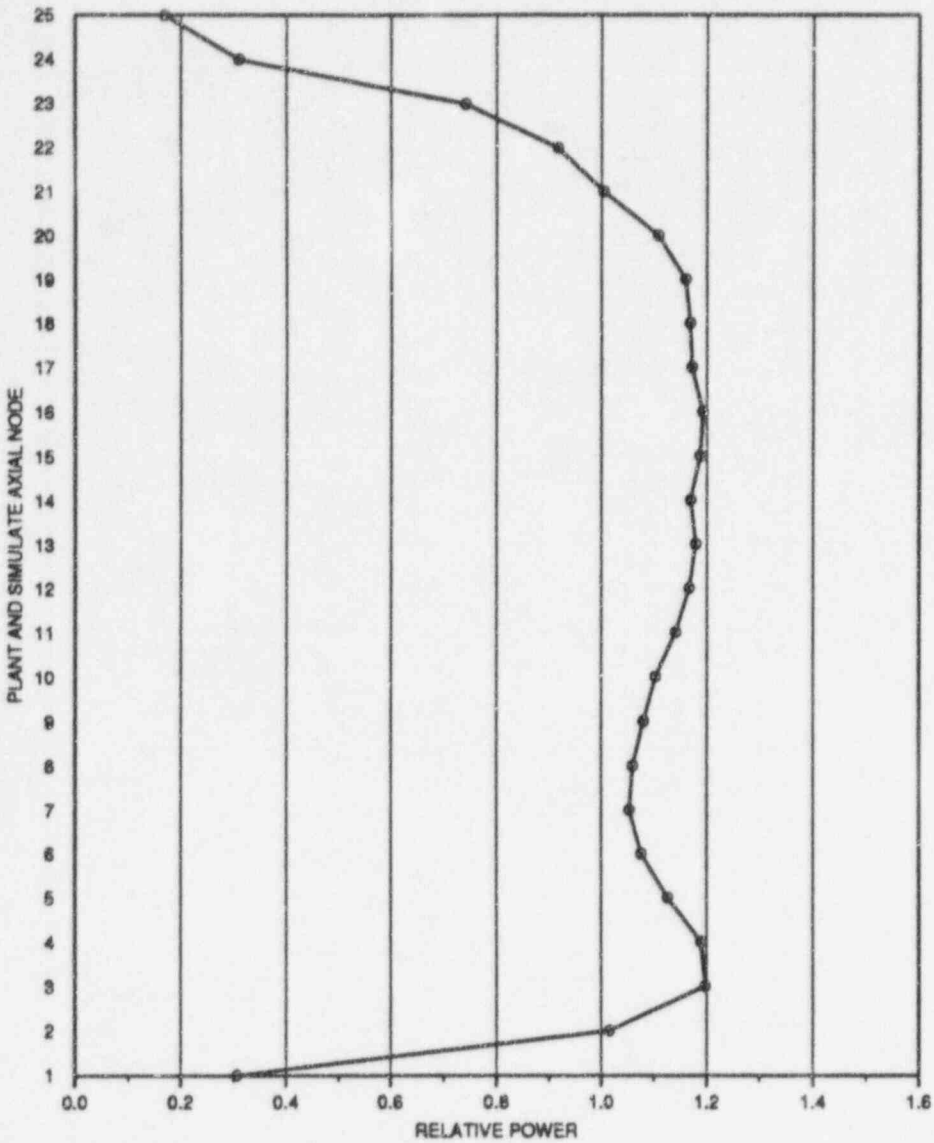

FIGURE 5.1.4

VY CYCLE 18 RODDED DEPLETION - ARO AT EOFPL,
CORE AVERAGE AXIAL POWER DISTRIBUTION

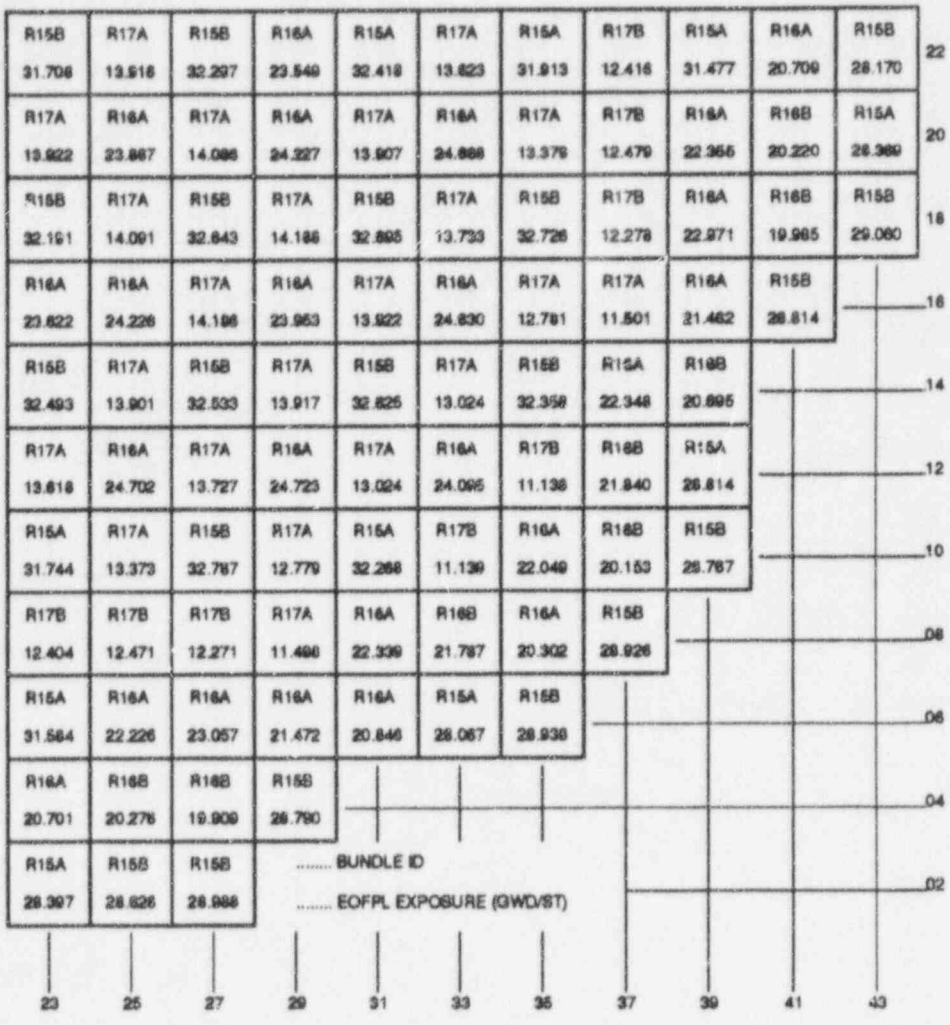

FIGURE 5.2.1

VY CYCLE 18 HALING DEPLETION, EOFPL BUNDLE AVERAGE EXPOSURES

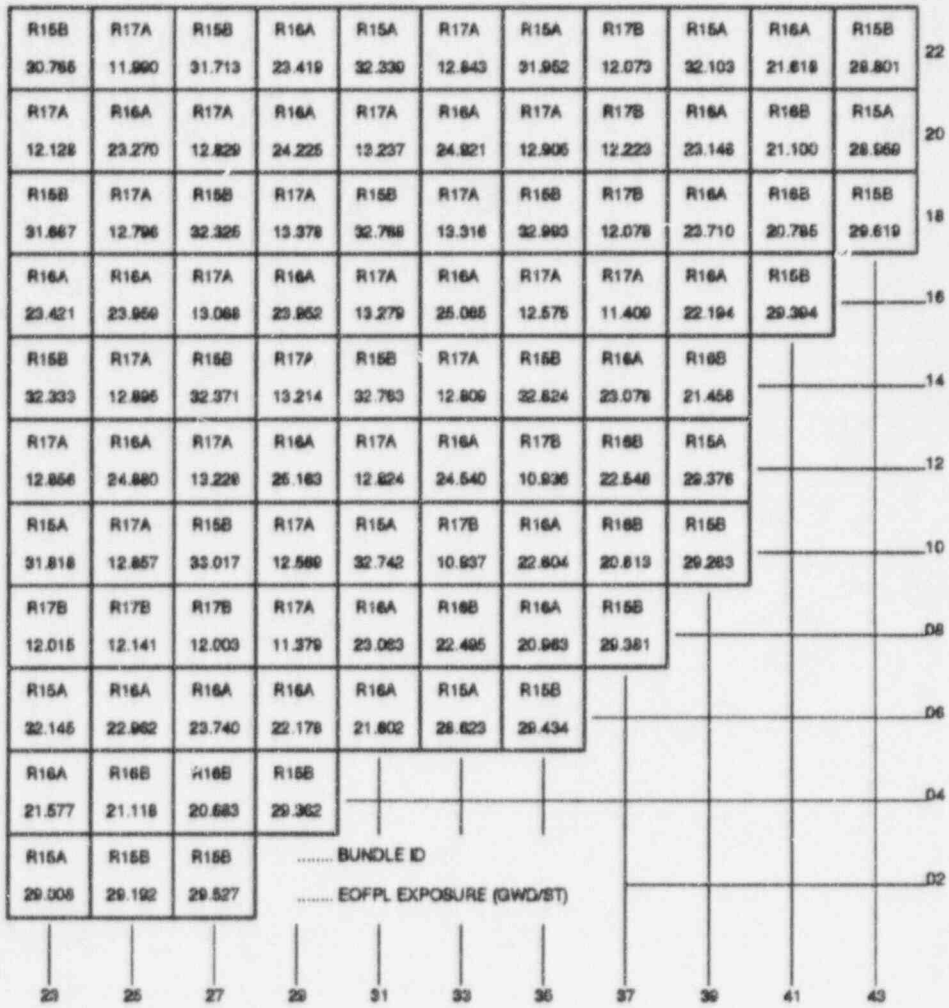

FIGURE 5.2.2

VY CYCLE 18 RODDED DEPLETION, EOFPL BUNDLE AVERAGE EXPOSURES

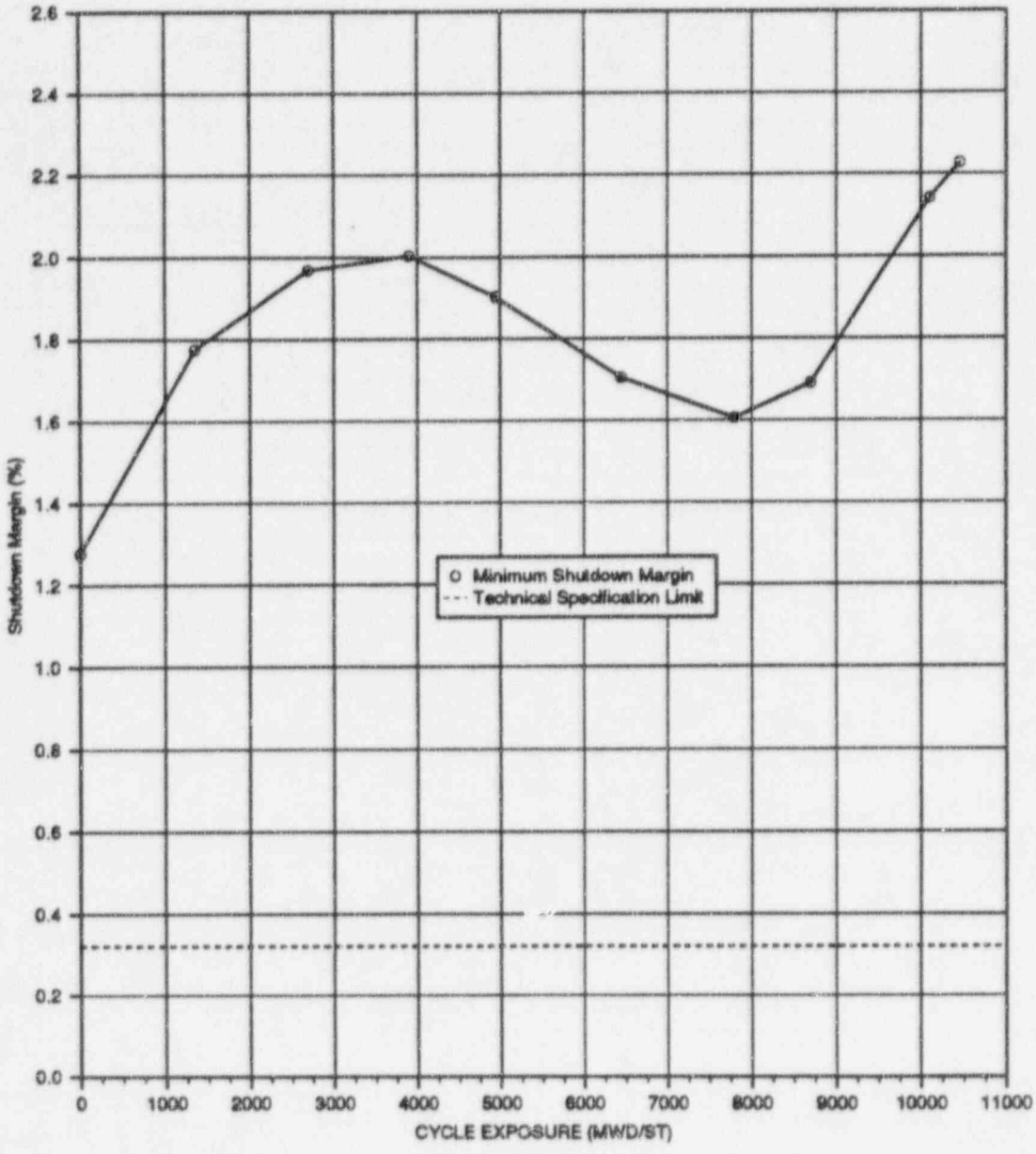

FIGURE 5.3.1

VY CYCLE 18 COLD SHUTDOWN MARGIN, IN %ΔK, VERSUS CYCLE EXPOSURE

6.0 THERMAL-HYDRAULIC DESIGN

6.1 Steady-State Thermal Hydraulics

Core steady-state thermal-hydraulic analyses for the Reload Cycle were performed using the FIBWR[16],[17],[18] computer code. The FIBWR code incorporates a detailed geometrical representation of the complex flow paths in a BWR core, and explicitly models the leakage flow to the bypass region and water rod flow. The FIBWR geometric models for each GE bundle type were benchmarked against vendor-supplied and plant thermal-hydraulic information.

Using the fuel bundle geometric models, a power distribution calculated by SIMULATE-3 and core inlet enthalpy, the FIBWR code calculates the core pressure drop and total bypass flow for several power and flow combinations. The core pressure drop and total bypass flow predicted by the FIBWR code were then used in setting the initial conditions for the system transient analysis model.

6.2 Reactor Limits Determination

Section 3.11 of the Technical Specifications requires that the plant assure the performance of the fuel rods by not exceeding the Minimum Critical Power Ratio (MCPR), the Maximum Linear Heat Generation Rate (MLHGR), and the Maximum Average Planar Linear Heat Generation Rate (MAPLHGR).

The Reload Cycle fuel has MCPR operating limits, shown in Appendix A. The MCPR is a combination of the Fuel Cladding Integrity Safety Limit (FCISL) and the change in a Critical Power Ratio (ΔCPR) which occurs during an anticipated operational transient. For Vermont Yankee FCISL is 1.07 [2]. CPR is defined as the ratio of the critical power (bundle power at which some point within the assembly experiences onset of boiling transition) to the operating bundle power. The objective for normal operation and anticipated transient events is to maintain nucleate boiling. Avoiding a transition to film boiling protects the fuel cladding integrity. Both the transient and normal MCPR operating limits are derived with the GEXL-Plus correlation[19], with appropriate coefficients representative of the Reload Cycle's fuel types. For core flows other than rated, the MCPR limits

must be adjusted by a generic factor, K_f[19]. The analysis, described in the Section 7.0, determines the Reload Cycle MCPR operating limits.

The Reload Cycle fuel has a Linear Heat Generation Rate (LHGR) limit of 14.4 kW/ft for all bundle types. The basis for this limit can be found in Reference 2.

The Reload Cycle fuel has Average Planar Linear Heat Generation Rate (APLHGR) limits, shown in Appendix A. The Maximum APLHGR (MAPLHGR) values are the most limiting of the fuel rod thermal-mechanical MAPLHGRs[20] and the LOCA analysis MAPLHGRs (Section 8.2). The fuel rod thermal-mechanical MAPLHGRs are the result of the GE fuel rod thermal-mechanical design analyses, described in Reference 2. These results assume that during steady-state: 1) the maximum LHGR is 14.4 kw/ft, 2) the maximum peak pellet exposure is 60.0 GWd/Mt, and 3) maximum operating time is 7.0 years. These results also assume that, during an anticipated operational transient, the thermal and mechanical overpower limits[21] are not exceeded. The transient analysis, described in Section 7.0, assures that the thermal and mechanical overpower limits are not exceeded. The LOCA analysis, described in Section 8.0, determines the LOCA analysis MAPLHGRs.

7.0 ABNORMAL OPERATIONAL TRANSIENT ANALYSIS

7.1 Transients Analyzed

Transient simulations are performed to assess the impact of certain transients on the heat transfer characteristics of the fuel. The purpose of this analysis is: 1) to determine the MCPR operating limit so that the FCISL is not violated for the transients considered, 2) to assure that the thermal and mechanical overpower limits are not exceeded during the transient, and 3) to demonstrate compliance with the ASME vessel code limits.

Past licensing analyses have shown that these transients result in the maximum MCPR:

1. Pressurization transients, including the generator load rejection with complete failure of the turbine bypass system and the turbine trip with complete failure of the turbine bypass system;

2. Loss of feedwater heating;

3. Local rod withdrawal error; and

4. Misloaded bundle error, including the rotated bundle error and the mislocated bundle error.

To demonstrate that the fuel rod thermal and mechanical overpowers are not exceeded, the maximum powers resulting from the pressurization, loss of feedwater heating and rod withdrawal error transients were compared to the criteria. To demonstrate compliance with ASME vessel code limits, the main steam isolation valves (MSIV) closing with failure of the MSIV position switch is also analyzed. Brief descriptions and the results of the transients analyzed are provided in the following sections.

7.2 Pressurization Transients Analysis

7.2.1 Methodology

The analysis involves two types of simulations. A system level simulation is performed to determine the overall plant response. Transient core inlet and exit conditions and normalized power from the system level calculation are then used to perform detailed thermal-hydraulic simulations of the fuel, referred to as "hot channel calculations." The hot channel simulations provide the bundle transient ΔCPR (the initial bundle CPR minus the MCPR experienced during the transient).

The system level simulations are performed with the one dimensional (1-D) kinetics RETRAN model[22],[23],[24]. The hot channel calculations are performed with the RETRAN[25],[26] and TCPYA01[27],[18],[23] computer codes. The GEXL-Plus correlation [19], contained in TCPYA01, evaluates the transient critical power ratio.

The hot channel transient ΔCPR calculations employ a two-part process, as illustrated by the flow chart in Figure 7.2.1. The first part involves a series of steady-state analyses performed with the FIBWR, RETRAN, and TCPYA01 computer codes. The FIBWR analyses utilize a one-channel model for each fuel type being analyzed, with bypass and water rod flow also modeled. The steady-state FIBWR analyses were performed at several power levels with other conditions (i.e., core pressure drop, system pressure, and core inlet enthalpy) held constant. The FIBWR code results provide a steady-state CPR, active channel flow (AF) and bypass flow (BPF) for each active channel power (AP).

The FIBWR conditions for channel power, channel flow, and bypass flow were then used as input to steady-state RETRAN/TCPYA01 hot channel calculations. Other assumptions are consistent with those in the FIBWR analysis. The Initial Critical Power Ratio (ICPR) is the result of the steady-state RETRAN/TCPYA01 analysis. These results allow for the development of functional relationships, describing AP as a function of ICPR, and AF and BPF as functions of AP for each fuel type. These relationships are used in the iterative process for determining the transient CPR, as shown in Figure 7.2.1.

The second part of the hot channel calculations determines the transient CPR performance. Because the ΔCPR for a given transient varies with Initial Critical Power Ratio (ICPR), the hot channel analysis is an iterative process. The objective of the hot channel iteration for each transient is to determine the hot channel initial conditions which result in reaching the FCISL. Each iteration requires a RETRAN hot channel run to calculate the transient enthalpies, flows, pressure and saturation properties at each time step. These are required for input to the TCPYA01 code. TCPYA01 is then used to calculate a CPR at each time step during the transient, from which a transient ΔCPR is derived.

In response to Reference 11, NRC Safety Evaluation for FROSSTEY-2, the hot channel methodology has considered the assumption of both fixed and time-varying power shapes. The fixed power shape assumes a 1.4 chopped cosine axial distribution which remains constant throughout the transient. The initial power shape for the time-varying power shape methodology is the Haling axial distribution used in the core wide analysis. The time-varying hot channel power distribution is assumed to be the same as that in the core wide analysis to account for the effects of transient power feedbacks and the scram. The transient MCPR limits are defined as the more conservative results from the fixed and varying shape analyses.

7.2.2 Initial Conditions and Assumptions

The initial conditions for the Reload Cycle are based on a reactor power level of 1664 MW_{th} which includes a 4.5% margin on the current licensed reactor power level of 1593 MW_{th}. This margin conservatively bounds the expected 2% calorimetric uncertainty. The reactor core flow is assumed to be 100% of rated. The core axial power distribution for each of the exposure points is based on the 3-dimensional SIMULATE-3 predictions associated with the generation of the reactivity data (Section 7.2.3). The core inlet enthalpy is set so that the amount of carryunder from the steam separators and the quality in the liquid region outside the separators is as close to zero as possible. For fast pressurization transients, this maximizes the initial pressurization rate and results in a more severe neutron power spike. A summary of the initial operating state used for the system simulations is provided in Table 7.2.1.

During the cycle, Vermont Yankee can adjust the core flow to account for reactivity changes rather than using the control rods. During this type of operation, core flow may be as low as 87% while at 100% power. To ensure the safety analysis bounds these conditions, transients are also analyzed at the limiting exposure statepoint at 1664 MW_{th} power and 87% flow. Limiting exposure is defined as the exposure which had the highest ΔCPR.

Assumptions specific to a particular transient are discussed in the section describing the transient. In general, the following assumptions are made for all transients:

1. Scram setpoints are at Technical Specification [12] limits.

2. Protective system logic delays are at equipment specification limits.

3. Safety/relief valve and safety valve capacities are based on Technical Specification rated values.

4. Safety/relief valve and safety valve setpoints are modeled as being at the Technical Specification upper limit. Valve responses are based on slowest specified response values.

5. Control rod drive scram speed is based on the Technical Specification limits. The analysis addresses a dual set of scram speeds, referred to as the "Measured" and the "67B" scram times. "Measured" refers to the faster scram times given in Section 3.3.C.1.1 of the Technical Specifications. "67B" refers to the slower scram times given in Section 3.3.C.1.2 of the Technical Specifications.

7.2.3 One-Dimensional Cross Sections and Kinetics Parameters

The one-dimensional (1-D) cross sections and kinetics parameters are generated as functions of fuel temperature, moderator density, and scram. The method[28] is outlined below.

A complete set of 1-D cross sections, kinetics parameters, and axial power distributions are generated from base states using the Haling depletion established for EOFPL, EOFPL-1000 MWd/St, EOFPL-2000 MWd/St, and BOC exposure statepoints. These statepoints are characterized by exposure and void history distributions, control rod patterns, and core thermal-hydraulic conditions. The latter are consistent with the assumed system transient conditions provided in Table 7.2.1.

The BOC base state is established by shuffling from the previously defined Current Cycle endpoint into the Reload Cycle loading pattern. A criticality search provides an estimate of the BOC critical rod pattern. The EOFPL and intermediate core exposure and void history distributions are calculated with a Haling depletion as described in Section 5.2. The EOFPL state is unrodded. The EOFPL-1000 MWd/St and EOFPL-2000 MWd/St exposure statepoints require base control rod patterns. These are developed to be as "black and white" as possible to minimize the scram reactivity, maximize the core average moderator density reactivity coefficient and, therefore, maximize the transient power response. Beginning with the rodded depletion configuration, all control rods which are more than half inserted are fully inserted, and all control rods which are less than half inserted are fully withdrawn. If the SIMULATE-3 calculated parameters are within operating limits, then this configuration becomes the base case. If the limits are exceeded, a minimum number of control rods are adjusted a minimum number of notches until the parameters fall within limits.

At each exposure statepoint, a SIMULATE-3 initial control state reference case is run. A series of perturbation cases are run with SIMULATE-3 to independently vary the fuel temperature, moderator temperature, and core pressure. All other variables normally associated with the SIMULATE-3 cross sections are held constant at the reference state. To obtain the effect of the control rod scram, another SIMULATE-3 reference case is run with all-rods-in. The perturbation cases described above are run again from this reference case. For each control state, a data set of kinetics parameters and cross sections is generated as a function of the perturbed variable. There is a table set for each of the 27 neutronic regions, 25 regions to represent the active core and one region each for the bottom and top reflectors.

7.2.4 Turbine Trip Without Bypass Transient (TTWOBP)

The transient is initiated by a rapid closure (0.1 second closing time) of the turbine stop valves. It is assumed that the steam bypass valves, which normally open to relieve pressure, remain closed. A reactor protection system signal is generated by the turbine stop valve closure switches. Control rod drive motion is conservatively assumed to occur 0.27 seconds after the start of turbine stop valve motion. The ATWS recirculation pump trip is assumed to occur at a setpoint of 1150 psig dome pressure. A pump trip time delay of 1.0 second is assumed to account for logic delay and M-G set generator field collapse. In simulating the transient, the bypass piping volume up to the valve chest is lumped into the control volume upstream of the turbine stop valves. Predictions of the salient system parameters at the three exposure points are shown in Figures 7.2.2 through 7.2.4 for the "Measured" scram time analysis.

7.2.5 Generator Load Rejection Without Bypass Transient (GLRWOBP)

The transient is initiated by a rapid closure (0.3 seconds closing time) of the turbine control valves. As in the case of the turbine trip transient, the bypass valves are assumed to fail. A reactor protection system signal is generated by the hydraulic fluid pressure switches in the acceleration relay of the turbine control system. Control rod drive motion is conservatively assumed to occur 0.28 seconds after the start of turbine control valve motion. The same modeling regarding the ATWS pump trip and bypass piping is used as in the turbine trip simulation. The influence of the accelerating main turbine generator on the recirculation system is simulated by specifying the main turbine generator electrical frequency as a function of time for the M-G set drive motors. The main turbine generator frequency curve is based on a 100% power plant startup test and is considered representative for the simulation. The system model predictions for the three exposure points are shown in Figures 7.2.5 through 7.2.7 for the "Measured" scram time analysis.

7.2.6 Pressurization Transient Analysis Results

The transients selected for consideration were analyzed at exposure points of EOFPL, EOFPL-1000 MWd/St, and EOFPL-2000 MWd/St. The transient results, reported in Table 7.2.2, correspond to the limiting bundle type in the core. The MCPR limits, in Table 7.2.2, are calculated by

adding the calculated ΔCPR to the FCISL. The worst ΔCPR for the pressurization transients include an adjustment to allow for the exposure window of ±600 MWd/St on Current Cycle and the exposure uncertainty on the Reload Cycle[7].

7.3 Loss of Feedwater Heating Transient Analysis

7.3.1 Loss of a Feedwater Heater (LOFWH) Results

A feedwater heater can be lost in such a way that the steam extraction line to the heater is shut off or the feedwater flow bypasses one of the heaters. In either case, the reactor will receive cooler feedwater, which will produce an increase in the core inlet subcooling, resulting in a reactor power increase.

The response of the system due to the loss of 100°F of the feedwater heating capability was analyzed. This represents the maximum expected feedwater temperature reduction for a single heater or group of heaters that can be tripped or bypassed by a single event. The system model used is the same as that used for the pressurization transient analyses (Section 7.2.1). The initial conditions and modeling assumptions discussed in Section 7.2.2 are applicable to this simulation.

Vermont Yankee has a scram setpoint of 120% of rated power as part of the Reactor Protection System (RPS) on high neutron flux. In this analysis, no credit was taken for scram on high neutron flux, thereby allowing the reactor power to reach its peak without scram. This approach was selected to provide a bounding and conservative analysis for events initiated from any power level.

The transient response of the system was evaluated at several exposures during the cycle, EOFPL-1000 MWd/St, EOFPL-2000 MWd/St, and BOC. The transient results, corresponding to the limiting bundle type in the core, are listed in Table 7.3.1. The MCPR limits in Table 7.3.1 are calculated by adding the calculated ΔCPR to the FCISL. The transient evaluation at EOFPL-1000 MWd/st was found to be the limiting case between BOC to EOFPL-1000 MWd/St. The results of the system response to a loss of 100°F feedwater heating capability evaluated at EOFPL-1000 MWd/St as predicted by the RETRAN code are presented in Figure 7.3.1.

7.3.2 Loss of Stator Cooling (LOSC) Results

In response to a loss of stator cooling, a turbine runback is initiated to reduce generator output to less than 29% of rated output. This runback is accomplished by bypassing main steam from the turbine directly to the main condenser. Since heating steam to the feedwater heaters is supplied from the turbine stages, the amount of steam available for feedwater heating is significantly reduced. The reduction of heating steam to the feedwater heaters results in a severe subcooling event.

For the analysis, the loss of stator cooling event is initiated at, or near, rated thermal power (maximum 104.5%). It is assumed that an instantaneous loss of extraction steam occurs to the Nos. 1-4 feedwater heaters of both feedwater trains. This is a conservative assumption, since there would not be a total loss of steam to the feedwater heaters, and the reduction in heating steam would occur over the several minutes required for the turbine runback. Also, no credit is taken for the heat capacity of structural materials in the process piping or feedwater heaters. This results in a stepwise decrease in feedwater inlet temperature as the feedwater travels through the feedwater piping to the reactor vessel.

The decrease in feedwater temperature results in a subsequent reduction in core inlet temperature. Due to the negative void coefficient, core thermal power increases. The transient is terminated by APRM high flux trip at 120% of rated core thermal power.

The transient response of the system was evaluated at several exposures during the cycle, EOFPL-1000 MWd/St, EOFPL-2000 MWd/St, and BOC. The transient results, corresponding to the limiting bundle type in the core, are listed in Table 7.3.2. The MCPR limits in Table 7.3.2 are calculated by adding the calculated ΔCPR to the FCISL. The transient evaluation at BOC was found to be limiting case between BOC and EOFPL-1000 MWd/St. The results of the system response to a loss of stator cooling evaluated at BOC as predicted by the RETRAN code are presented in Figure 7.3.2. To assure that the thermal overpower limits are not exceeded, the MAPLHGR limits in Appendix A were modified according to Reference 41.

7.4 Overpressurization Analysis Results

Compliance with ASME vessel code limits is demonstrated by an analysis of the Main Steam Isolation Valves (MSIV) closing with failure of the MSIV position switch scram. EOFPL conditions were analyzed. The system model used is the same as that used for the transient analysis (Section 7.2.1). The initial conditions and modeling assumptions discussed in Section 7.2.2 are applicable to this simulation.

The transient is initiated by a simultaneous closure of all MSIVs. A 3.0 second closing time, which is the minimum time in Technical Specification Table 4.7.2, is assumed. A reactor scram signal is generated on APRM high flux. Control rod drive motion is conservatively assumed to initiate 0.28 seconds after reaching the high flux setpoint. The system response is shown in Figure 7.4.1 for the "Measured" scram time analysis.

The maximum pressures at the bottom of the reactor vessel calculated for the "Measured" scram time analysis and for the "67B" scram time analysis are given in Table 7.4.1. These results are within the ASME code overpressure design limit which is 110% of the vessel design pressure. Vermont Yankee's design pressure is 1250 psig so the maximum pressure limit is 1375 psig.

7.5 Local Rod Withdrawal Error Transient Results

The rod withdrawal error (RWE) is a local core transient caused by an operator erroneously withdrawing a control rod in the continuous withdrawal mode. If the core is operating at its operating limits for MCPR at the time of the error, then withdrawal of a control rod could increase both local and core power levels with the potential for overheating the fuel.

There is a broad spectrum of core conditions and control rod patterns which could be present at the time of such an error. For most normal situations it would be possible to fully withdraw a control rod without violating the FCISL.

The MCPR operating limit for the RWE is defined at each Rod Block Monitor (RBM) System setpoint so that the FCISL is not violated. The consequences of the error depend on the local power

increase, the initial MCPR of the neighboring locations and the ability of the RBM to stop the withdrawing rod before MCPR reaches the FCISL.

The most severe transient postulated begins with the core operating according to normal procedures and within normal operating limits. The operator makes a procedural error and attempts to fully withdraw the maximum worth control rod at maximum withdrawal speed. The core limiting locations are close to the error rod. They experience the spatial power shape transient as well as the overall core power increase.

The core conditions and control rod pattern are conservatively modeled for the licensing bounding case by specifying the following set of concurrent worst case assumptions:

1. The rod should have high reactivity worth. The worst rod is identified by running the full RWE analysis for the control rods as found in the normal control rod patterns of the rodded depletion. Every control rod sequence is checked. From this examination, the control rods that result in the highest worth and highest ΔCPR are identified. Licensing test case rod patterns are then developed to further exaggerate the worth and ΔCPR impact of the rod to be withdrawn.

   The test patterns are developed with xenon-free conditions. The xenon-free condition and the additional control rod inventory needed to maintain criticality exaggerates the worth of the withdrawn control rod when compared to normal operation with normal xenon levels.

2. The core is modeled at 104.5% power and 100% flow.

3. The core power distribution is adjusted with the available control rods to place the locations within the four by four array of bundles around the error rod as close to the operating limits as possible.

4. Of the many patterns tested, the pattern with the most limiting ΔCPR results is selected as the bounding case.

The RBM System's ability to terminate the bounding case is evaluated on the following bases:

1. Technical Specifications allow each of the separate RBM channels to remain operable if at least half of the Local Power Range Monitor (LPRM) inputs on each level are operable. For the interior locations tested in this analysis, there are a maximum of four LPRM inputs per level. One RBM channel averages the inputs from the A and C levels; the other channel averages the inputs from the B and D levels. Considering the inputs for a single channel, there are eleven failure combinations of none, one and two failed LPRM strings. The RBM channel responses are evaluated separately at these eleven input failure conditions. Then, for each channel taken separately, the lowest response as a function of error rod position is chosen for comparison to the RBM setpoint.

2. The event is analyzed separately in each of the four quadrants of the core due to the differing LPRM string physical locations relative to the error rod.

Technical Specifications require that both RBM channels be operable during normal operation. Thus, the first channel calculated to intercept the RBM setpoint is assumed to stop the rod. To allow for control system delay times, the rod is assumed to move two inches after the intercept and stop at the following notch.

The analysis is performed using SIMULATE-3. The two separate cases presented here are selected from numerous explicit SIMULATE-3 analyses. Case 1 analyzes the bounding event with zero xenon, initiated from 104.5% power and 100% flow. This case also assumes the worst case abnormal rod pattern configuration which results in the initial MCPR being as low as possible. Case 2 is the worst of all the rod withdrawal transients analyzed from 100% power, 100% flow, equilibrium xenon, and normal rod patterns used in the rodded depletion. The worst transient ΔCPR results for both cases are shown in Table 7.5.1. The ΔCPR values are evaluated such that the implied MCPR operating limit equals FCISL + ΔCPR. This is done by conserving the figure of merit (ΔCPR/ICPR) shown by the SIMULATE-3 calculations. The transient ΔCPR results for Case 1 will be used to set the operating MCPR limits. Case 2 results are bounded by the Case 1 results by at least 0.02 ΔCPR margin to assure that the exposure uncertainties on the Current Cycle and the Reload Cycle are

accounted for. This method also provides valid operating MCPR values that bound expected operating conditions.

The Case 1 (bounding event) RBM channel responses are shown in Figures 7.5.1 and 7.5.2. They also show the control rod position at the point where the RBM channel response first intercepts the RBM setpoint.

7.6 Misloaded Bundle Error Analysis Results

7.6.1 Rotated Bundle Error

The primary result of a bundle rotation is a large increase in local pin peaking and the associated R-factor as higher enrichment pins are placed adjacent to the surrounding wide water gaps. In addition, there may be a small increase in reactivity, depending on the exposure and void fraction states. The R-factor increase results in a CPR reduction. The objective of the analysis is to ensure that, in the worst possible rotation, the FCISL is not violated with the most limiting bundles on their operating limits.

To analyze the CPR response, rotated bundle R-factors as a function of exposure are developed by adding the largest possible ΔR-factor resulting from a rotation to the exposure dependent R-factors of the properly oriented bundles. Using these rotated bundle R-factors, the MCPR values resulting from a bundle rotation are determined using SIMULATE-3. This is done for each control rod sequence throughout the cycle. The process is repeated with the K-infinity of the limiting bundle modified slightly to account for the increase in reactivity resulting from the rotation. For each sequence, the MCPR for the properly oriented bundles is adjusted by a ratio necessary to place the corresponding rotated bundle's CPR on its FCISL. The adjusted MCPRs at each exposure is the rotated bundle operating limit for the rotated bundle error.

Because the BP8DWB335 fuel designs exhibit a significant increase in R-factor with rotation early in exposure, the impact upon the rotated bundle ΔCPR is high at BOC. This effect soon drops off with exposure. Therefore, the operating MCPR limit resulting from a rotation is presented in Table 7.6.1 versus cycle exposure.

7.6.2 Mislocated Bundle Error

Mislocating a high reactivity assembly into a region of high neutron importance results in a location of high relative assembly average power. Since the assembly is assumed to be properly oriented (not rotated), R-factors used for the mislocated bundle are the standard values for the given fuel type.

The analysis uses multiple SIMULATE-3 cases to examine the effects of explicitly mislocating every older interior assembly in a quarter core with a fresh or once-burned assembly. Because of symmetry, the results apply to the whole core. Edge bundles are not examined because they are never limiting, due to neutron leakage.

The effect of the successive mislocations is examined for every control rod sequence throughout the cycle. For each sequence, the MCPR for the properly loaded core is compared to the MCPR of the misloaded core at the misloaded location. The MCPR for the properly loaded core is adjusted by a ratio necessary to place the mislocated assembly on the FCISL. The maximum of these adjusted MCPRs is the mislocated bundle operating limit. The results of the mislocated bundle analysis are given in Table 7.6.2.

7.7 Transient Analysis Results

The results of this transient analysis has: 1) determined the MCPR operating limit so that the FCISL is not violated for the transients considered, 2) assured that the thermal and mechanical overpower limits are not exceeded during the transient, and 3) demonstrated compliance with the ASME vessel code limits.

The MCPR operating limits for the Reload Cycle are calculated by adding the calculated ΔCPR to the FCISL at each of the exposure statepoints for each transient. Table 7.7.1 lists the limiting transient for each statepoint. For an exposure interval between statepoints, the highest MCPR limit at either end is assumed to apply to the whole interval. The highest calculated MCPR limits for the Reload Cycle for each of the exposure intervals for the various scram speeds and for the various rod block lines are provided in Appendix A. These MCPR operating limits are valid for operation of

the Reload Cycle at full power up to 10644 MWd/St and for operation during coastdown beyond EOFPL.

TABLE 7.2.1

VY CYCLE 18 SUMMARY OF SYSTEM TRANSIENT MODEL
INITIAL CONDITIONS FOR TRANSIENT ANALYSES

Core Thermal Power (MW_{th})	1664.0
Turbine Steam Flow ($10^6 lb_m/hr$)	6.75
Total Core Flow ($10^6 lb_m/hr$)	48.0
Core Bypass Flow ($10^6 lb_m/hr$)*	6.28
Core Inlet Enthalpy (BTU/lb_m)	523.2
Steam Dome Pressure (psia)	1034.7
Turbine Inlet Pressure (psia)	985.7
Total Recirculation Drive Flow ($10^6 lb_m/hr$)	23.7
Core Plate Differential Pressure (psi)	20.4
Narrow Range Water Level (in.)	162.0
Average Fuel Gap Conductance	(See Section 4.2)

* Includes water rod flow.

TABLE 7.2.2

VY CYCLE 18 PRESSURIZATION TRANSIENT ANALYSIS RESULTS

Transient	Exposure Statepoint	Peak Prompt Power (Fraction of Initial Value)	Peak Average Heat Flux (Fraction of Initial Value)	ΔCPR*	Transient MCPR Limits
Turbine Trip Without Bypass, "Measured" Scram Time	EOFPL	2.80378	1.19541	0.25	1.32
	EOFPL-1000	2.24381	1.14296	0.20	1.27
	EOFPL-2000	1.25154	1.00000	0.04	1.11
Turbine Trip Without Bypass, "67B" Scram Time	EOFPL	3.12172	1.23971	0.27	1.34
	EOFPL-1000	2.63805	1.19536	0.23	1.30
	EOFPL-2000	1.64655	1.04145	0.08	1.15
Generator Load Rejection Without Bypass, "Measured" Scram Time	EOFPL	2.81519	1.17663	0.23	1.30
	EOFPL-1000	2.34636	1.12670	0.19	1.26
	EOFPL-2000	1.13637	1.00000	0.02	1.09
Generator Load Rejection Without Bypass, "67B" Scram Time	EOFPL	3.30268	1.23750	0.27	1.34
	EOFPL-1000	2.92611	1.19323	0.23	1.30
	EOFPL-2000	1.60336	1.01760	0.05	1.12

* The worst ΔCPR for TTWOBP and GLRWOBP includes a 0.01 ΔCPR adjustment to allow for the exposure window of ±600 MWd/St on Current Cycle and the exposure uncertainty on the Reload Cycle.

TABLE 7.3.1

VY CYCLE 18 LOSS OF FEEDWATER HEATER TRANSIENT RESULTS

Transient	Exposure Statepoint	Peak Prompt Power (Fraction of Initial Value)	Peak Average Heat Flux (Fraction of Initial Value)	ΔCPR	Transient MCPR Limits
Loss of 100°F Feedwater Heating	EOFPL-1000	1.24680	1.15373	0.12	1.19
	EOFPL-2000	1.14354	1.14440	0.11	1.18
	BOC	1.17041	1.14530	0.11	1.18

TABLE 7.3.2

VY CYCLE 18 LOSS OF STATOR COOLING TRANSIENT RESULTS

Transient	Exposure Statepoint	Peak Prompt Power (Fraction of Initial Value)	Peak Average Heat Flux (Fraction of Initial Value)	ΔCPR	Transient MCPR Limits
Loss of Stator Cooling	EOFPL-1000	1.23165	1.12990	0.11	1.18
	EOFPL-2000	1.19910	1.18716	0.13	1.20
	BOC	1.19806	1.18498	0.13	1.20

TABLE 7.4.1

VY CYCLE 18 OVERPRESSURIZATION ANALYSIS RESULTS

Conditions	Maximum Pressure at Reactor Vessel Bottom (psig)
"Measured" Scram Time	1251
"67B" Scram Time	1278

TABLE 7.5.1

VY CYCLE 18 ROD WITHDRAWAL ERROR ANALYSIS RESULTS

Rod Block Monitor Setpoint	Bounding Case ΔCPR	Worst Normal ΔCPR	Transient MCPR Limits
104	0.15	0.13	1.22
105	0.16	0.14	1.23
106	0.16	0.14	1.23
107	0.20	0.18	1.27
108	0.26	0.18	1.33

TABLE 7.6.1

VY CYCLE 18 ROTATED BUNDLE ANALYSIS RESULTS

Exposure (GWd/St)	Transient MCPR Limit
0.0	1.39
4.0	1.35
5.5	1.29
6.5	1.25
10.0	1.25

TABLE 7.6.2

VY CYCLE 18 MISLOCATED BUNDLE ANALYSIS RESULTS

Transient MCPR Limit
1.15

TABLE 7.7.1

VY CYCLE 18 LIMITING TRANSIENTS

Rod Block Monitor Setpoint	Scram Time	Exposure (GWd/St)	Limiting Transient	Transient MCPR Limit
108	Measured	0.0	Rotated Bundle	1.39
		4.0	Rotated Bundle	1.35
		5.5*	Rod Withdrawal Error	1.33
108	"67B"	0.0	Rotated Bundle	1.39
		4.0	Rotated Bundle	1.35
		5.5	Rod Withdrawal Error	1.33
		9.035*	Turbine Trip	1.34
107	Measured	0.0	Rotated Bundle	1.39
		4.0	Rotated Bundle	1.35
		5.5	Rotated Bundle	1.29
		6.5	Rod Withdrawal Error	1.27
		9.035*	Turbine Trip	1.32
107	"67B"	0.0	Rotated Bundle	1.39
		4.0	Rotated Bundle	1.35
		5.5	Rotated Bundle	1.29
		6.5	Rod Withdrawal Error	1.27
		8.035	Turbine Trip	1.30
		9.035*	Turbine Trip	1.34
106	Measured	0.0	Rotated Bundle	1.39
		4.0	Rotated Bundle	1.35
		5.5	Rotated Bundle	1.29
		6.5	Rotated Bundle	1.25
		8.035	Turbine Trip	1.27
		9.035*	Turbine Trip	1.32
106	"67B"	0.0	Rotated Bundle	1.39
		4.0	Rotated Bundle	1.35
		5.5	Rotated Bundle	1.29
		6.5	Rotated Bundle	1.25
		8.035	Turbine Trip	1.30
		9.035*	Turbine Trip	1.34

* Transient MCPR is limiting from this exposure to EOFPL.

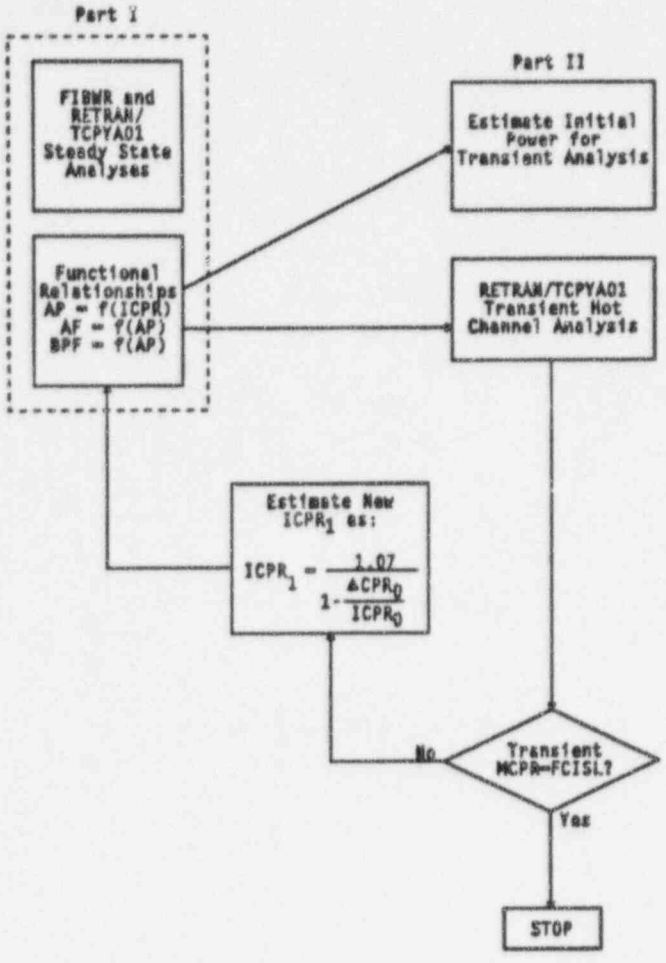

FIGURE 7.2.1

FLOW CHART FOR THE CALCULATION OF ΔCPR USING THE RETRAN/TCPYA01 CODES

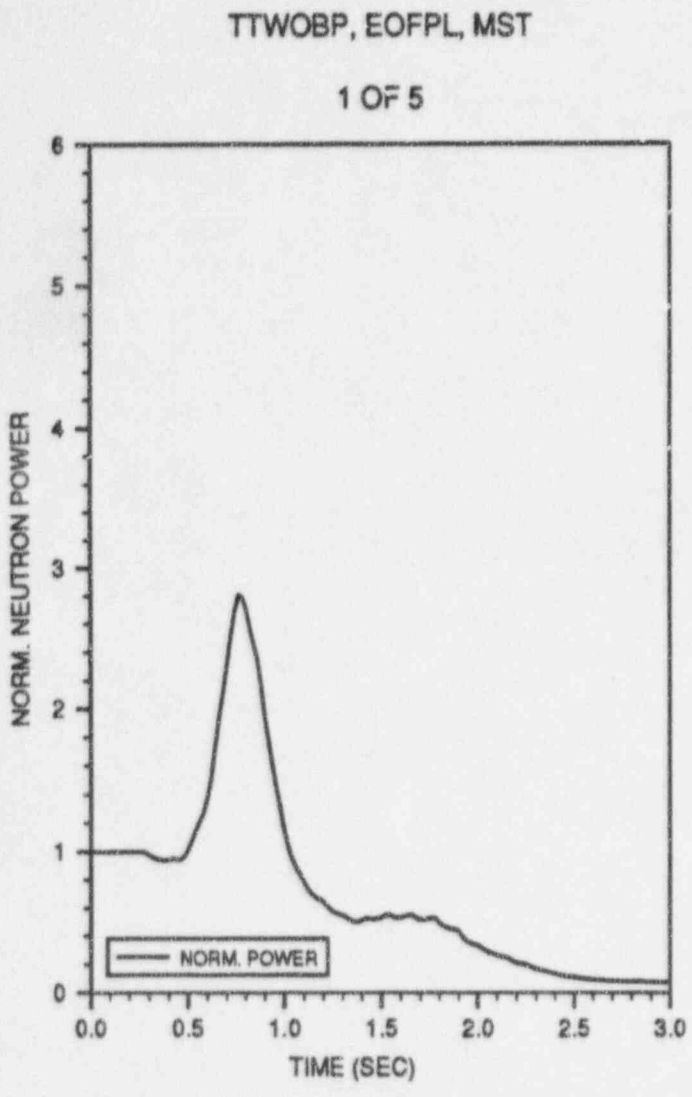

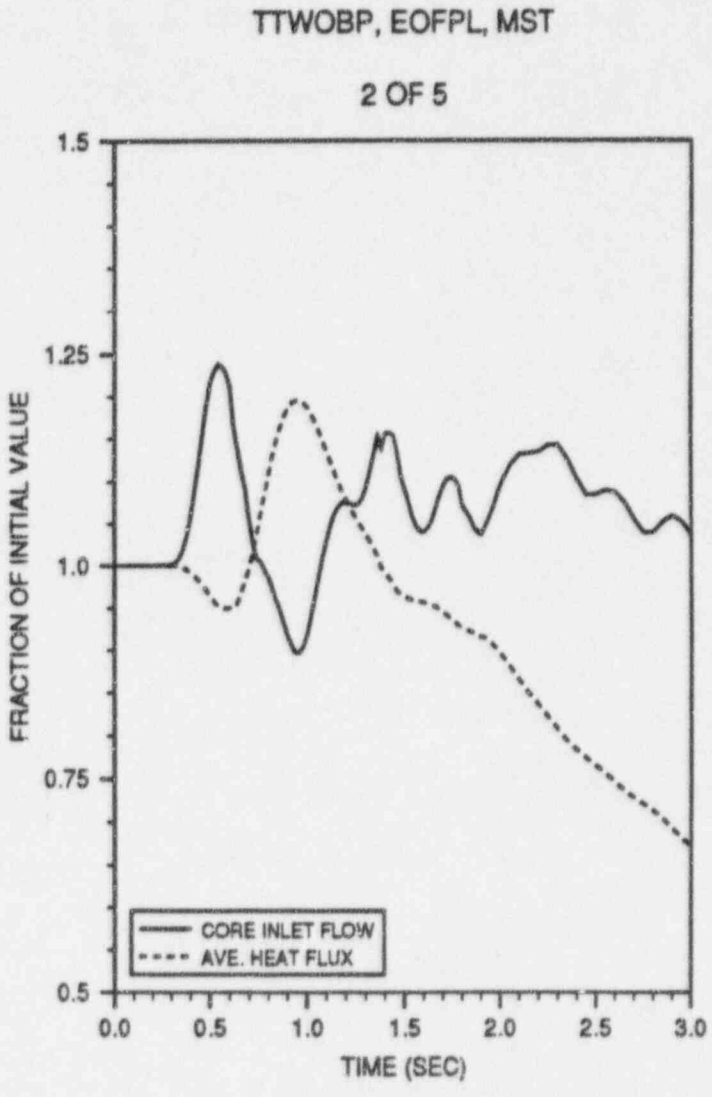

FIGURE 7.2.2

TURBINE TRIP WITHOUT BYPASS, EOFPL18
TRANSIENT RESPONSE VERSUS TIME, "MEASURED" SCRAM TIME

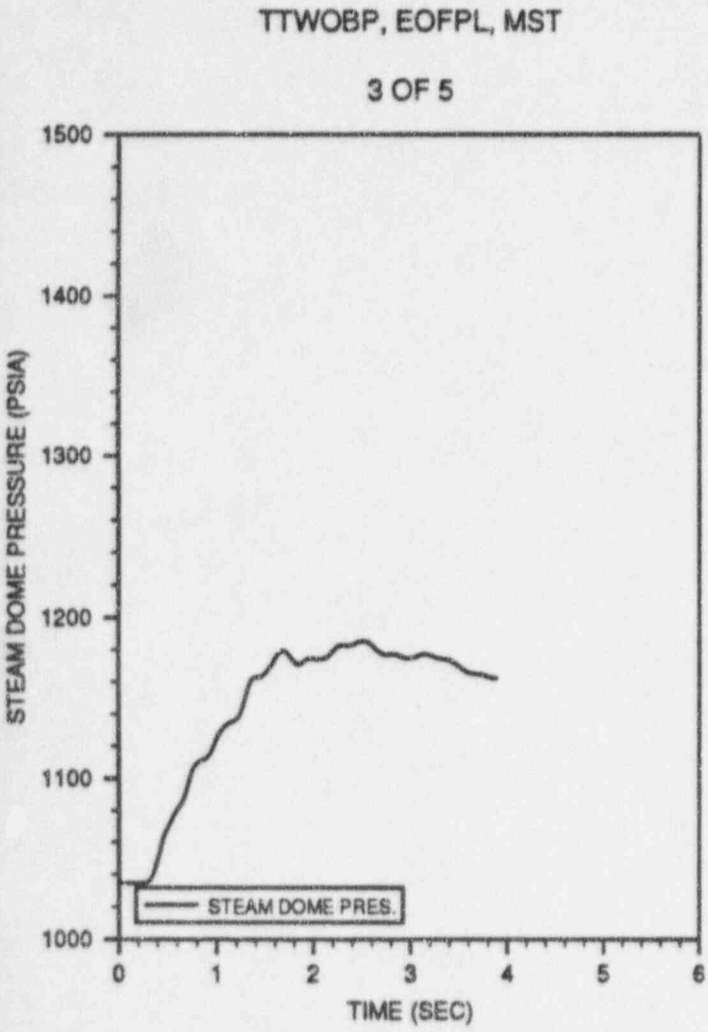

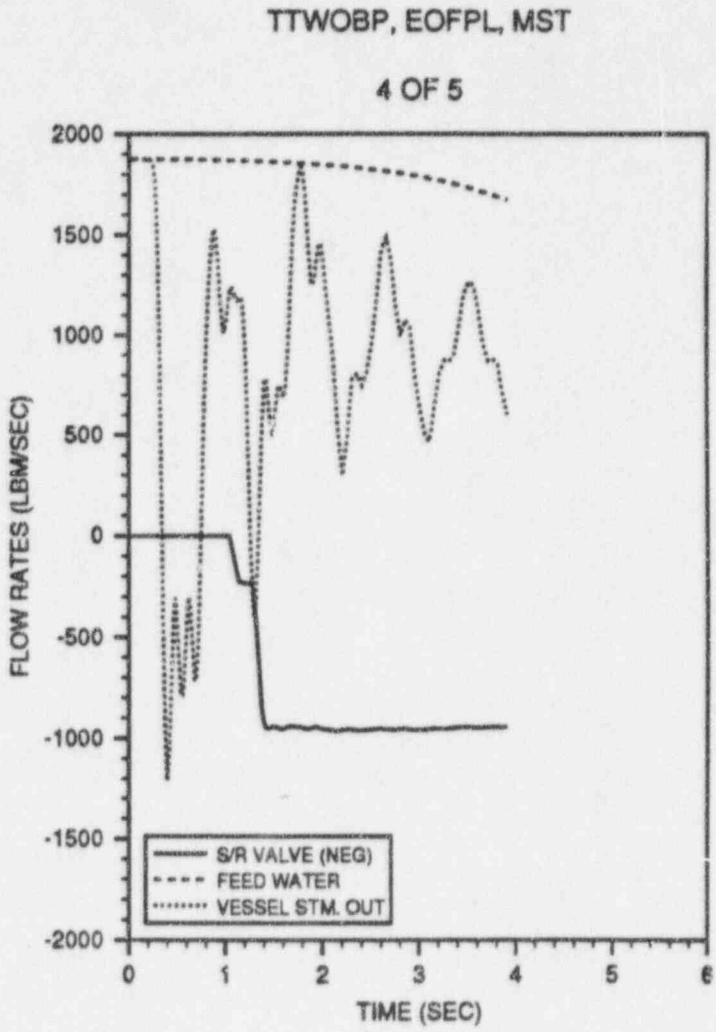

FIGURE 7.2.2
(Continued)

TURBINE TRIP WITHOUT BYPASS, EOFPL18
TRANSIENT RESPONSE VERSUS TIME, "MEASURED" SCRAM TIME

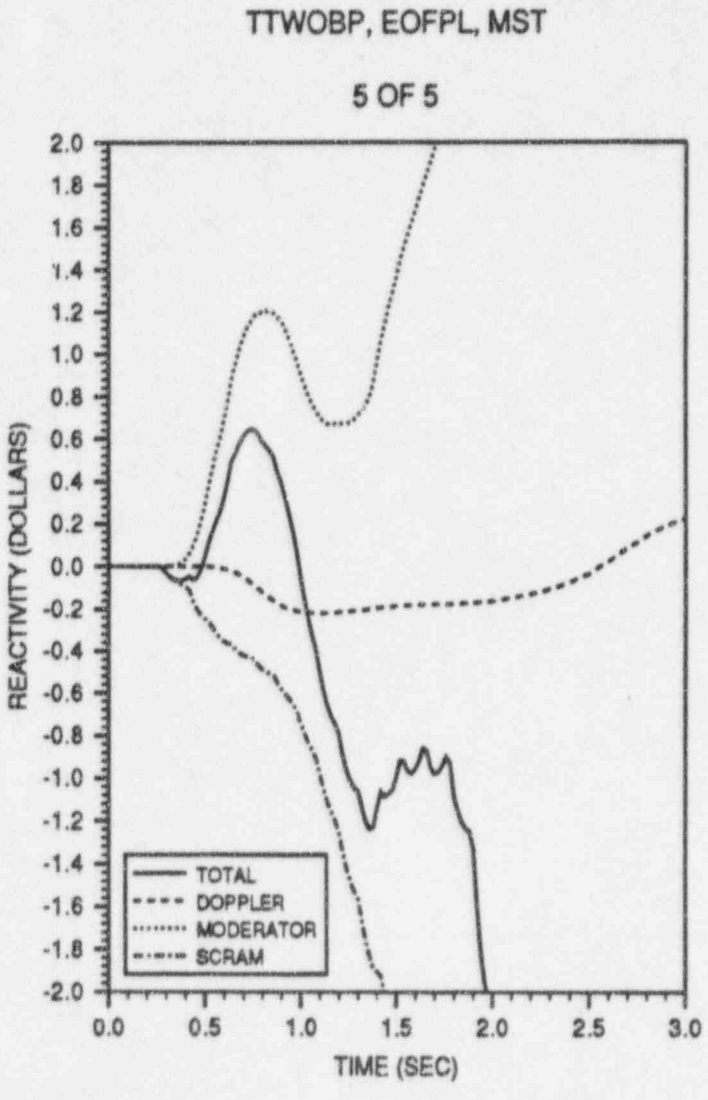

FIGURE 7.2.2
(Continued)

TURBINE TRIP WITHOUT BYPASS, EOFPL18
TRANSIENT RESPONSE VERSUS TIME, "MEASURED" SCRAM TIME

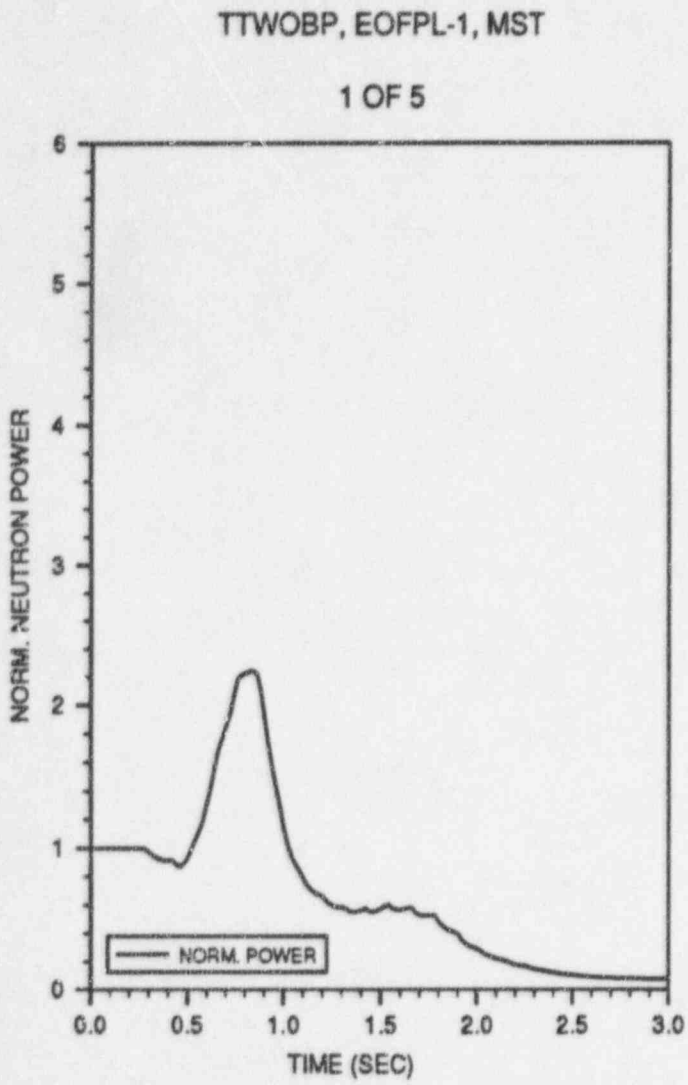

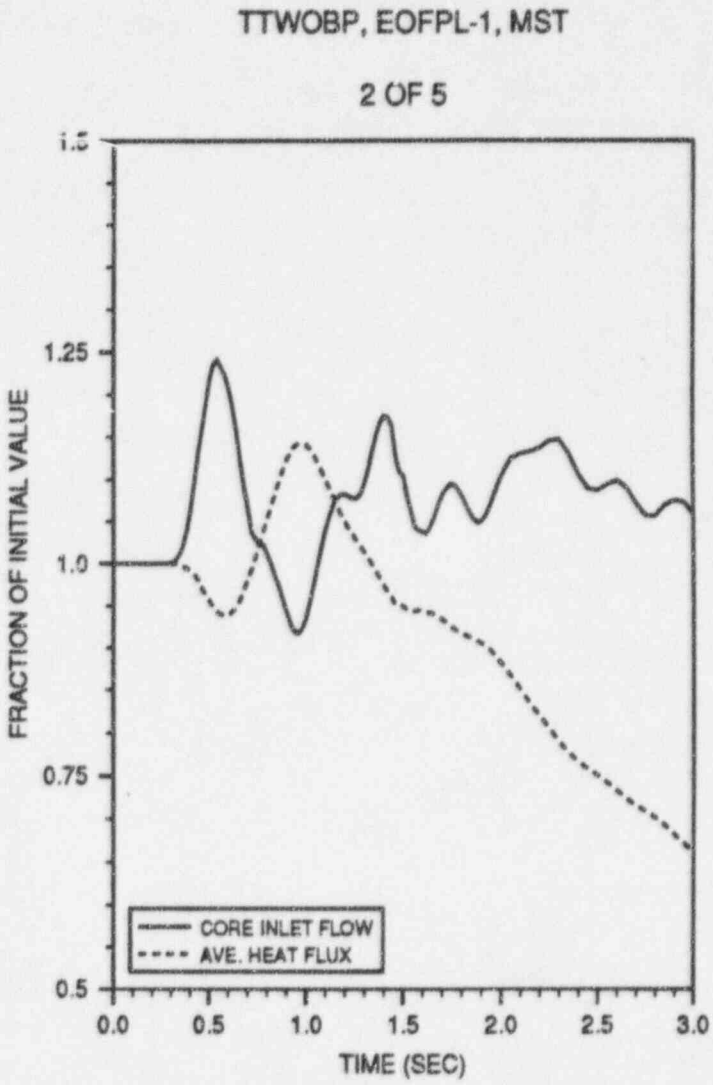

FIGURE 7.2.3

TURBINE TRIP WITHOUT BYPASS, EOFPL18-1000 MWD/ST
TRANSIENT RESPONSE VERSUS TIME, "MEASURED" SCRAM TIME

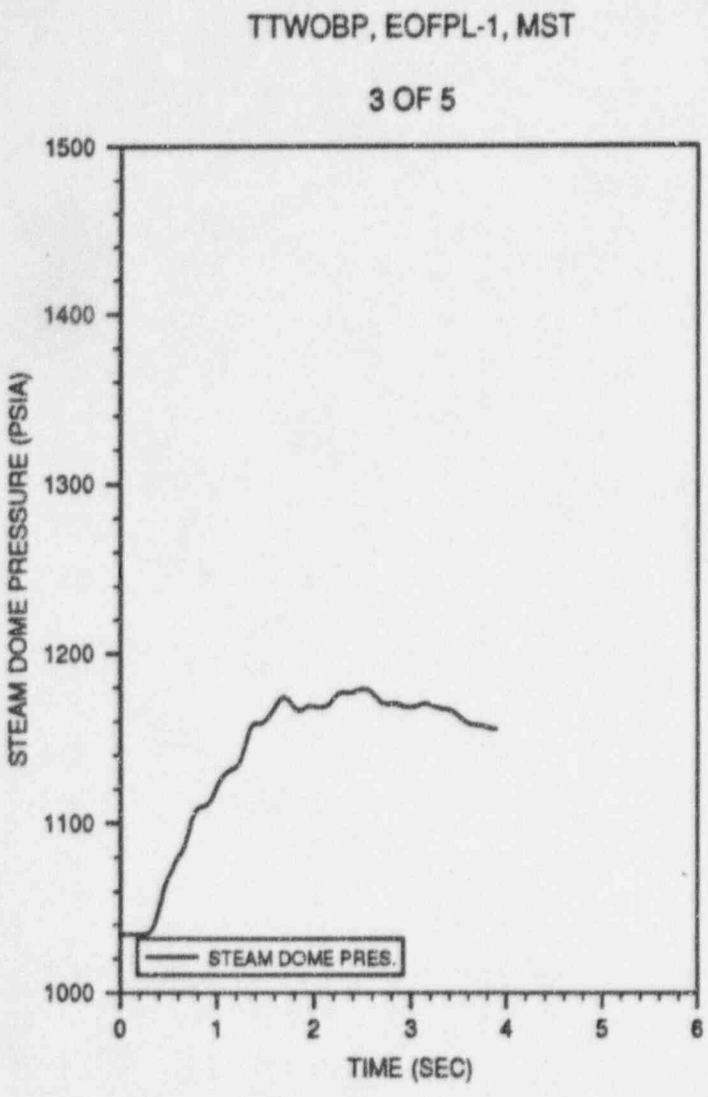

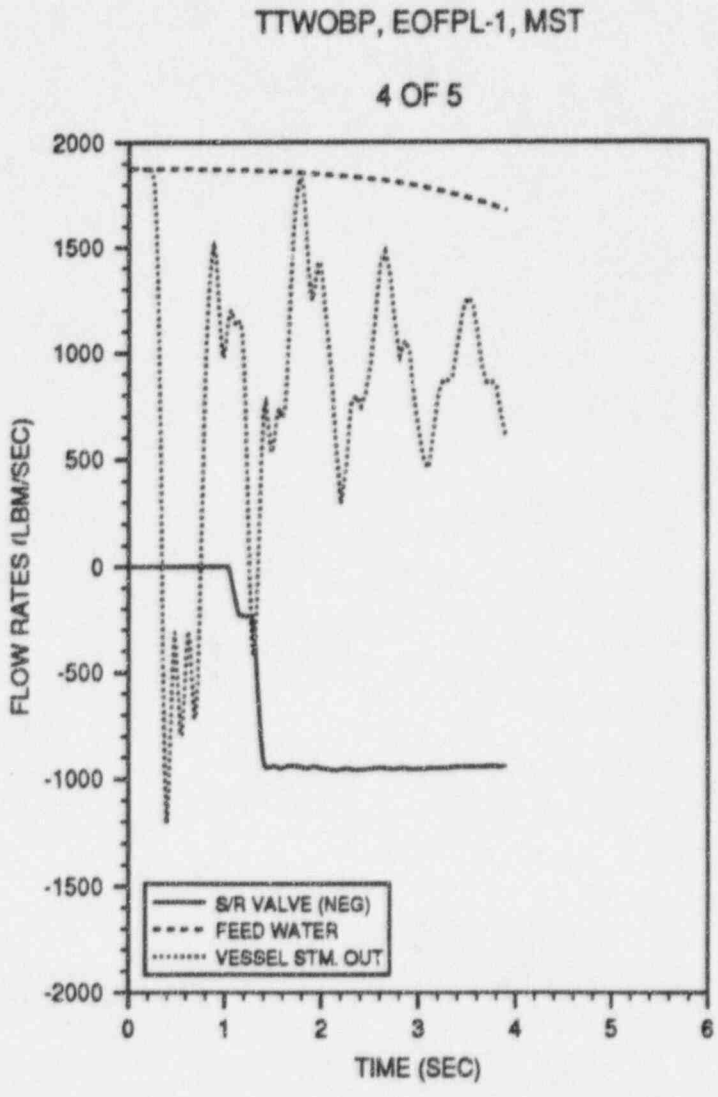

FIGURE 7.2.3
(Continued)

TURBINE TRIP WITHOUT BYPASS, EOFPL18-1000 MWD/ST
TRANSIENT RESPONSE VERSUS TIME, "MEASURED" SCRAM TIME

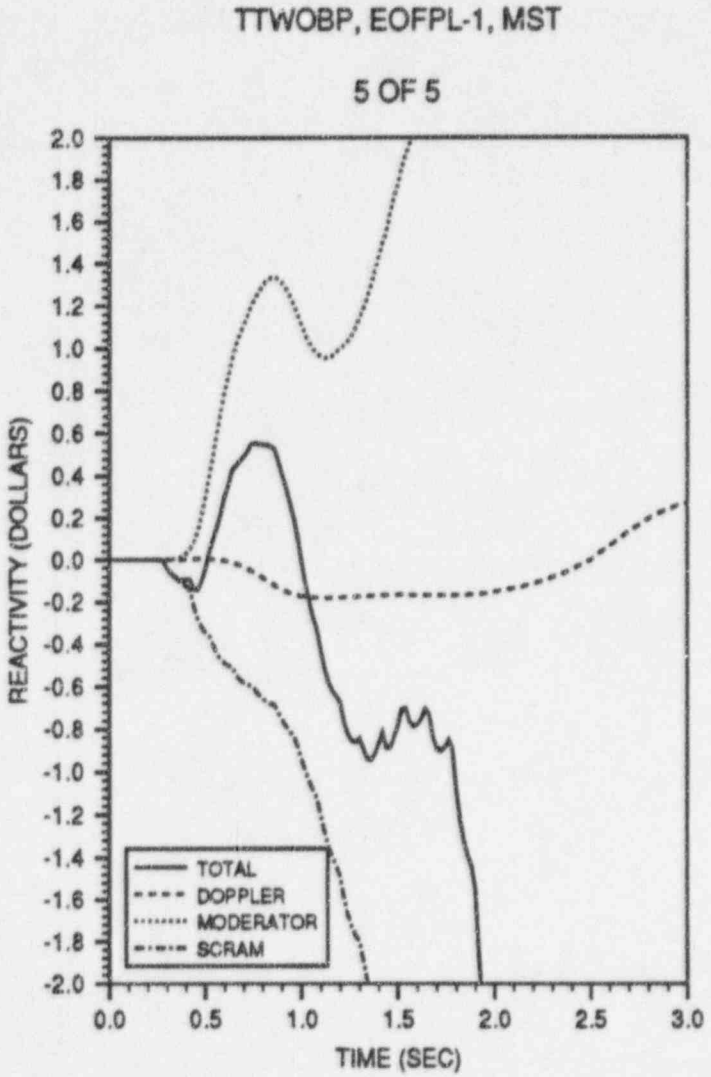

FIGURE 7.2.3
(Continued)

TURBINE TRIP WITHOUT BYPASS, EOFPL18-1000 MWD/ST
TRANSIENT RESPONSE VERSUS TIME, "MEASURED" SCRAM TIME

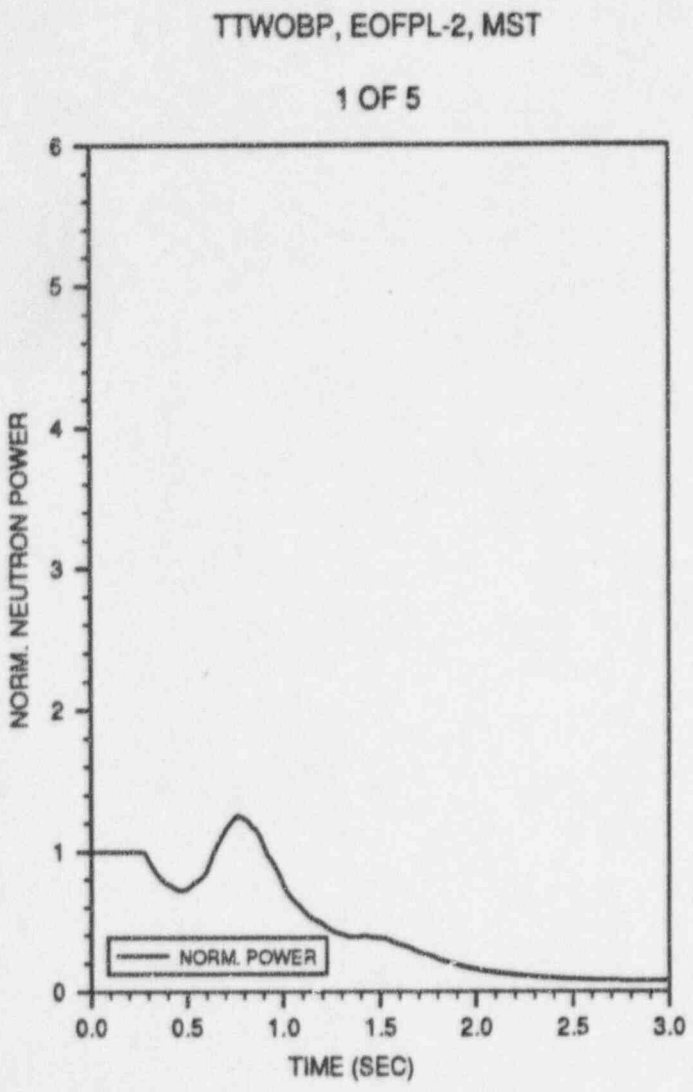

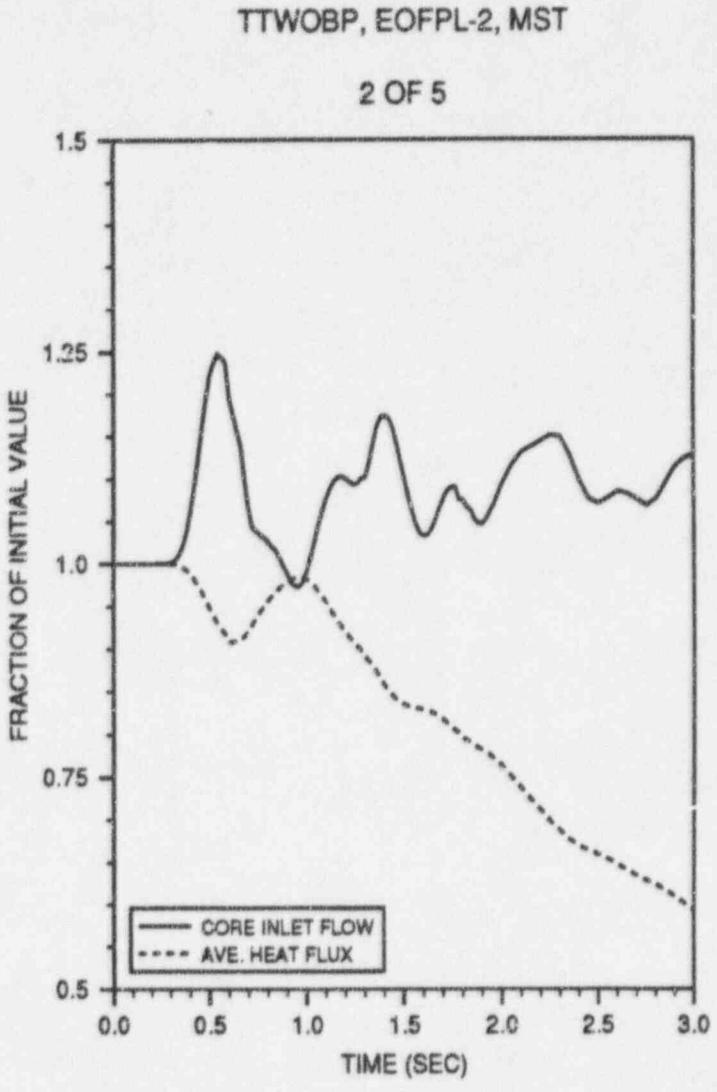

FIGURE 7.2.4

TURBINE TRIP WITHOUT BYPASS, EOFPL18-2000 MWD/ST
TRANSIENT RESPONSE VERSUS TIME, "MEASURED" SCRAM TIME

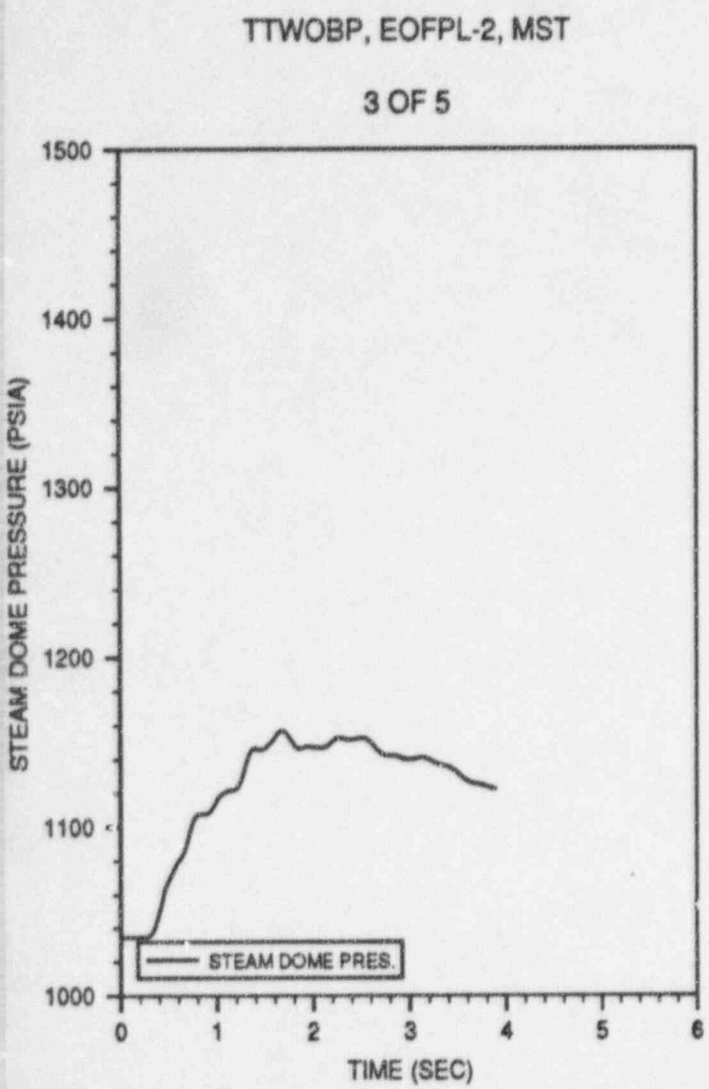

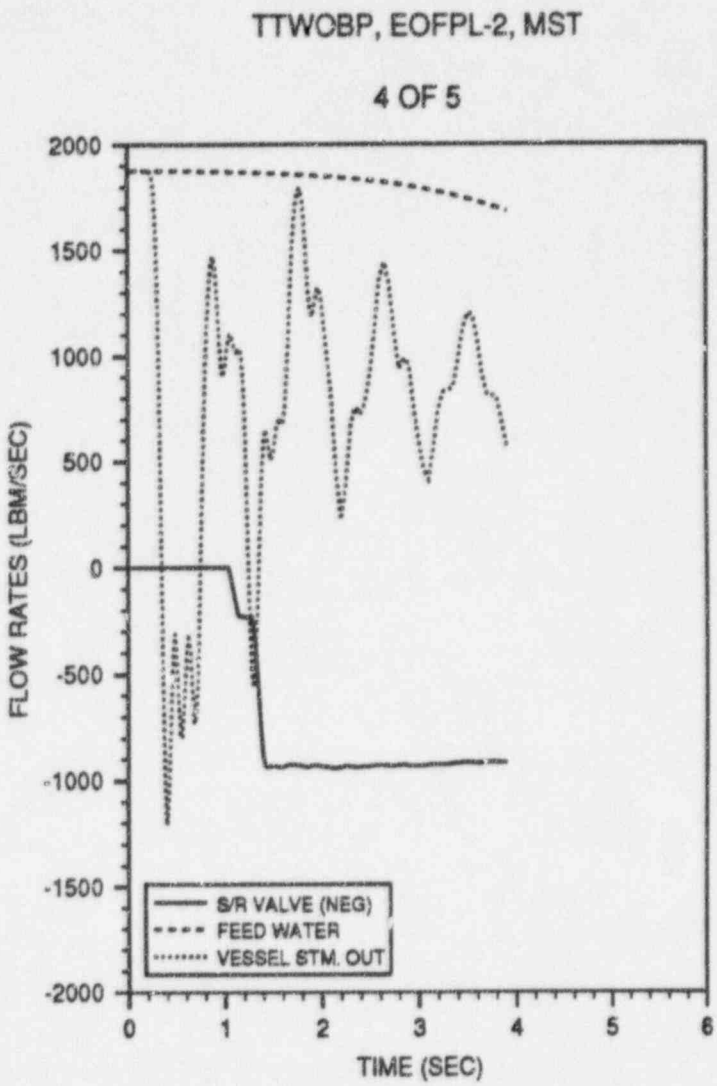

FIGURE 7.2.4
(Continued)

TURBINE TRIP WITHOUT BYPASS, EOFPL18-2000 MWD/ST
TRANSIENT RESPONSE VERSUS TIME, "MEASURED" SCRAM TIME

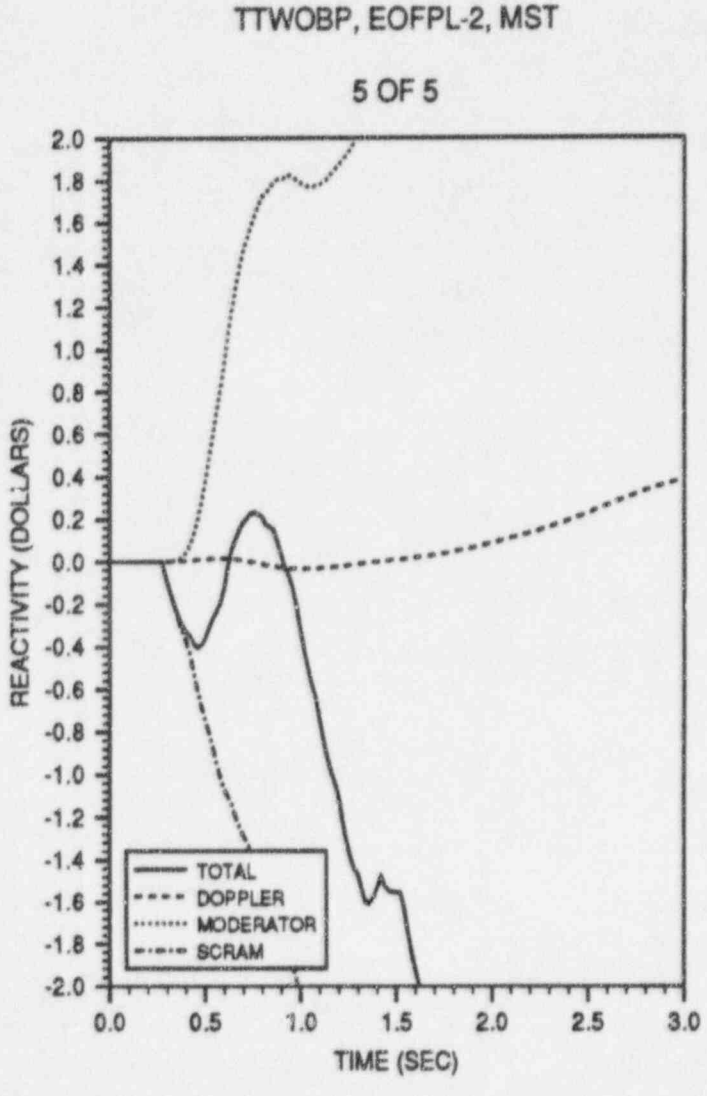

FIGURE 7.2.4
(Continued)

TURBINE TRIP WITHOUT BYPASS, EOFPL18-2000 MWD/ST
TRANSIENT RESPONSE VERSUS TIME, "MEASURED" SCRAM TIME

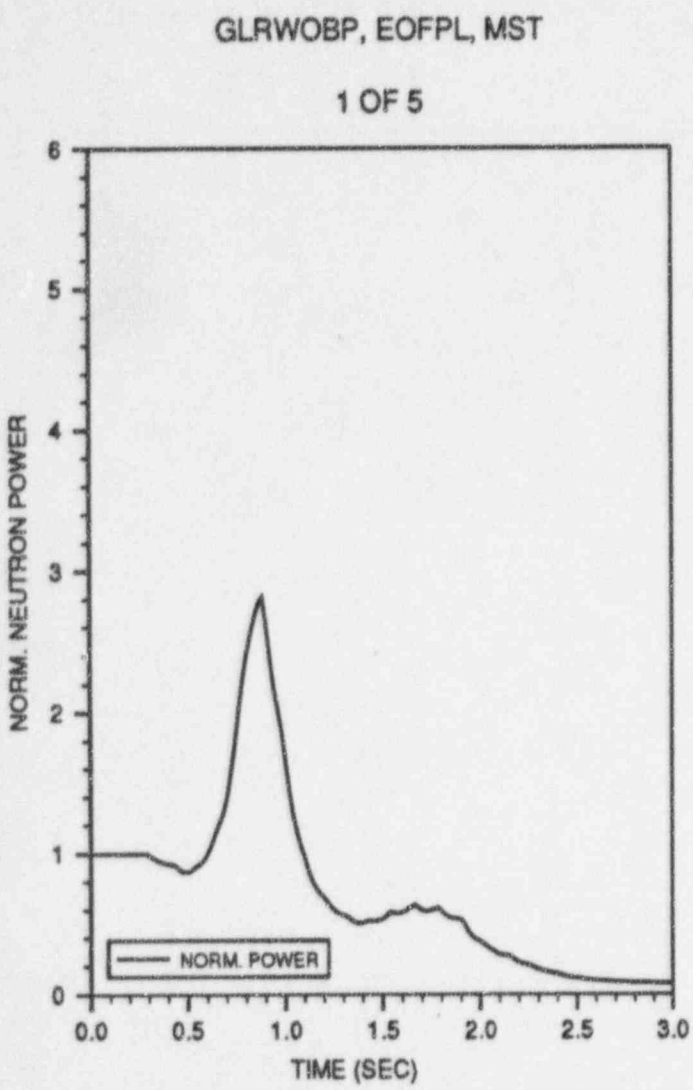

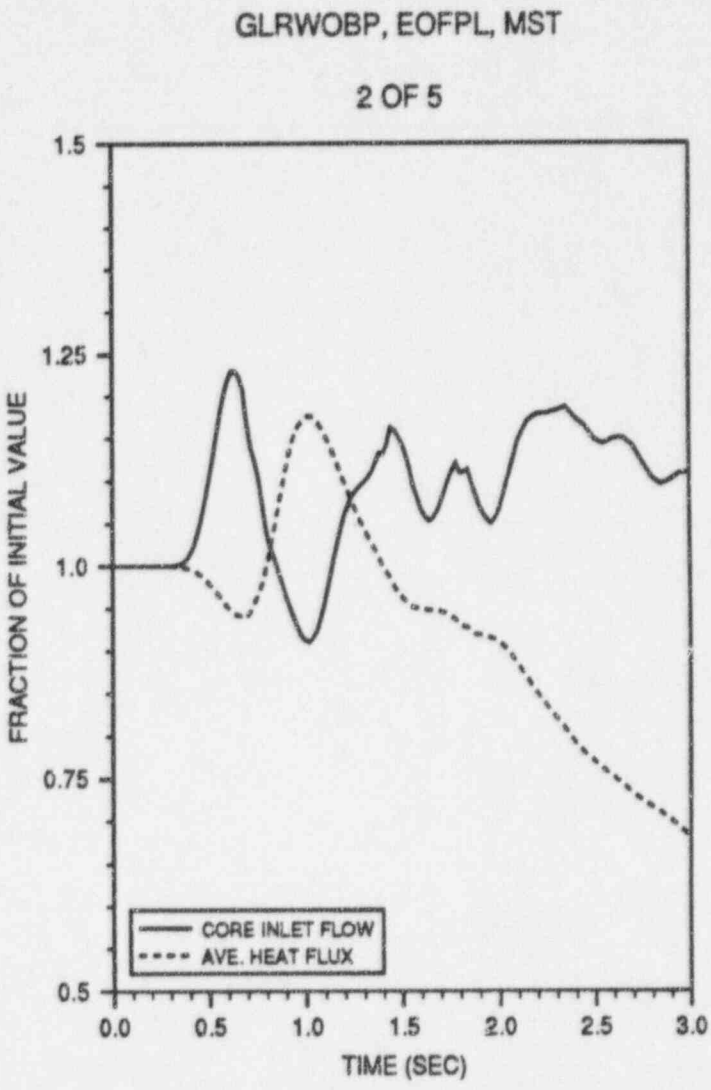

FIGURE 7.2.5

GENERATOR LOAD REJECTION WITHOUT BYPASS, EOFPL18
TRANSIENT RESPONSE VERSUS TIME, "MEASURED" SCRAM TIME

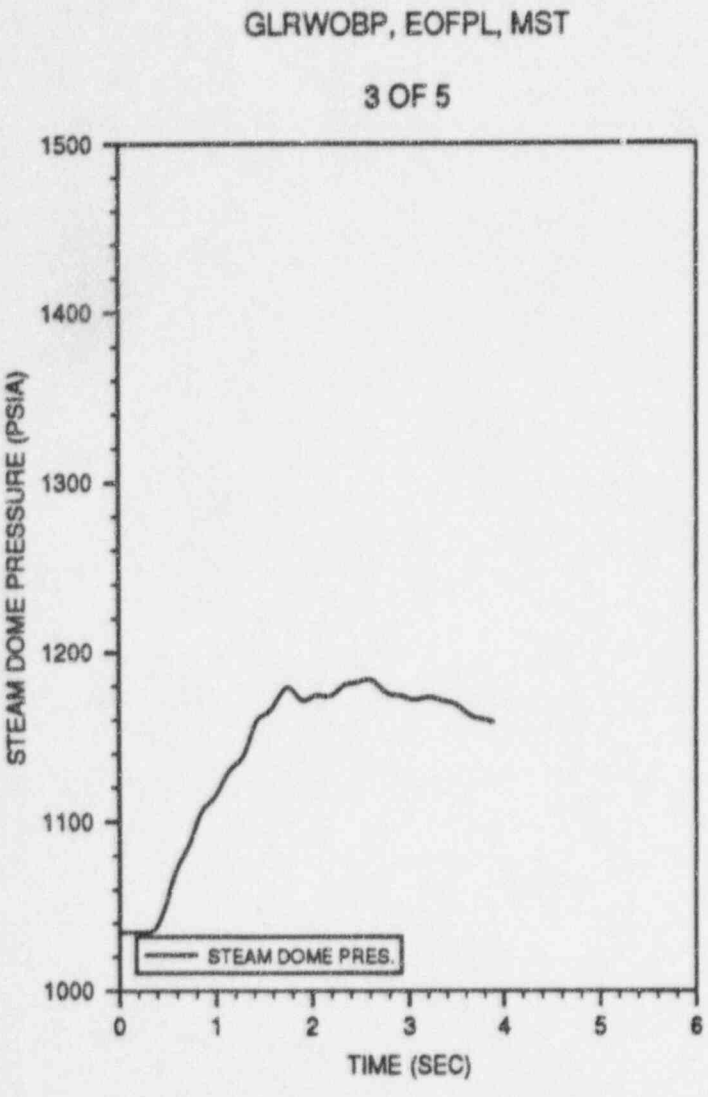

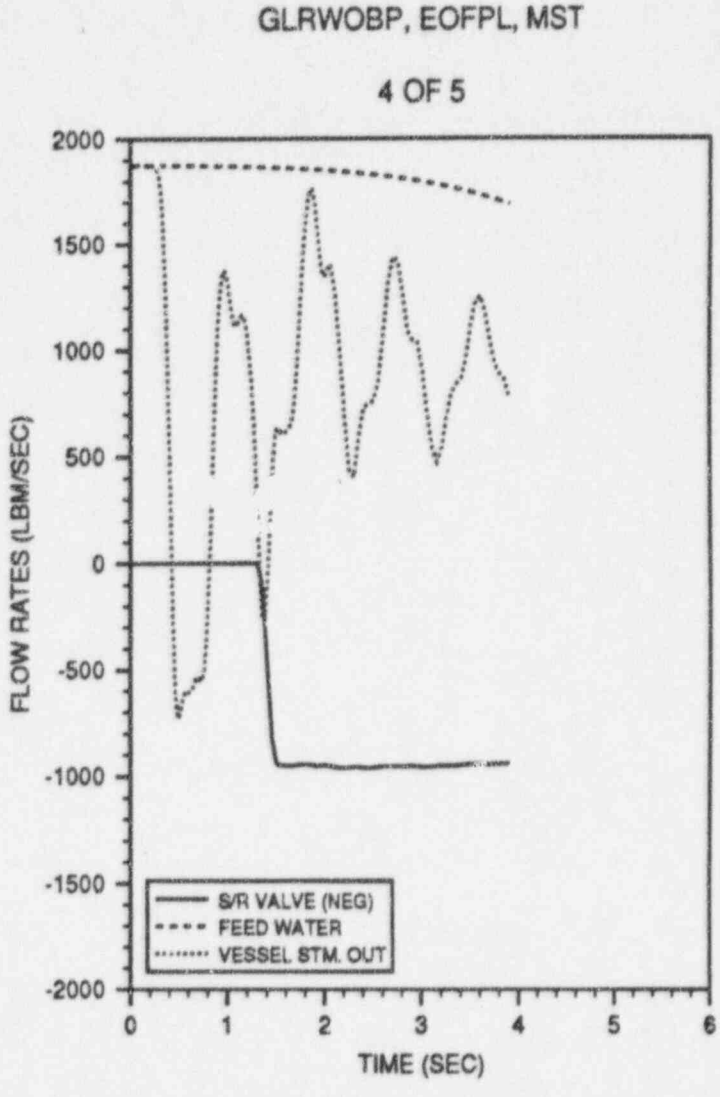

FIGURE 7.2.5
(Continued)

GENERATOR LOAD REJECTION WITHOUT BYPASS, EOFPL18
TRANSIENT RESPONSE VERSUS TIME, "MEASURED" SCRAM TIME

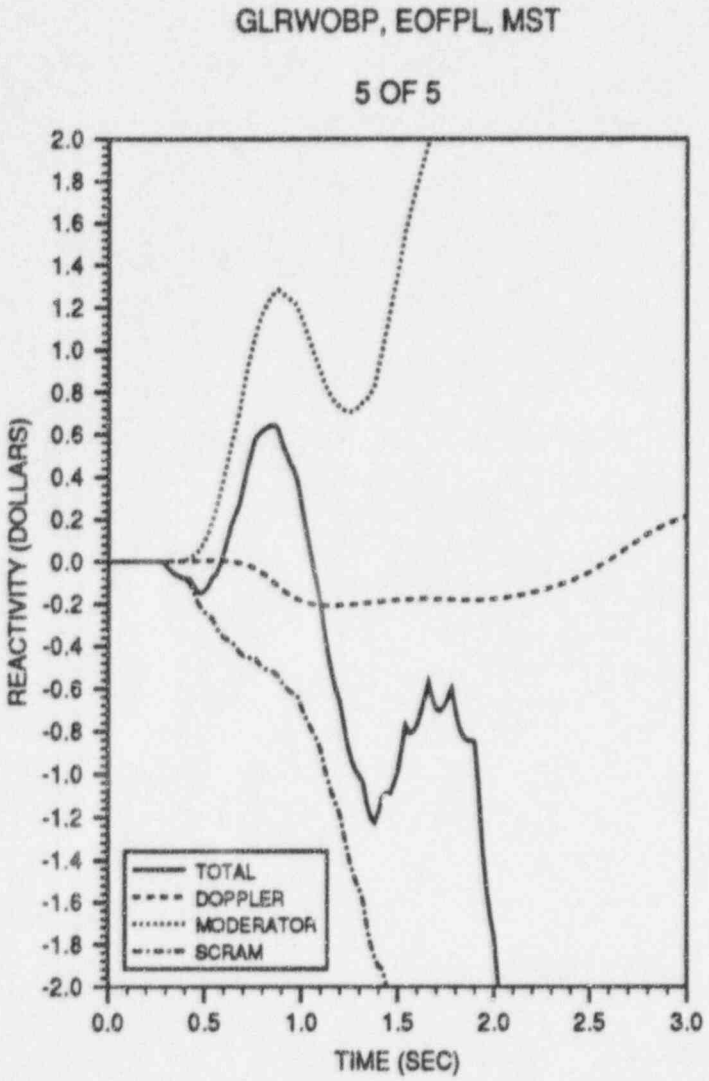

FIGURE 7.2.5
(Continued)

GENERATOR LOAD REJECTION WITHOUT BYPASS, EOFPL18
TRANSIENT RESPONSE VERSUS TIME, "MEASURED" SCRAM TIME

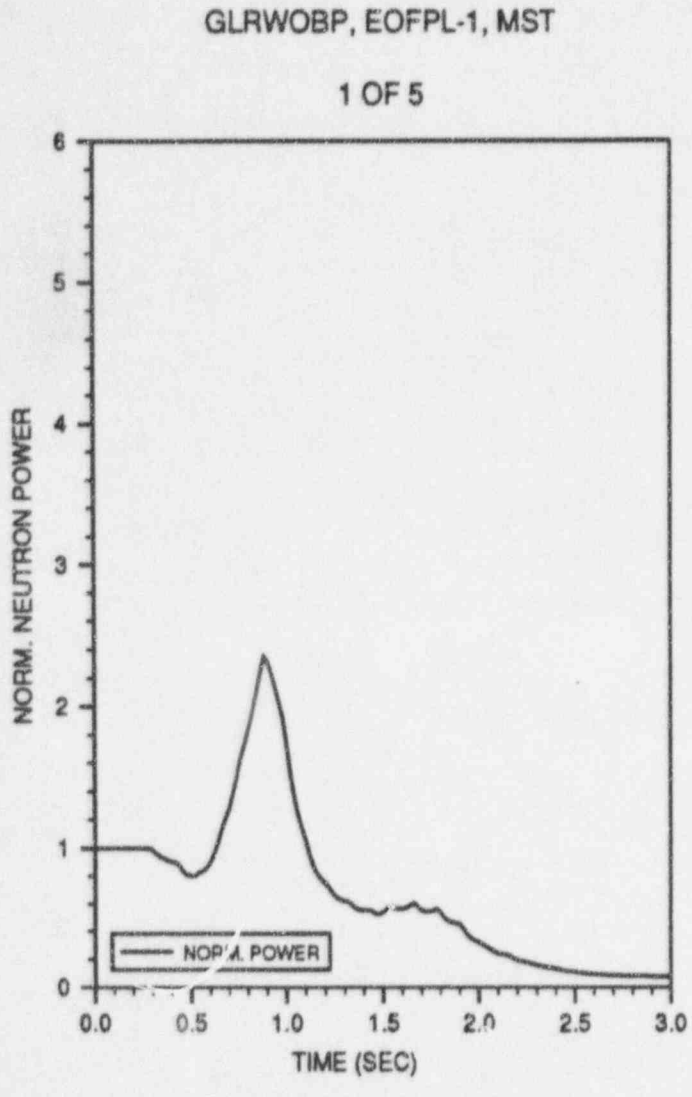

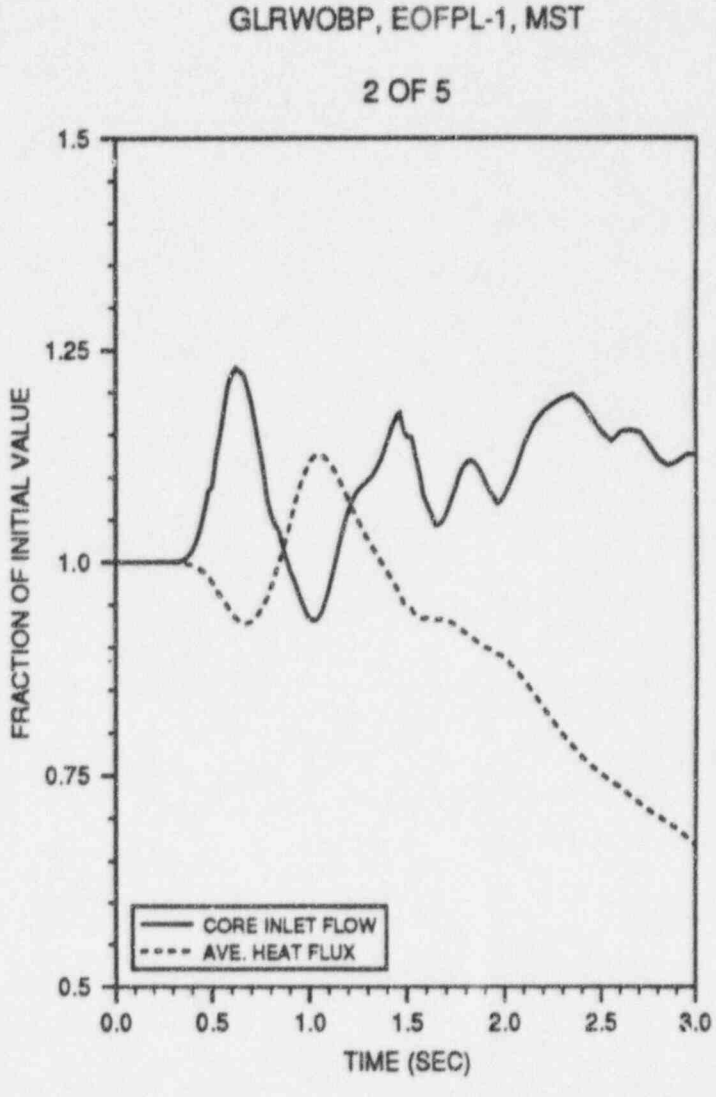

FIGURE 7.2.6

GENERATOR LOAD REJECTION WITHOUT BYPASS, EOFPL18-1000 MWD/ST
TRANSIENT RESPONSE VERSUS TIME, "MEASURED" SCRAM TIME

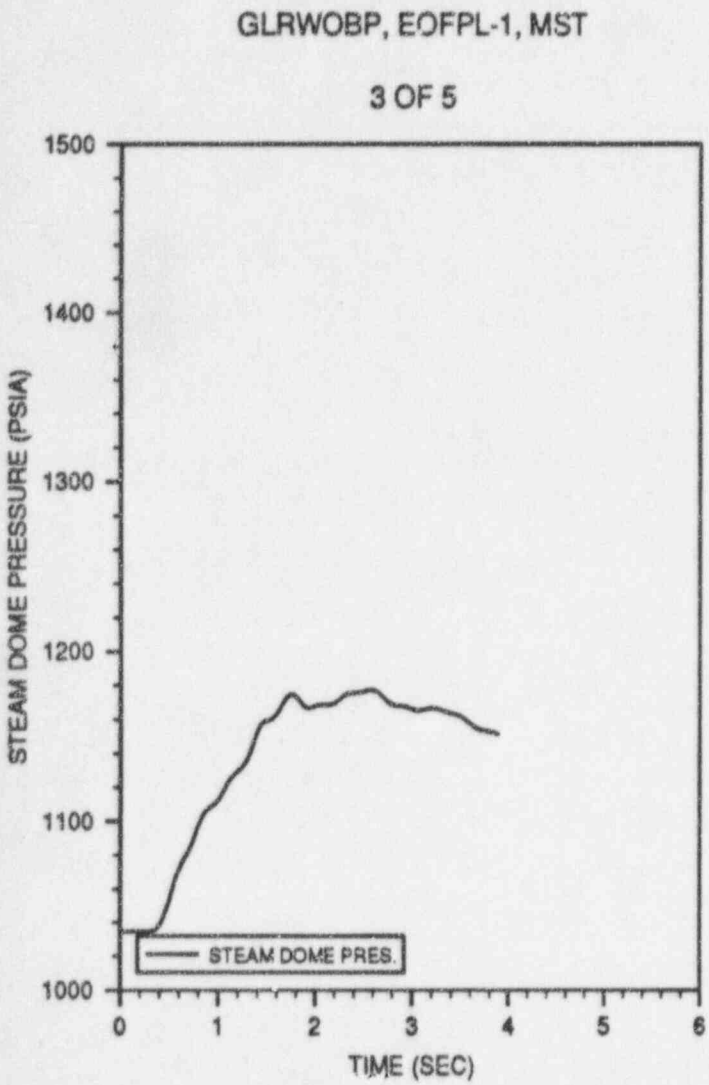

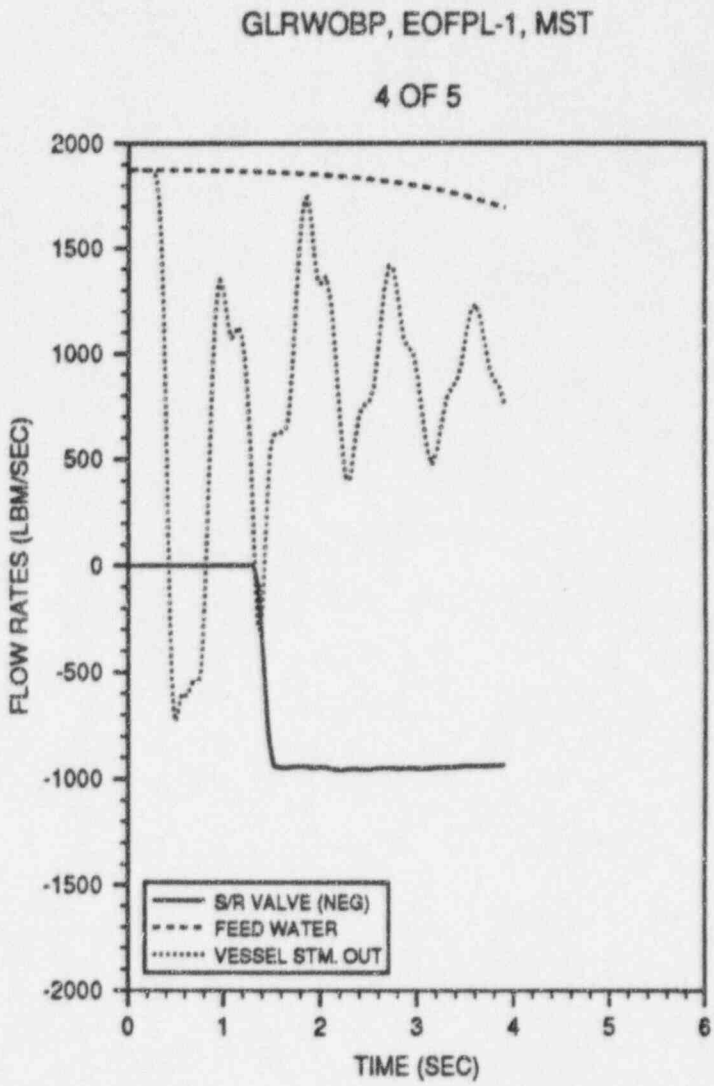

FIGURE 7.2.6
(Continued)

GENERATOR LOAD REJECTION WITHOUT BYPASS, EOFPL18-1000 MWD/ST
TRANSIENT RESPONSE VERSUS TIME, "MEASURED" SCRAM TIME

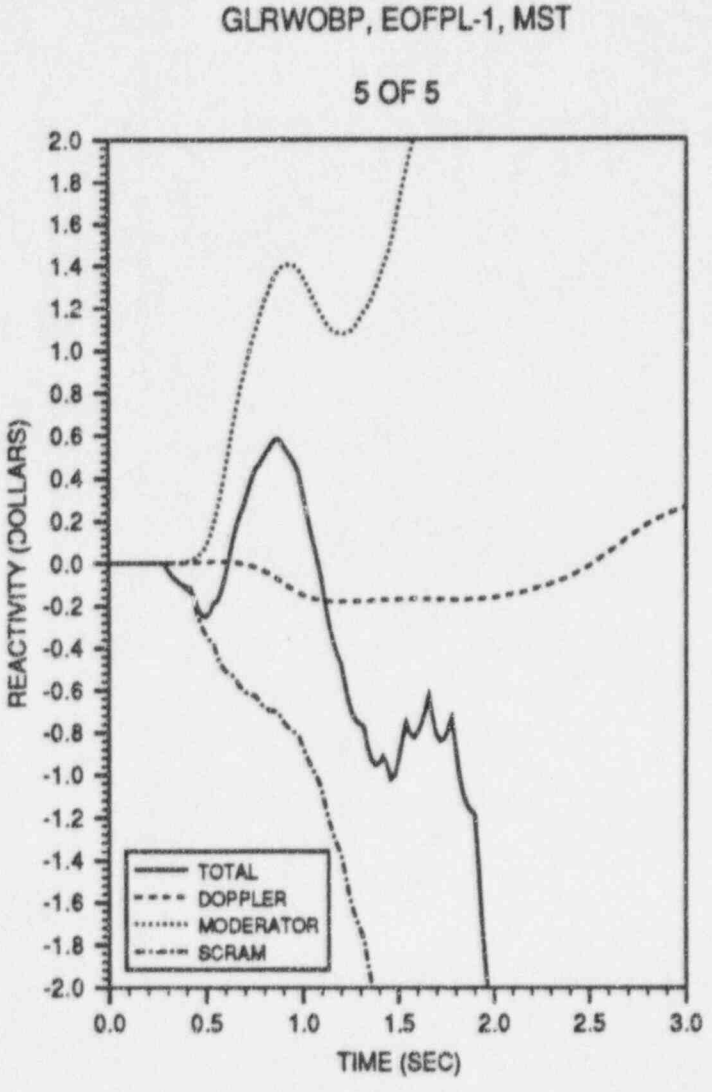

FIGURE 7.2.6
(Continued)

GENERATOR LOAD REJECTION WITHOUT BYPASS, EOFPL18-1000 MWD/ST
TRANSIENT RESPONSE VERSUS TIME, "MEASURED" SCRAM TIME

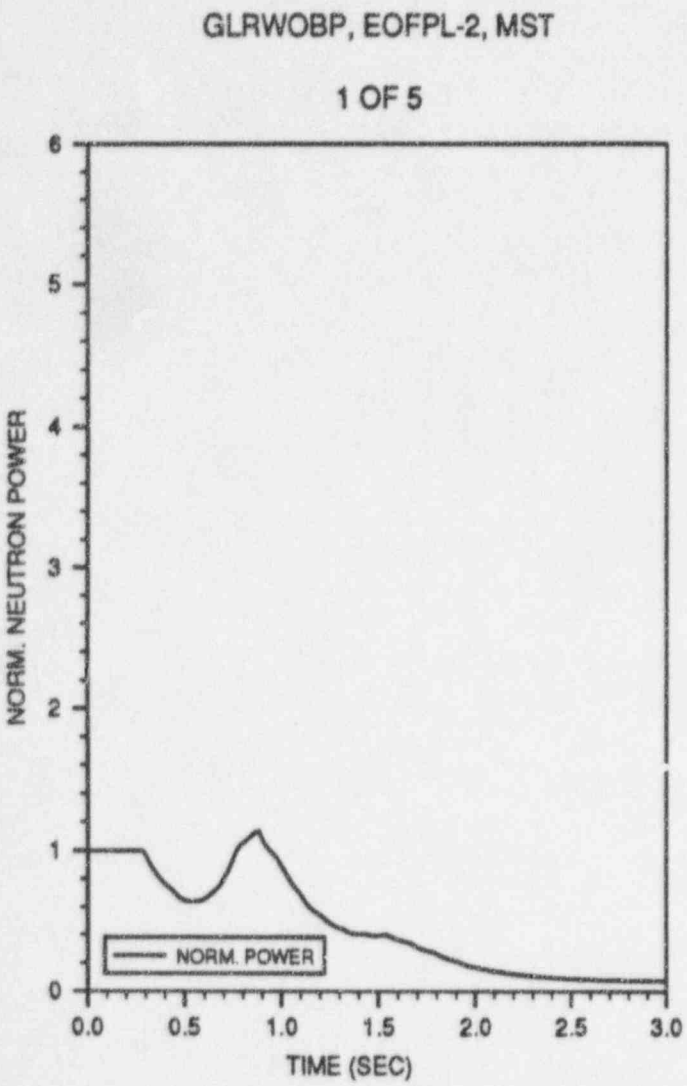

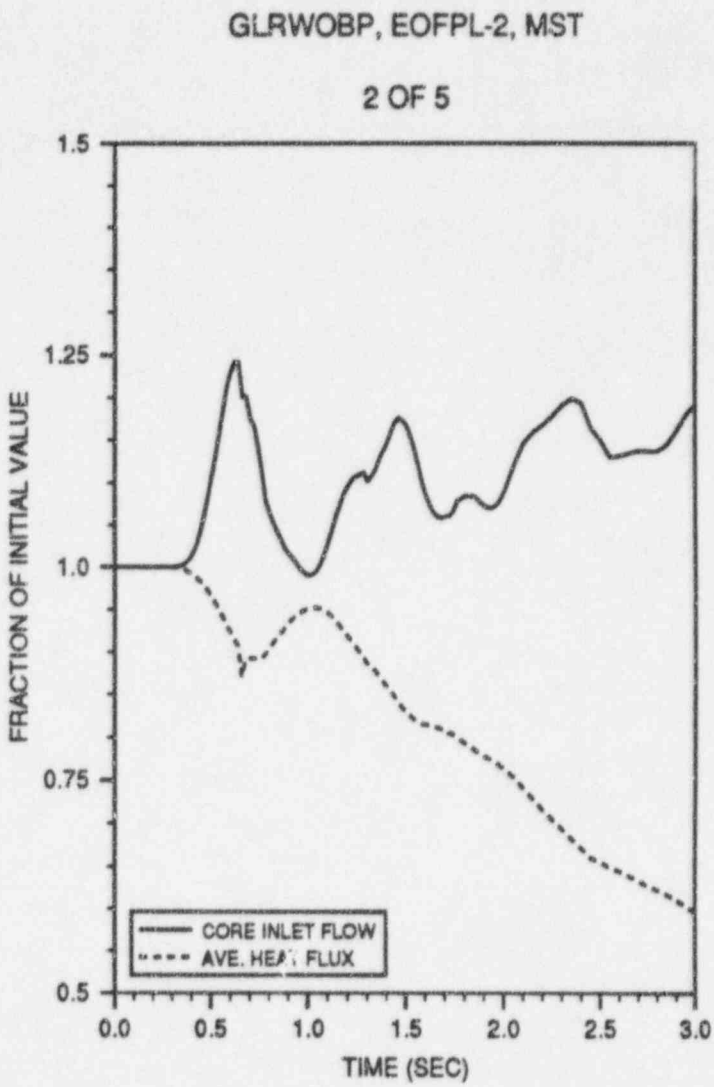

FIGURE 7.2.7

GENERATOR LOAD REJECTION WITHOUT BYPASS, EOFPL18-1000 MWD/ST
TRANSIENT RESPONSE VERSUS TIME, "MEASURED" SCRAM TIME

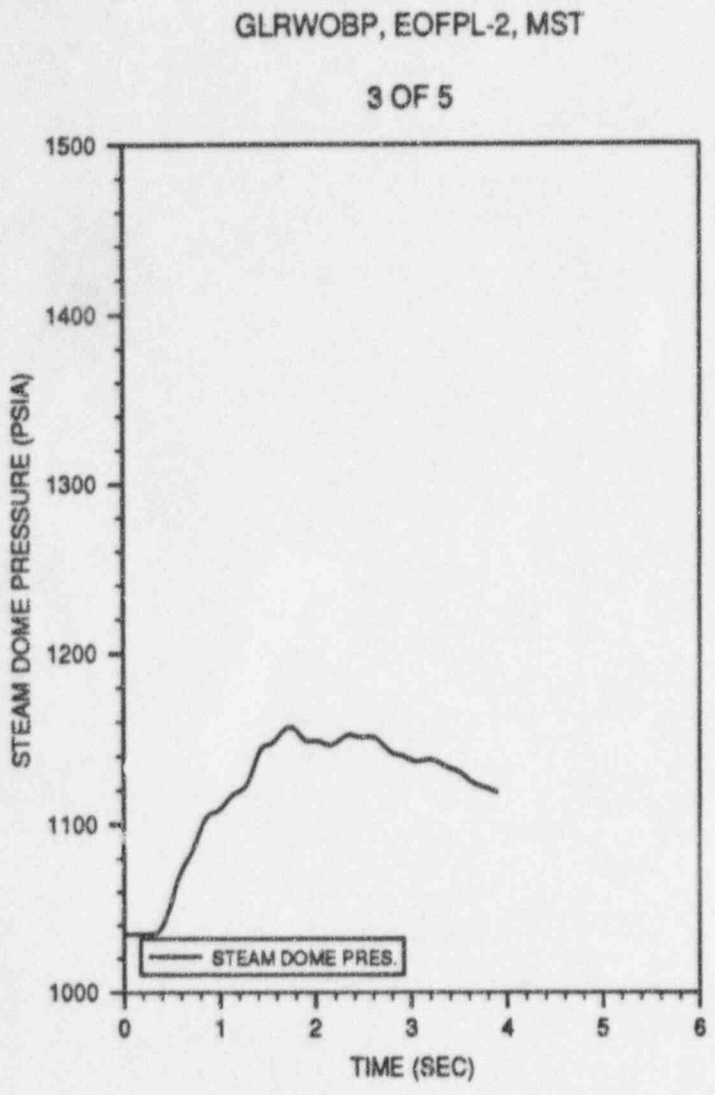

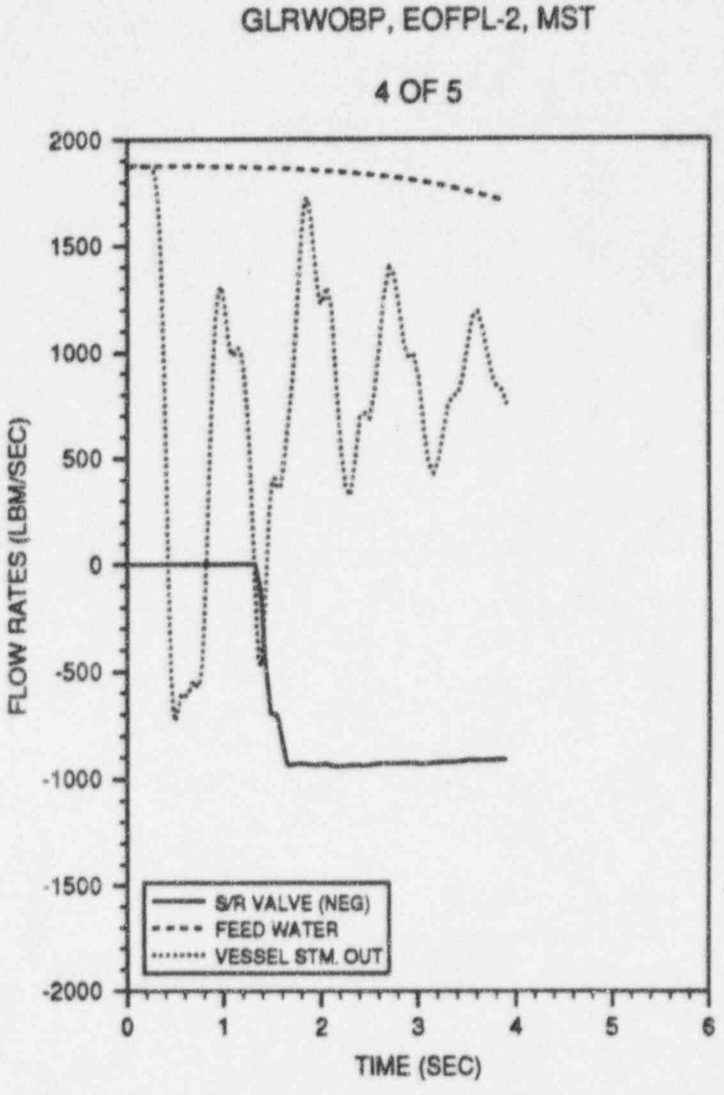

FIGURE 7.2.7
(Continued)

GENERATOR LOAD REJECTION WITHOUT BYPASS, EOFPL18-1000 MWD/ST
TRANSIENT RESPONSE VERSUS TIME, "MEASURED" SCRAM TIME

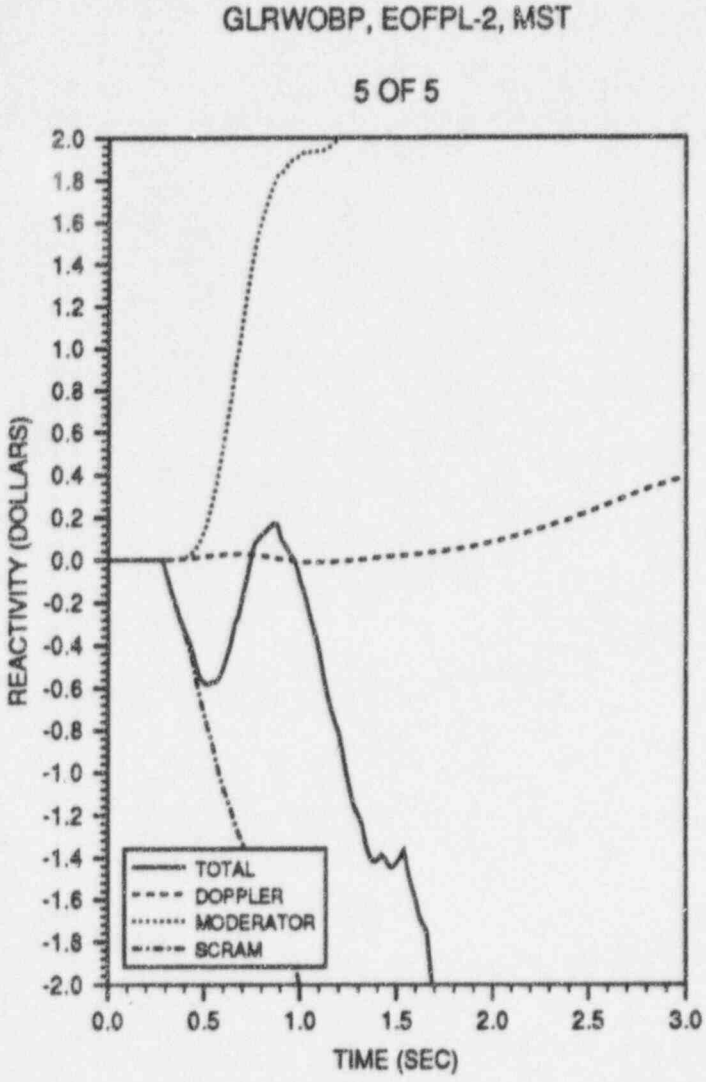

FIGURE 7.2.7
(Continued)

GENERATOR LOAD REJECTION WITHOUT BYPASS, EOFPL18-1000 MWD/ST
TRANSIENT RESPONSE VERSUS TIME, "MEASURED" SCRAM TIME

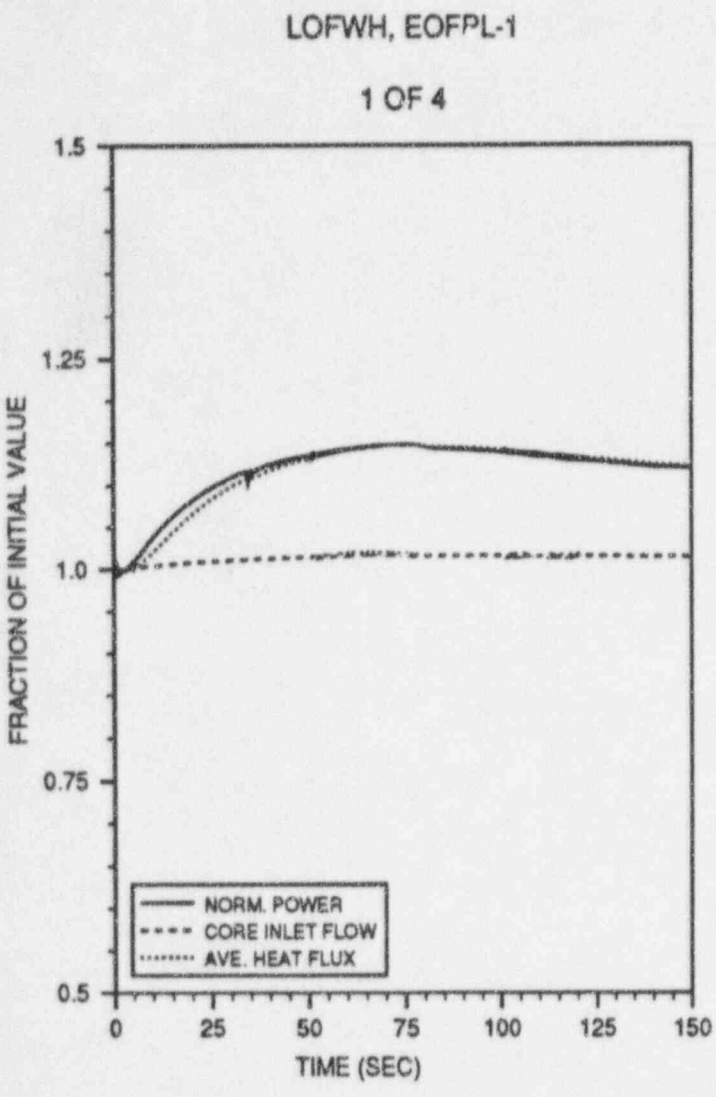

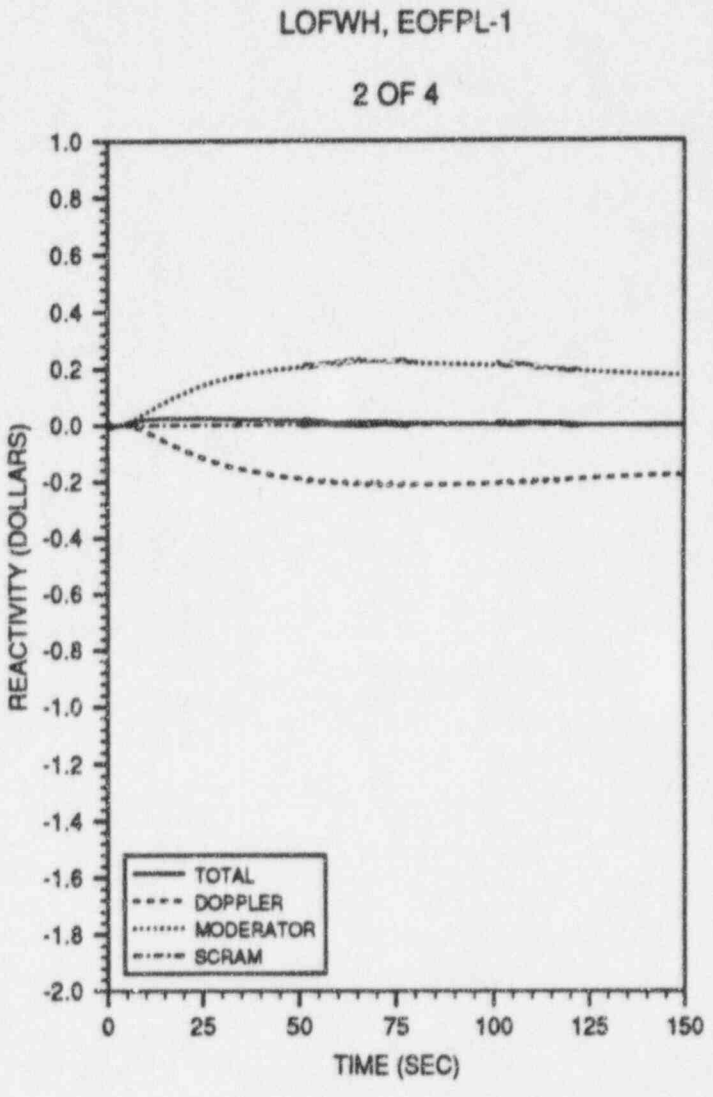

FIGURE 7.3.1

LOSS OF 100°F FEEDWATER HEATER (LIMITING CASE)
TRANSIENT RESPONSE VERSUS TIME

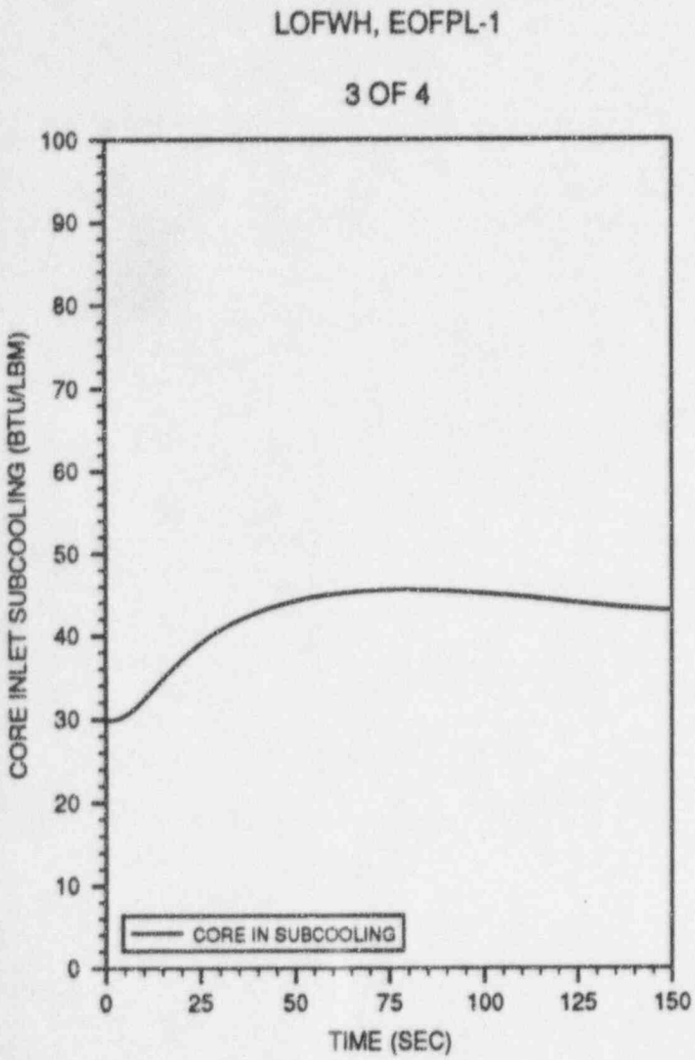

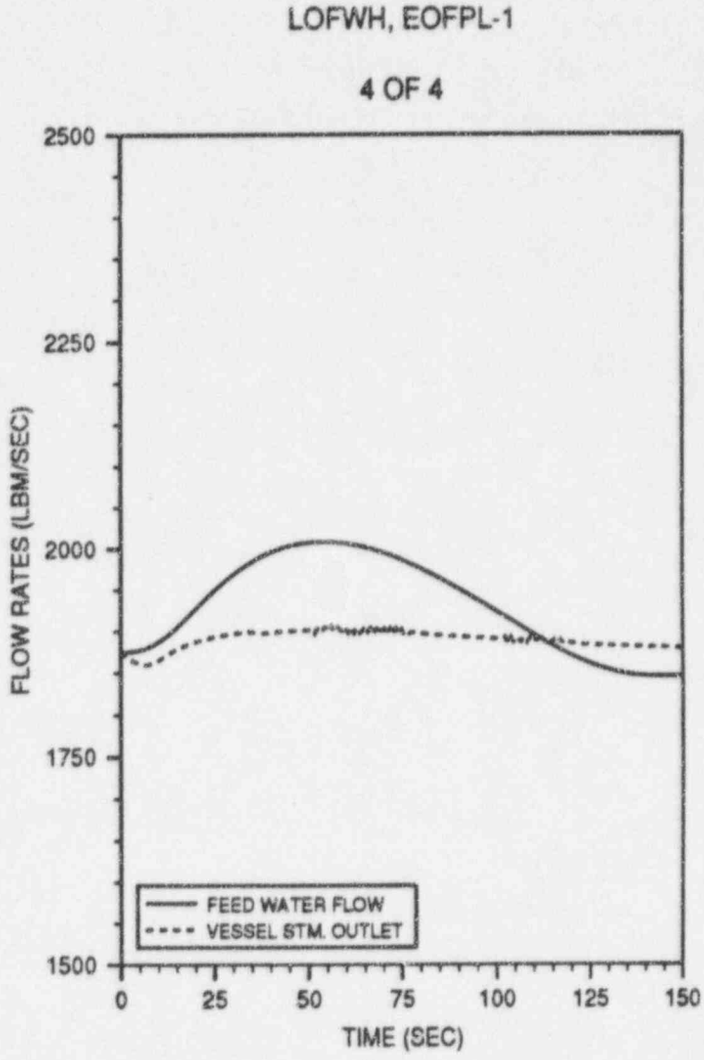

FIGURE 7.3.1
(Continued)

LOSS OF 100°F FEEDWATER HEATER (LIMITING CASE)
TRANSIENT RESPONSE VERSUS TIME

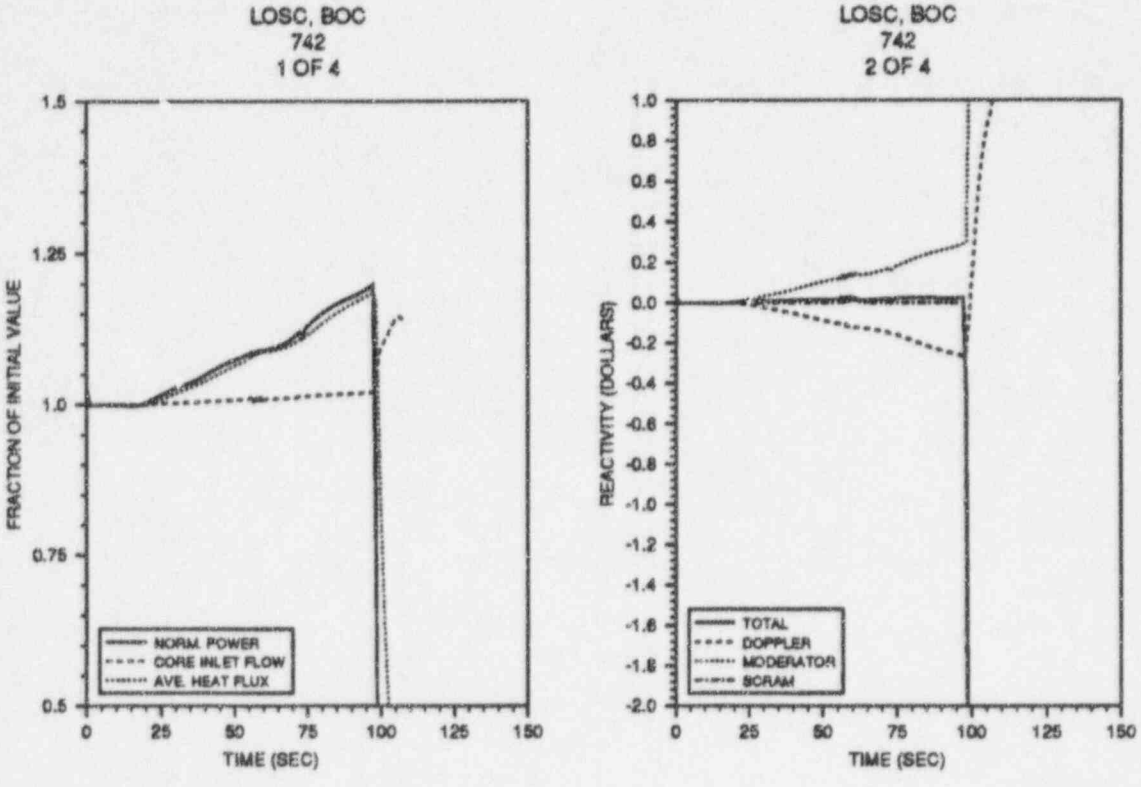

FIGURE 7.3.2

LOSS OF STATOR COOLING TRANSIENT RESPONSE VERSUS TIME

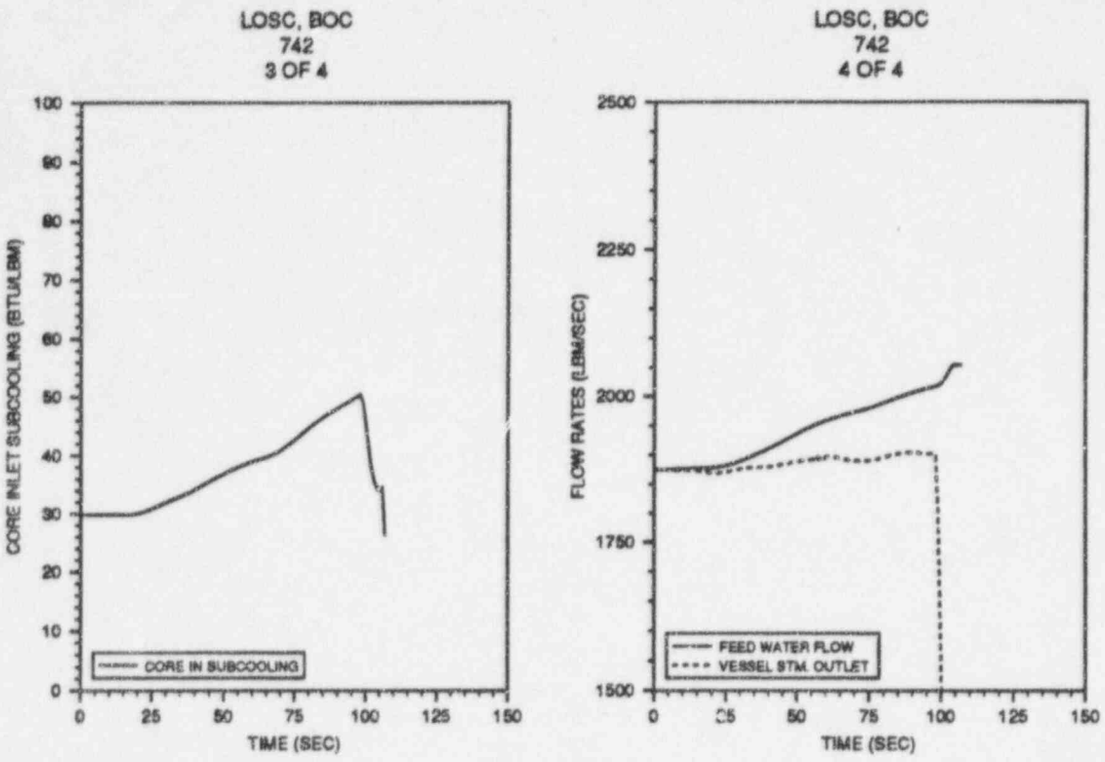

FIGURE 7.3.2
(Continued)

LOSS OF STATOR COOLING TRANSIENT RESPONSE VERSUS TIME

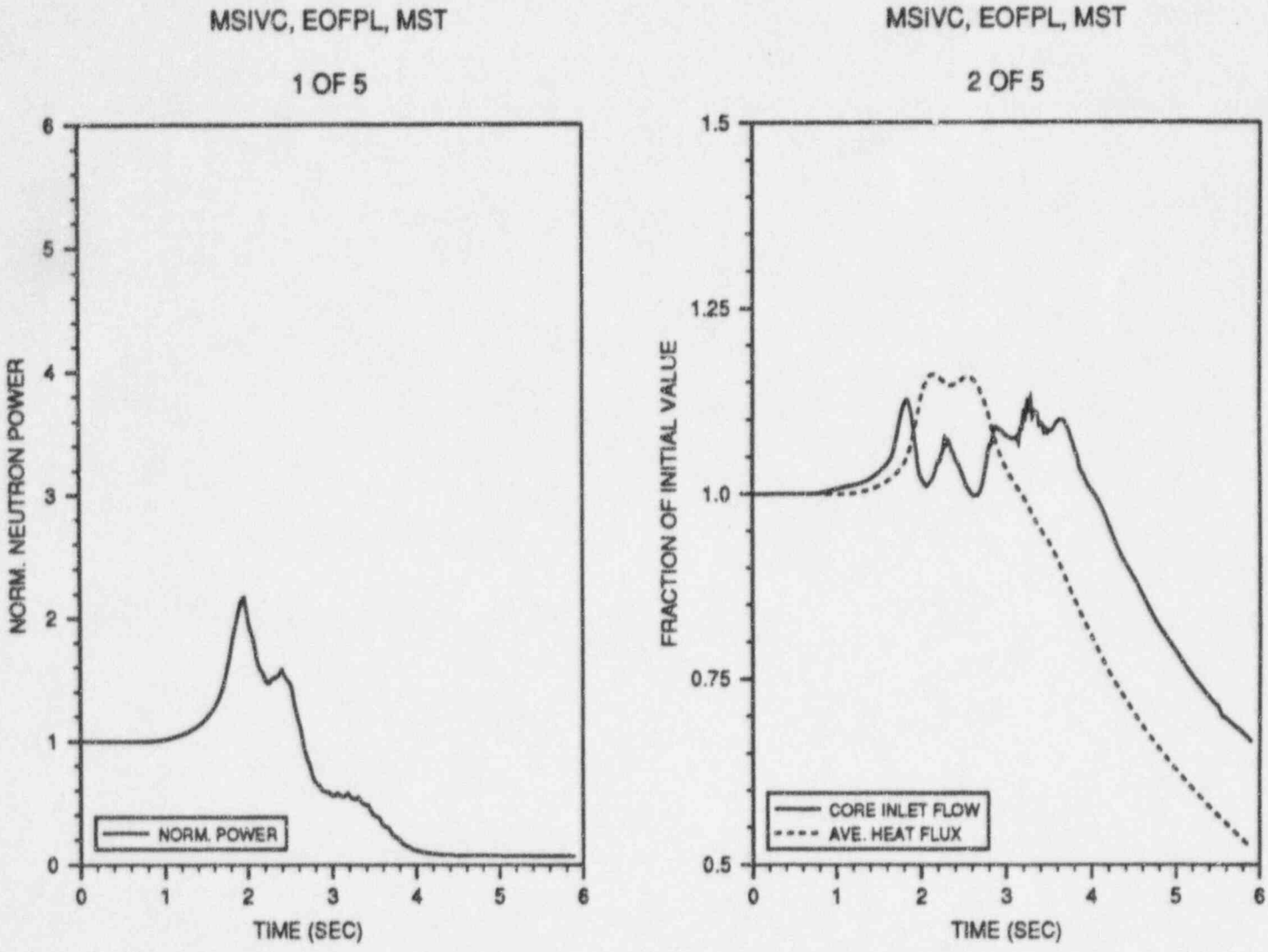

FIGURE 7.4.1

MSIV CLOSURE, FLUX SCRAM, EOFPL18
TRANSIENT RESPONSE VERSUS TIME, "MEASURED" SCRAM TIME

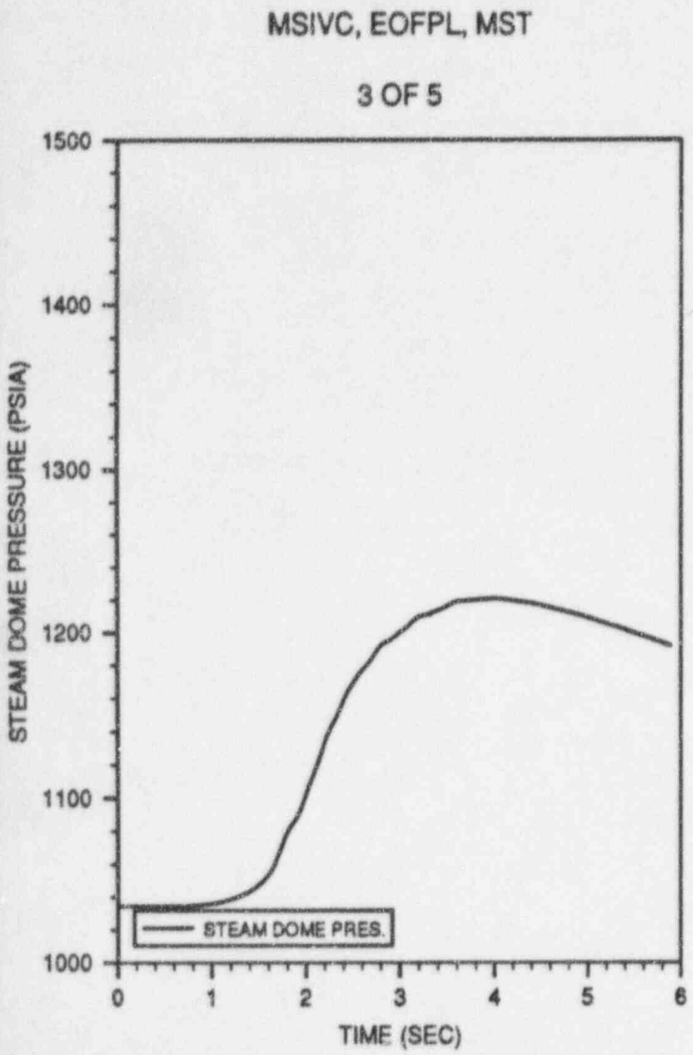

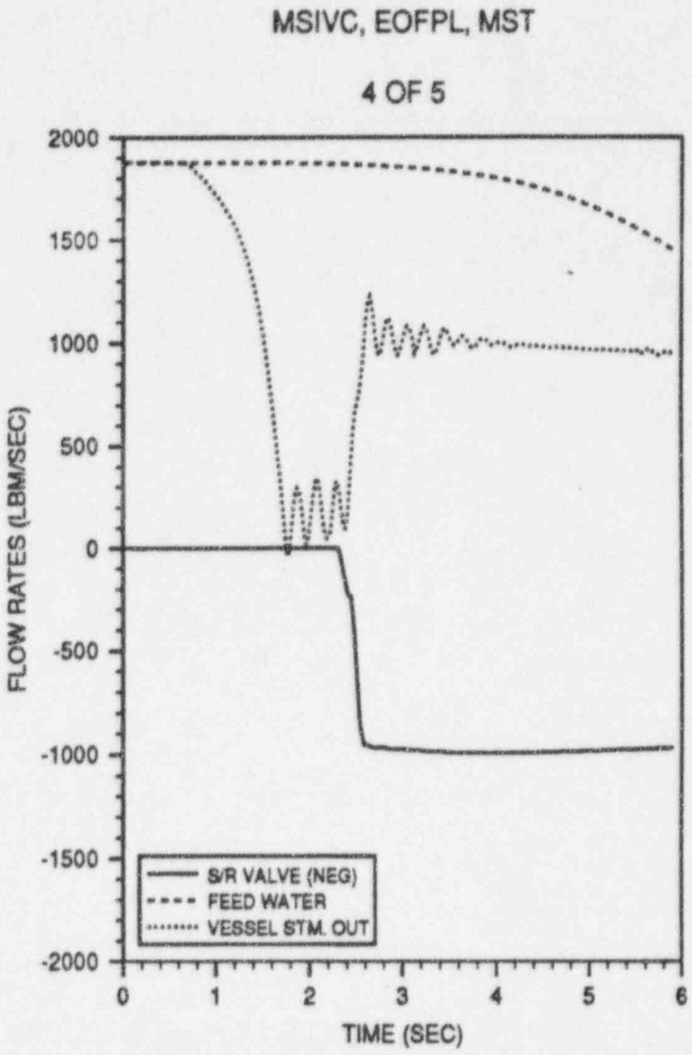

FIGURE 7.4.1
(Continued)

MSIV CLOSURE, FLUX SCRAM, EOFPL18
TRANSIENT RESPONSE VERSUS TIME, "MEASURED" SCRAM TIME

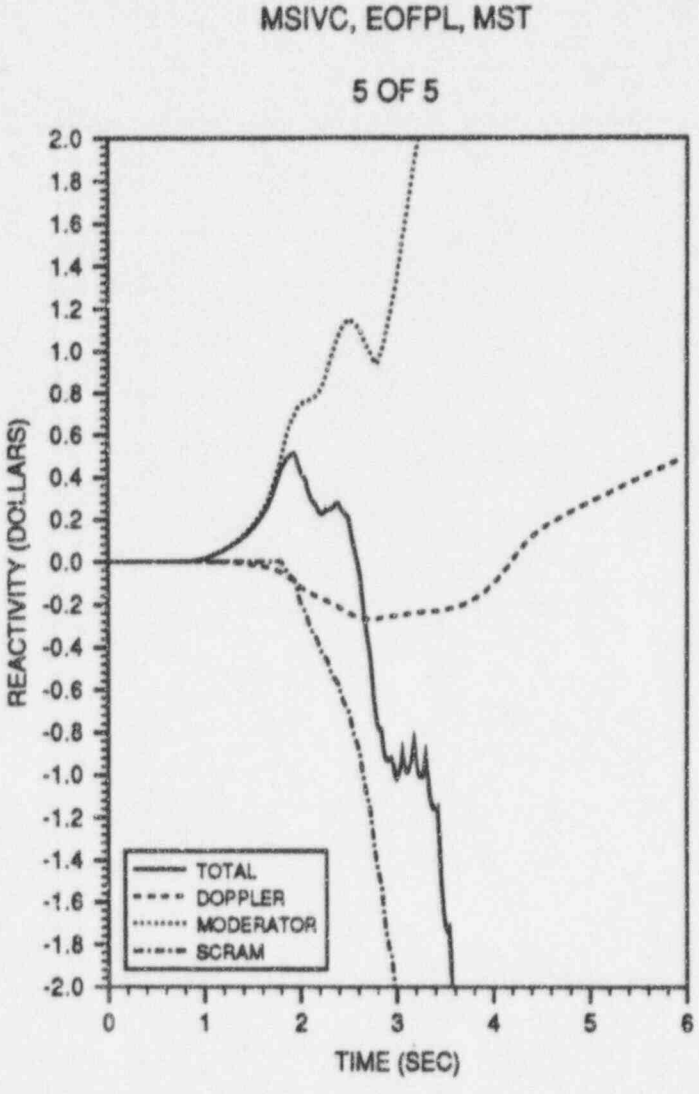

FIGURE 7.4.1
(Continued)

MSIV CLOSURE, FLUX SCRAM, EOFPL18
TRANSIENT RESPONSE VERSUS TIME, "MEASURED" SCRAM TIME

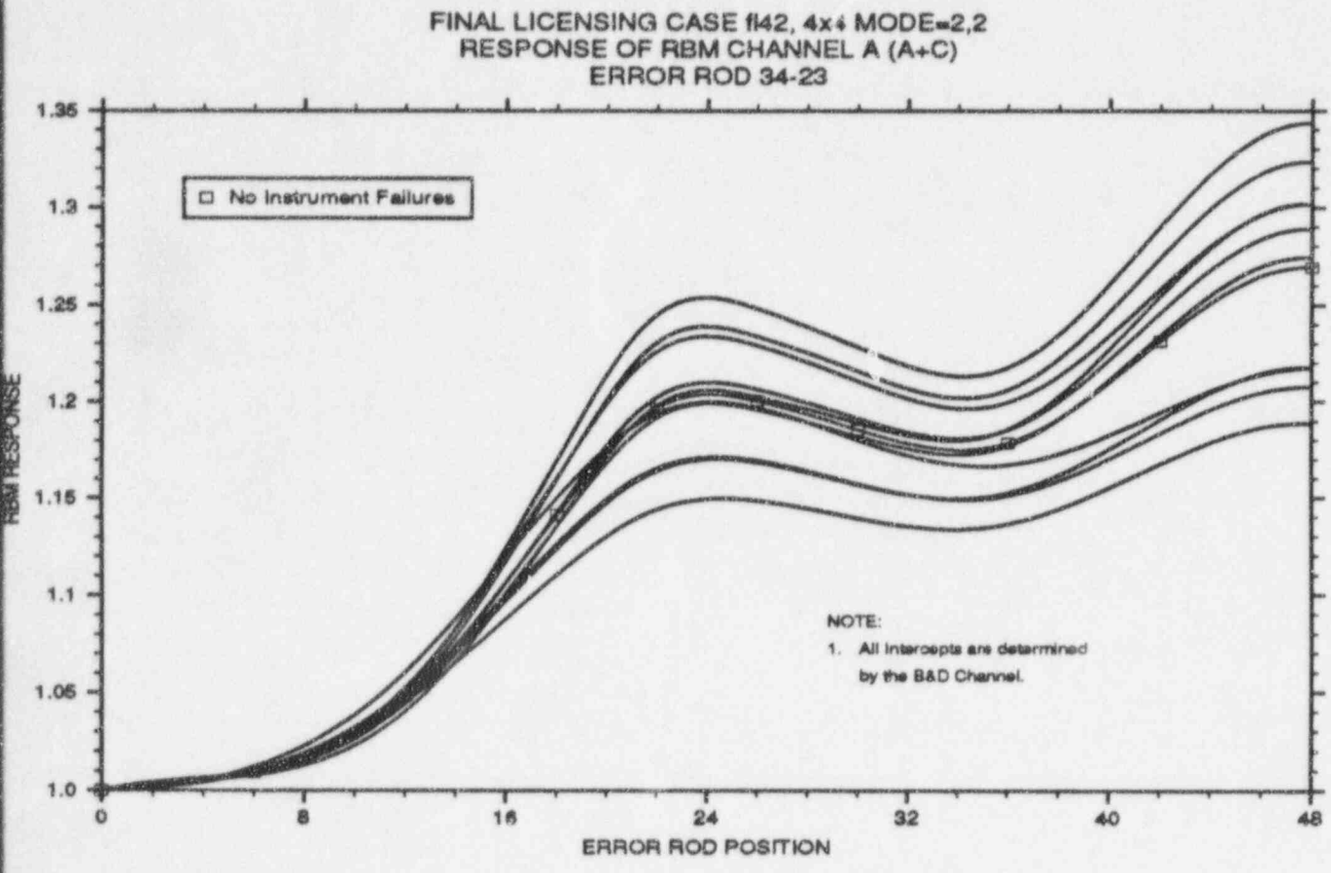

FIGURE 7.5.1

VY CYCLE 18 RWE CASE 1 - SETPOINT INTERCEPTS DETERMINED BY THE A AND C CHANNELS

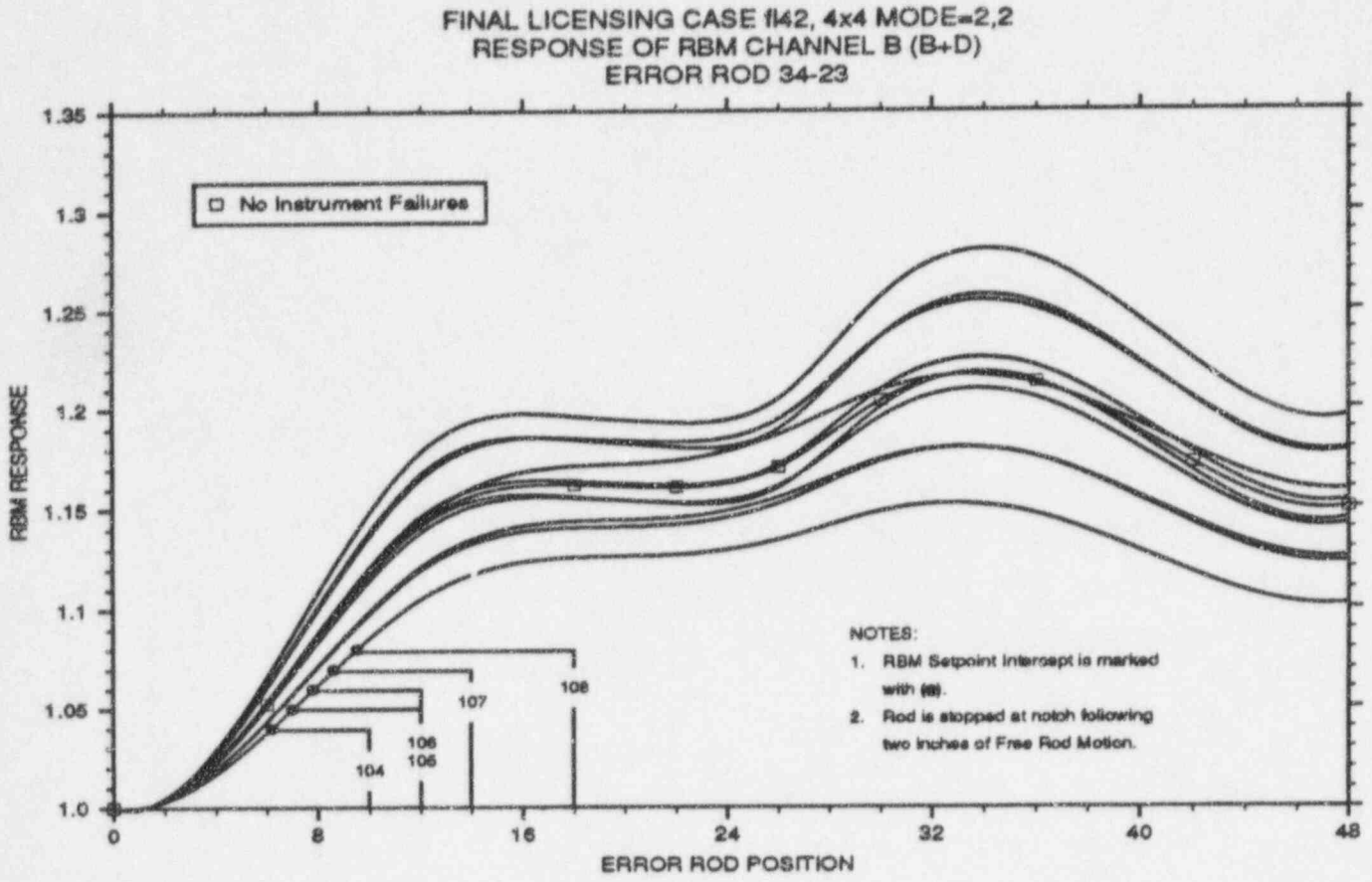

FIGURE 7.5.2

VY CYCLE 18 RWE CASE 1 - SETPOINT INTERCEPTS DETERMINED BY THE B AND D CHANNELS

8.0 DESIGN BASIS ACCIDENT ANALYSIS

8.1 Control Rod Drop Accident Results

The control rod sequences are a series of rod withdrawal and banked withdrawal instructions specifically designed to minimize the worths of individual control rods. The sequences are examined so that, in the event of the uncoupling and subsequent free fall of the rod, the incremental rod worth is acceptable. Incremental rod worth refers to the fact that rods beyond Group 2 are banked out of the core and can only fall the increment from full-in to the rod drive withdrawal position. Acceptable worth is one which produces a maximum fuel enthalpy less than 280 calories per gram.

Some out-of-sequence control rods could accrue potentially high worths. However, the Rod Worth Minimizer (RWM) will prevent withdrawing an out-of-sequence rod, if accidentally selected. The RWM is functionally tested before each startup.

The sequence in the RWM will take the plant from All Rods In (ARI) to well above 20% core thermal power. Above 20% power even multiple operator errors will not create a potential rod drop situation above 280 calories per gram[29],[30],[31]. Below 20% power, however, the sequences must be examined for incremental rod worth. This is done throughout the cycle using the full core, xenon-free SIMULATE-3 model.

Both the A and B sequences were examined at various exposures throughout the cycle. For startup, the rods are grouped, as shown in Figures 8.1.1 and 8.1.2, and are pulled in numerical order. All the rods in one group are pulled out before the pulling of the next group begins. The rods in the first two groups are individually pulled from full-in to full-out. Beyond Group 2, the rods are banked out using procedures[32],[33] which reduce the rod incremental worths.

The potentially high worths that occur in pulling the rods in Group 1 are ignored because the reactor is subcritical in Group 1. Therefore, if a rod drops from any configuration in the first group, its excess reactivity contribution to the Rod Drop Accident (RDA) is zero. Successive reloads of axially zoned fuel have extended this subcriticality situation to the second group as well.

The second group of rods was examined using the following analysis method[34]. Both the A and B sequences were examined. It was found that the highest worth rod was the first rod in the second group. Any of the first four rod arrays, shown in Figures 8.1.1 and 8.1.2, may be designated as the first group pulled. However, a specific second group must follow as Table 8.1.1 illustrates. For added conservatism, each of the high worth rods in the second group were checked; i.e., one at a time, they were assigned to be the first rod pulled. This assures that in any sequence the actual worths will always be less than those calculated here.

Only that portion of the control rod worth above the SIMULATE-3 cold critical eigenvalue contributes to the rod drop accident. For conservatism, "critical" was defined as the SIMULATE-3 average cold critical K_{eff} minus 1% ΔK (reactivity anomaly criteria). The results of the Group 2 calculations, as presented in Table 8.1.2, fit under the bounding analysis of References 29 through 31.

Beyond Group 2, the rods are banked out of the core. This generally limits the incremental worth of a single rod drop; however, virtually all of the pre-drop cases in Group 3 are critical. Therefore, the entire dropped rod worth contributes toward the RDA excess reactivity insertion. The method used to evaluate Group 3 involved pulling Groups 1 and 2 out and banking Group 3 to varying positions. The types of cases examined included:

1. Banked positions 04, 08, 12, and 48 (full-out).

2. Group 3 rods pulled out of sequence, creating high flux regions.

3. Xenon-free conditions, both cold moderator and "standby" (i.e., 1020 psia).

4. Group 3 rods dropping from 00 (full-in) to the appropriate banked position.

5. Stuck rods from previously pulled Group 1 or 2 dropping from 00 to 48.

The highest worth results from the Group 3 analysis fit under the Group 2 results, presented in Table 8.1.2.

8.2 Loss-of-Coolant Accident Analysis

The LOCA analysis, performed in accordance with 10CFR50 Appendix K and the Safety Evaluation Reports[35][36], demonstrates that Vermont Yankee, operating within the assumed conditions, complies with the LOCA limits specified in 10CFR50. 46.

The LOCA analysis for the Reload Cycle is a combination of cycle specific analysis and a base analysis for Cycle 17[37]. Both analyses use the NRC-approved codes, FROSSTEY-2[11] and RELAP5YA[38]. The base analysis provided the break spectrum and the single failure conditions. The Reload Cycle analysis provided the verification that the base analysis was valid for the Reload Cycle given changes in the reactivity and the UNIX system configuration. All other assumed initial conditions and assumptions are the same for both analyses. Table 8.2.1 lists some of the key input assumptions but Reference 37 provides a more detailed listing of the input assumptions.

The base analysis was performed for a combination of break size, break location, and single failure conditions. The break sizes range from 0.05 ft^2 to 7.28 ft^2. Five break locations were analyzed: main steam line, core spray line, feedwater line, recirculation loop suction and recirculation loop discharge. Five possible single failures were evaluated: low pressure coolant injection valve, high pressure coolant injection, DC power supply, diesel generator and one automatic depressurization system valve. The impact of the Gd_2O_3 on initial volume average temperature and material properties was included. The PCT results for the limiting break 0.6 ft^2 with loss of DC power was 1778.1°F.

The Reload Cycle analysis was performed for the limiting break size and two single failure conditions. The PCT results for the limiting break 0.6 ft^2 with loss of DC power was 1788.9°F which is a 10.8°F increase in PCT compared to the base analysis results. For the same size break with LPCI injection valve failure, the PCT for the Reload Cycle was 1770.4°F, an increase of 26.2°F compared to the base analysis. The Reload Cycle analysis also showed that the break spectrum performed for the base analysis remains valid for the Reload Cycle.

The combined analysis results, in terms of peak cladding temperature (PCT), are shown in Figure 8.2.1. The break spectrum PCT results for Reload Cycle were obtained by increasing the base analysis results by the maximum change in PCT from the Reload Cycle analysis, 26.2°F. These

results show that the limiting break is 0.6 ft^2 in the recirculation loop at the pump discharge with one DC power supply as the single failure and loss of offsite power coincident with the break opening. Overall, the calculated peak clad temperatures are well below the 2200°F limit of 10CFR 50.46. The analysis also shows compliance with the other 10CFR 50.46 limits: total cladding oxidation at the peak location is less than 17%; hydrogen generated in the core is less than 1%; and the core retains a coolable geometry with no clad rupture.

During the cycle, Vermont Yankee can adjust the core flow to account for reactivity changes rather than using the control rods. During this type of operation, core flow may be as low as 87% while at 100% power. To ensure the safety analysis bounds these conditions, the LOCA analysis was analyzed at 1698 MW_{th} power and 87% flow. The results showed that the 100% flow case bounded the low flow case.

The analysis showed that the MAPLHGR limits are not limited by a LOCA. Therefore, the MAPLHGR limits are set based on the thermal-mechanical analysis of the bundle from Reference 18. They are provided in Appendix A for all the fuel types in the Reload Cycle, as a function of average planar exposure. The analysis also verified that the single loop MAPLHGR multiplier, 0.83, is valid for the Reload Cycle.

8.3 Refueling Accident Results

If any assembly is damaged during refueling, then a fraction of the fission product inventory could be released to the environment. The source term for the refueling accident is the maximum gap activity within any bundle. The source term includes contributions from both noble gases and iodines. The calculation of maximum gap activity is based on the MAPLHGRs, the maximum operating fuel centerline temperatures, and maximum bundle burnup.

The fuel rod gap activity, internal pressure and centerline temperature for the Reload Cycle are bounded by the values used in Section 14.9 of the FSAR[39].

TABLE 8.1.1

CONTROL ROD DROP ANALYSIS - ROD ARRAY PULL ORDER

The order in which rod arrays are pulled is specific once the choice of the first group is made.

First Group Pulled Is:	Second Group Pulled Must Be:	Successive Group Is Banked Out
Array 1	Array 2	Arrays 3 or 4
Array 2	Array 1	Arrays 3 or 4
Array 3	Array 4	Arrays 1 or 2
Array 4	Array 3	Arrays 1 or 2

TABLE 8.1.2

VY CYCLE 18 CONTROL ROD DROP ANALYSIS RESULTS

Maximum Incremental Rod Worth Calculated Cold, Xenon-Free	0.80% ΔK
Bounding Analysis Worth for Enthalpy Less than 280 Calories per Gram [29],[30],[31]	1.30% ΔK

TABLE 8.2.1

LOCA ANALYSIS ASSUMPTIONS

Core Thermal Power (MW_{th})	1698.3
Total Core Flow ($10^6 lb_m/hr$)	48.0
Reactor Vessel Pressure (psia)	1067.0
Recirculation Loop Flow ($10^6 lb_m/hr$) - Each Loop	12.3
Feedwater Flow ($10^6 lb_m/hr$)	6.93
Feedwater Temperature (°F)	377.0
Water Level Above Top of Enriched Fuel (in.)	130.0
Containment Drywell Pressure (psia)	16.5
Containment Wetwell Pressure (psia)	14.7
Containment Wetwell Liquid Temperature (°F)	165.0
Maximum Bundle Power (MW_{th})	7.3
Maximum Average Planar Linear Heat Generation Rate (kW/ft)	13.6*
Maximum Linear Heat Generation Rate (kW/ft)	14.4**

* Plus Calorimetric and TIP Reading Uncertainties (8.9%)

** Plus Calorimetric and TIP Reading Uncertainties (9.2%)

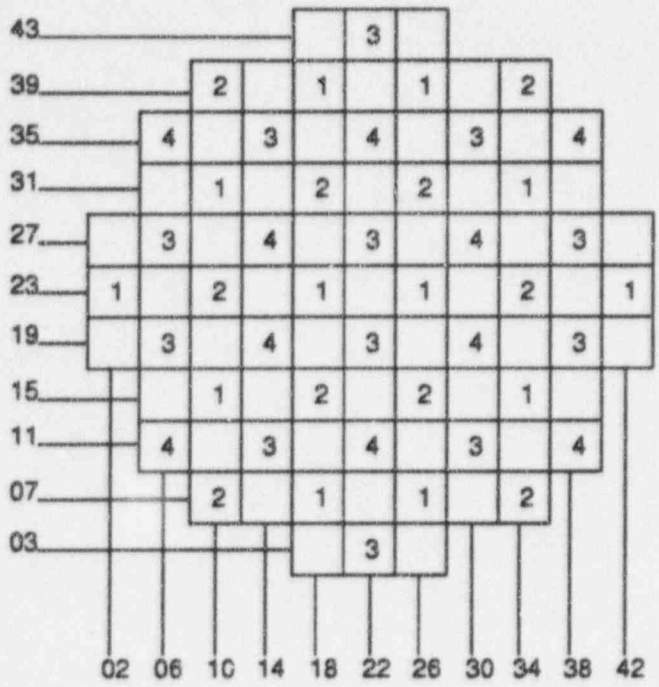

FIGURE 8.1.1

FIRST FOUR ROD ARRAYS PULLED IN THE A SEQUENCES

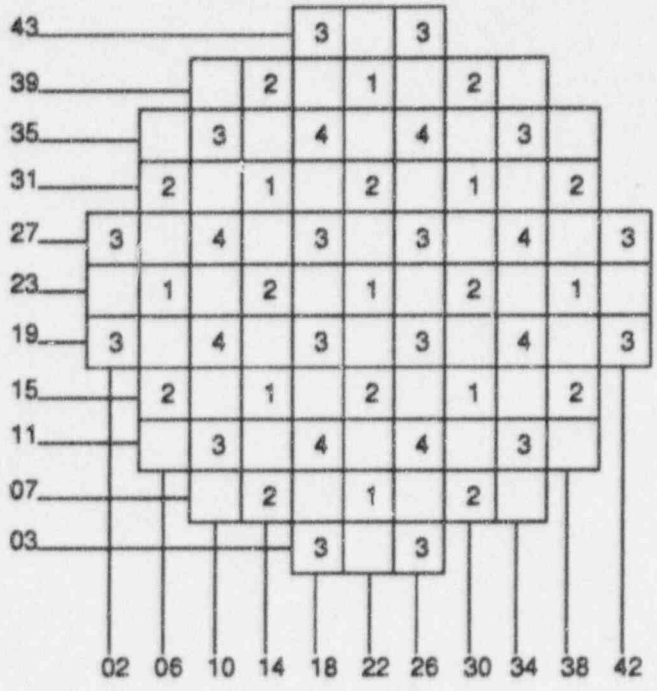

FIGURE 8.1.2

FIRST FOUR ROD ARRAYS PULLED IN THE B SEQUENCES

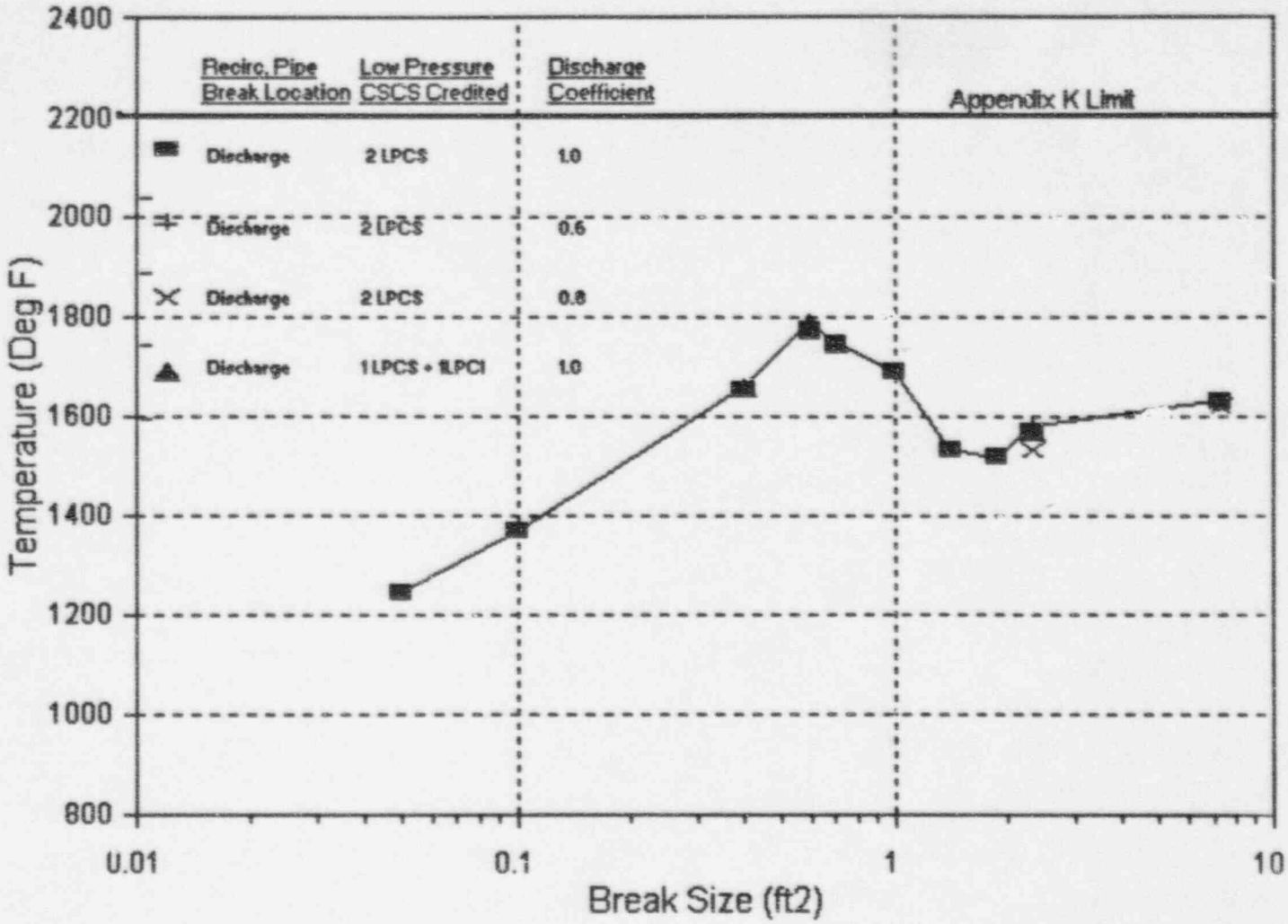

FIGURE 8.2.1

LOCA ANALYSIS RESULTS, PEAK CLADDING TEMPERATURE VERSUS BREAK SIZE

9.0 STARTUP PROGRAM

Following refueling and prior to vessel reassembly, fuel assembly position and orientation will be verified and videotaped by underwater television.

The Vermont Yankee Startup Program will include process computer data checks, shutdown margin demonstration, in-sequence critical measurement, rod scram tests, power distribution comparisons, TIP reproducibility, and TIP symmetry checks. The content of the Startup Test Report will be similar to that sent to the Office of Inspection and Enforcement in the past[40].

10.0 CONCLUSION

This report presented the design information, calculational results, and operating limits pertinent to the operation of the Reload Cycle. The core is designed to consist of 120 new GE-9B fuel bundles and 248 irradiated GE-9B fuel bundles. The shutdown margin for the Reload Cycle is greater than the Technical Specification limit of 0.32% ΔK. The bundles used in the Reload Cycle do not exceed the Technical Specification limit of 1.31 K_∞ for storage in the spent fuel pool or the new fuel storage facility. The transient analysis has: 1) determined the MCPR operating limits so that the FCISL is not violated for the transients considered, 2) assured that the thermal and mechanical overpower limits are not exceeded during the transient, and 3) demonstrated compliance with the ASME vessel code limits. The control rod drop worth is less than the bounding analysis which demonstrates a maximum fuel enthalpy less than the Technical Specification limit of 280 calories per gram. The LOCA analysis demonstrates compliance with the acceptance criteria specified in 10CFR50.46. The fuel rod gap activity, internal pressure and centerline temperature are bounded by the values used in Section 14.9 of the FSAR which demonstrates the limits of 10CFR100 are not exceeded for a refueling accident.

REFERENCES

1. K. J. Morrissey, Vermont Yankee Cycle 16 Summary Report, YAEC-1878 (April 1994).

2. General Electric Company, General Electric Standard Application for Reactor Fuel (GESTARII), NEDE-24011-P-A-10, GE Company Proprietary, February 1991, as amended.

3. Letter, D. T. Weiss to J. M. Buchheit, "GE9B Bundle Nuclear Design Reports for Reload 14," DTW89168, October 6, 1989.

4. Letter, D. T. Weiss to R. T. Yee, "Fuel Bundle Nuclear Design Reports for Vermont Yankee Reload 16," DTW92194, September 3, 1992.

5. A. S. DiGiovine, J. P. Gorski, and M. A. Tremblay; SIMULATE-3 Validation and Verification; YAEC-1659-A (September 1988).

6. R. A. Woehlke, et al.; MICBURN-3/CASMO-3/TABLES-3/SIMULATE-3 Benchmarking of Vermont Yankee Cycles 9 through 13; YAEC-1683-A (March 1989).

7. B. Y. Hubbard, et al.; End-of-Full-Power-Life Sensitivity Study for the Revised BWR Licensing Methodology; YAEC-1822 (October 1991).

8. VYNPC Letter to USNRC, "Vermont Yankee LOCA Analysis Method: FROSSTEY Fuel Performance Code (FROSSTEY-2)," FVY 87-116 (December 16, 1987).

9. VYNPC Letter to USNRC, "Response to Request for Additional Information - FROSSTEY-2 Fuel Performance Code," BVY 91-024 (March 6, 1991).

10. VYNPC Letter to USNRC, "FROSSTEY-2 Fuel Performance Code - Vermont Yankee Response to Remaining Concerns," BVY 92-54 (May 15, 1992).

11. USNRC Letter to L. A. Tremblay, SER, "Vermont Yankee Nuclear Power Station, Safety Evaluation of FROSSTEY-2 Computer Code (TAC No. M68216)," NVY 92-178 (September 24, 1992).

12. Appendix A to Operating License DPR-28 Technical Specifications and Bases for Vermont Yankee Nuclear Power Station, Docket No. 50-271.

13. VYNPC Letter to USNRC, "Inverted Control Rod Poison Tubes at Vermont Yankee," WVY 75-51 (May 16, 1975).

14. USNRC Letter to G. C. Andognini, "Change to Bases," (June 6, 1975).

15. A. S. DiGiovine, et al.; CASMO-3 Validation; YAEC-1363-A (April 1988).

16. A. A. F. Ansari, Methods for the Analysis of Boiling Water Reactors: Steady-State Core Flow Distribution Code (FIBWR), YAEC-1234 (December 1980).

REFERENCES

(Continued)

17. A. A. F. Ansari, R. R. Gay, and B. J. Gitnick; FIBWR: A Steady-State Core Flow Distribution Code for Boiling Water Reactors - Code Verification and Qualification Report; EPRI NP-1923; Project 1754-1 Final Report, July 1981.

18. USNRC Letter to J. B. Sinclair, SER, "Acceptance for Referencing in Licensing Actions for the Vermont Yankee Plant of Reports: YAEC-1232,YAEC-1238, YAEC-1299P, and YAEC-1234," NVY 82-157 (September 15, 1982).

19. General Electric Company, GEXL-Plus Correlation Application to BWR 2-6 Reactors GE6 through GE9 Fuel, NEDE-31598P, GE Company Proprietary, July 1989.

20. Letter, D. T. Weiss to R. T. Yee, "Mechanical MAPLHGRs for Vermont Yankee Reload 16," DTW93136, June 3, 1993.

21. Letter, D. T. Weiss to R. T. Yee, "Fuel Rod Thermal-Mechanical Performance Limits," DTW92260, November 19, 1992.

22. A. A. F. Ansari and J. T. Cronin, Methods for the Analysis of Boiling Water Reactors: A Systems Transient Analysis Model (RETRAN), YAEC-1233, (April 1981).

23. USNRC Letter to R. L. Smith, SER, "Amendment No. 70 to Facility License No. DPR-28," (November 27, 1981).

24. V. Chandola, M. P. LeFrancois, and J. D. Robichaud; Application of One-Dimensional Kinetics to Boiling Water Reactor Transient Analysis Methods; YAEC-1693-A, Revision 1 (November 1989).

25. Electric Power Research Institute, RETRAN - A Program for One-Dimensional Transient Thermal-Hydraulic Analysis of Complex Fluid Flow Systems, CCM-5, December 1978.

26. USNRC Letter to T. W. Schnatz, SER, "Acceptance for Referencing of Licensing Topical Reports: EPRI CCM-5 and EPRI NP-1850-CCM," (September 4, 1984).

27. A. A. F. Ansari, K. J. Burns, and D. K. Beller; Methods for the Analysis of Boiling Water Reactors: Transient Critical Power Ratio Analysis (RETRAN-TCPYA01); YAEC-1299P (March 1982).

28. J. T. Cronin, Method for Generation of One-Dimensional Kinetics Data for RETRAN-02, YAEC-1694-A (June 1989).

29. General Electric Company; C. J. Paone, et al.; Rod Drop Accident Analysis for Large Boiling Water Reactors; NEDO-10527; March 1972.

REFERENCES

(Continued)

30. General Electric Company; R. C. Stirn, et al.; Rod Drop Accident Analysis for Large Boiling Water Reactors Addendum No. 1, Multiple Enrichment Cores with Axial Gadolinium; NEDO-10527, Supplement 1; July 1972.

31. General Electric Company; R. C. Stirn, et al.; Rod Drop Accident Analysis for Large Boiling Water Reactor Addendum No. 2 Exposed Cores; NEDO-10527, Supplement 2; January 1973.

32. General Electric Company, C. J. Paine, Banked Position Withdrawal Sequence, NEDO-21231, January 1977.

33. General Electric Company, D. Radcliffe and R. E. Bates, Reduced Notch Worth Procedure, SIL-316, November 1979.

34. M. A. Sironen, Vermont Yankee Cycle 14 Core Performance Analysis Report, YAEC-1706 (October 1988).

35. USNRC Letter to L. A. Tremblay, SER, "Safety Evaluation for Vermont Yankee Nuclear Power Station RELAP5YA LOCA Analysis Methodology (TAC No. M74595)," NVY 92-192 (October 21, 1992).

36. USNRC Letter to R. W. Capstick, SER, "Approval of Use of Thermal-Hydraulic Code RELAP5YA (TAC No. 60193)," NVY 87-136 (August 25, 1987).

37. L. Schor, et al.; Vermont Yankee Loss-of-Coolant Accident Analysis; YAEC-1772 (June 1993).

38. Report, RELAP5YA, A Computer Program for Light-Water Reactor System Thermal-Hydraulic Analysis, YAEC-1300P-A, Revision 0, October 1982; Revision 1, July 1993.

39. Vermont Yankee Nuclear Power Station Final Safety Analysis Report, December 1991.

40. Letter from L. A. Tremblay to USNRC, "Cycle 17 Startup Test Report," BVY 94-03 (January 13, 1994).

41. Letter, P. J. Savoia, GE, to R. T. Yee, "Transmittal of Modified Thermal Mechanical MAPLHGR Limits for Vermont Yankee Cycle 18 Loss of Stator Cooling Event," PJS 95106, dated July 25, 1995.

APPENDIX A

CALCULATED OPERATING LIMITS

The MCPR operating limits for the Reload Cycle are calculated by adding the calculated ΔCPR to the FCISL. This is done for each of the analyses in Section 7.0 at each of the exposure statepoints. For an exposure interval between statepoints, the highest MCPR limit at either end is assumed to apply to the whole interval.

Table A.1 provides the highest calculated MCPR limits for the Reload Cycle for each of the exposure intervals for the various scram speeds and for the various rod block lines. These MCPR operating limits are valid for operation of the Reload Cycle at full power up to 10644 MWd/St and for operation during coastdown beyond EOFPL.

Tables A.2 through A.5 provide the most limiting calculated MAPLHGR limits for all the fuel types in the Reload Cycle. These values bound the lattice-specific MAPLHGR limits for all the enriched lattice zones in each fuel type. The MAPLHGR limits were revised for the LOSC transient results[41].

TABLE A.1

VERMONT YANKEE NUCLEAR POWER STATION
CYCLE 18 MCPR OPERATING LIMITS

Value of "N" in RBM Equation[1]	Average Control Rod Scram Time	Cycle Exposure Range	MCPR Operating Limit[2,3]
42%	Equal to or better than L.C.O. 3.3.C.1.1	0.0 to 4000 MWd/St	1.39
		4000 to 5500 MWd/St	1.35
		5500 to 10644 MWd/St	1.33
	Equal to or better than L.C.O. 3.3.C.1.2	0.0 to 4000 MWd/St	1.39
		4000 to 5500 MWd/St	1.35
		5500 to 9035 MWd/St	1.33
		9035 to 10644 MWd/St	1.34
41%	Equal to or better than L.C.O. 3.3.C.1.1	0.0 to 4000 MWd/St	1.39
		4000 to 5500 MWd/St	1.35
		5500 to 6500 MWd/St	1.29
		6500 to 9035 MWd/St	1.27
		9035 to 10644 MWd/St	1.32
	Equal to or better than L.C.O. 3.3.C.1.2	0.0 to 4000 MWd/St	1.39
		4000 to 5500 MWd/St	1.35
		5500 to 6500 MWd/St	1.29
		6500 to 8035 MWd/St	1.27
		8035 to 9035 MWd/St	1.30
		9035 to 10644 MWd/St	1.34
≤ 40%	Equal to or better than L.C.O. 3.3.C.1.1	0.0 to 4000 MWd/St	1.39
		4000 to 5500 MWd/St	1.35
		5500 to 6500 MWd/St	1.29
		6500 to 8035 MWd/St	1.25
		8035 to 9035 MWd/St	1.27
		9035 to 10644 MWd/St	1.32
	Equal to or better than L.C.O. 3.3.C.1.2	0.0 to 4000 MWd/St	1.39
		4000 to 5500 MWd/St	1.35
		5500 to 6500 MWd/St	1.29
		6500 to 8035 MWd/St	1.25
		8035 to 9035 MWd/St	1.30
		9035 to 10635 MWd/St	1.34

(1) The Rod Block Monitor (RBM) trip setpoints are determined by the equation shown in Table 3.2.5 of the Technical Specifications.

(2) The current analysis for the MCPR operating limits does not include the 7X7, 8X8, 8X8R or P8X8R fuel types. On this basis, if any of these fuel types are to be reinserted, they will be evaluated in accordance with 10CFR50.59 to ensure that the above limits are bounding for these fuel types.

(3) MCPR operating limits should be increased by 0.01 for the single loop operation.

TABLE A.2

MAPLHGR VERSUS AVERAGE PLANAR EXPOSURE FOR BP8DWB311-10GZ

Plant: Vermont Yankee

Fuel Type: BP8DWB311-10GZ

Average Planar Exposure	MAPLHGR Limits (kW/ft)	
(MWd/St)	Two-Loop Operation	Single-Loop Operation*
0.00	10.93	9.07
200.00	11.00	9.13
1,000.00	11.13	9.24
2,000.00	11.32	9.40
3,000.00	11.52	9.56
4,000.00	11.64	9.66
5,000.00	11.77	9.77
6,000.00	11.92	9.89
7,000.00	12.11	10.05
8,000.00	12.34	10.24
9,000.00	12.59	10.45
10,000.00	12.83	10.65
12,500.00	13.00	10.79
15,000.00	12.81	10.63
20,000.00	12.24	10.16
25,000.00	11.55	9.59
35,000.00	10.24	8.50
45,000.00	8.76	7.27
50,735.00	5.91	4.91

* MAPLHGR limits for single-loop operation are obtained by multiplying the two-loop operation MAPLHGR limits by 0.83.

TABLE A.3

MAPLHGR VERSUS AVERAGE PLANAR EXPOSURE FOR BP8DWB311-11GZ

Plant: Vermont Yankee

Fuel Type: BP8DWB311-11GZ

Average Planar Exposure	MAPLHGR Limits (kW/ft)	
(MWd/St)	Two-Loop Operation	Single-Loop Operation*
0.00	10.93	9.07
200.00	11.00	9.13
1,000.00	11.13	9.24
2,000.00	11.32	9.40
3,000.00	11.52	9.56
4,000.00	11.64	9.66
5,000.00	11.77	9.77
6,000.00	11.92	9.89
7,000.00	12.11	10.05
8,000.00	12.34	10.24
9,000.00	12.59	10.45
10,000.00	12.83	10.65
12,500.00	13.00	10.79
15,000.00	12.81	10.63
20,000.00	12.24	10.16
25,000.00	11.55	9.59
35,000.00	10.24	8.50
45,000.00	8.76	7.27
50,735.00	5.91	4.91

* MAPLHGR limits for single-loop operation are obtained by multiplying the two-loop operation MAPLHGR limits by 0.83.

TABLE A.4

MAPLHGR VERSUS AVERAGE PLANAR EXPOSURE FOR BP8DWB335-10GZ

Plant: Vermont Yankee

Fuel Type: BP8DWB335-10GZ

Average Planar Exposure	MAPLHGR Limits (kW/ft)	
(MWd/St)	Two-Loop Operation	Single-Loop Operation*
0.00	11.29	9.37
200.00	11.34	9.41
1,000.00	11.48	9.53
2,000.00	11.69	9.70
3,000.00	11.92	9.89
4,000.00	12.17	10.10
5,000.00	12.43	10.32
6,000.00	12.68	10.52
7,000.00	12.87	10.68
8,000.00	13.06	10.84
9,000.00	13.24	10.99
10,000.00	12.99	10.78
12,500.00	12.84	10.66
15,000.00	12.65	10.50
20,000.00	11.93	9.90
25,000.00	11.26	9.35
35,000.00	9.88	8.20
45,000.00	8.38	6.96
50,593.00	5.65	4.69

* MAPLHGR limits for single-loop operation are obtained by multiplying the two-loop operation MAPLHGR limits by 0.83.

TABLE A.5

MAPLHGR VERSUS AVERAGE PLANAR EXPOSURE FOR BP8DWB335-11GZ

Plant: Vermont Yankee

Fuel Type: BP8DWB335-11GZ

Average Planar Exposure	MAPLHGR Limits (kW/ft)	
(MWd/St)	Two-Loop Operation	Single-Loop Operation*
0.00	11.28	9.36
200.00	11.33	9.40
1,000.00	11.43	9.49
2,000.00	11.60	9.63
3,000.00	11.80	9.79
4,000.00	12.04	9.99
5,000.00	12.30	10.21
6,000.00	12.53	10.40
7,000.00	12.73	10.57
8,000.00	12.94	10.74
9,000.00	13.13	10.90
10,000.00	12.99	10.78
12,500.00	12.84	10.66
15,000.00	12.65	10.50
20,000.00	11.93	9.90
25,000.00	11.26	9.35
35,000.00	9.88	8.20
45,000.00	8.38	6.96
50,593.00	5.65	4.69

* MAPLHGR limits for single-loop operation are obtained by multiplying the two-loop operation MAPLHGR limits by 0.83.